

Spring 5-2014

Using LiDAR to Map the Geomorphology of the Swift River Region of the White Mountain National Forest, New Hampshire

Cameron A. Held
cheld@bates.edu

Follow this and additional works at: http://scarab.bates.edu/geology_theses

Recommended Citation

Held, Cameron A., "Using LiDAR to Map the Geomorphology of the Swift River Region of the White Mountain National Forest, New Hampshire" (2014). *Standard Theses*. 15.
http://scarab.bates.edu/geology_theses/15

This Open Access is brought to you for free and open access by the Student Scholarship at SCARAB. It has been accepted for inclusion in Standard Theses by an authorized administrator of SCARAB. For more information, please contact batesscarab@bates.edu.

Using LiDAR to Map the Geomorphology of the Swift River Region of the White Mountain National Forest, New Hampshire

An Honors Thesis

Presented to
The Faculty of the Department of Geology
Bates College

in partial fulfillment of the requirements for the
Degree of Bachelor of Science

by
Cameron Held
Lewiston, Maine
March 21, 2014

Abstract

Recently, geomorphologic mapping techniques have undergone rapid developments as high-resolution ortho-imagery and digital elevation models augment traditional field-based surveying methods. Utilizing 2011-2012 LiDAR data, this project maps and classifies the geomorphology of the Swift River region of the White Mountains of New Hampshire. LiDAR Hillshade maps with illuminations/elevations of 315/45 and 45/45 produced the best images to view the complexities of the landscape. Analysis of the bare ground LiDAR has allowed new landscape units to be recognized and mapped, including: 1) depositional and erosional floodplain fluvial features (approximately 15% of the study area); 2) stream incision features on slopes (average grade of 18° - 40°); 3) glacially streamlined features (310° azimuth of orientation); 4) other glacial landforms such as glacial lake terraces; 5) and stoss and lee bedrock features (with dominant fracture orientations of 5°, 40°, and 130°) among others. There is no variation in the lineament analysis of the Jurassic bedrock using the methodology of Mabee et al. (1994), but a strong correlation to the field-measured joints in those units from Pangaeon rifting. Further analysis of the landscape geomorphology focused on where the polygons overlapped, creating areas of mixed landscape units (ex. overlap of glacial depositional and fluvial erosional polygons or of fractured bedrock and glacial depositional regions). This study shows that LiDAR can be successfully used to map the bedrock and surficial landscape geomorphology of large, remote regions of land that were previously unable to be viewed due to the dense tree canopy.

Chapter 1: Introduction

1.1 Purpose

Recently, geologic mapping techniques have undergone rapid development as traditional field-based surveying methods are replaced with high-resolution orthoimagery and digital elevation models. LiDAR, a laser based range-finding technology was first used for geologic mapping in the late 1990s. Due to technological advances and increased availability, it has only recently started to be used extensively in research. Data generated with this method shows subtle topographic expressions at a resolution previously unachievable. As a result, it is an extremely useful tool for geologic research; in particular for geomorphic studies of tectonic, glacial, hillslope, and fluvial processes (e.g. Pavlis and Bruhn, 2010; Pavlis et al., 2010; Haugerud et al., 2003).

In March of 2012, a region of the White Mountain National Forest near the Swift River was flown with LiDAR for a soil study carried out by the Natural Resources Conservation Service. This data, also available for geologic research and mapping, invited further research. Hillshade images rendered from this LiDAR data on ArcGIS show topographic variations that represent faults, fractures, striations, glacial streamline features, hillslope slumps and landslides, as well as fluvial systems (Roering *et al.*, 2013). This imagery in conjunction with the *Bedrock Geologic Map of New Hampshire* (Lyons et al., 1997), can be used to conduct a completely remote lineament and geomorphology analysis of the terrain in ArcGIS. Yet, while LiDAR opens up opportunities to identify unseen lineaments and features and to quickly map large areas, it cannot replace on the ground fieldwork, thus selective field analysis is still necessary.

LiDAR mapping in the Swift River region of the White Mountain National

Forest has provided an opportunity to employ and test relatively new remote sensing techniques to map bedrock features, glacial features, and post-glacial landforms. This effort has resulted in the generation of a geomorphic map of this remote region of the White Mountain National Forest. The map, produced using the new LiDAR data of the region, and checked with ground-truthing of the joint data will offers new insights on the geology of the region, as well as the potential applications of high resolution remote sensing, like LiDAR, to supplement the necessary field surveys in any mapped region.

1.2 Geomorphology and Remote Sensing

From the early days of geologic investigation through 1972, all geomorphology was determined by on location field research (Roering *et al.*, 2013). Detailed sketches, showing morphologic features of a study area, accompanied most geologic work predating 1900. The advent of relatively portable and inexpensive photography in the early twentieth century greatly increased the objectivity of field location documentation as compared to sketches. Improved surveying techniques over the next several decades allowed for improved location precision and more accurate elevation mapping. Geomorphologists were still severely limited however- an experienced surveying team could often take only 30-40 topographic data points in a day (Roering *et al.*, 2013). This restricted studies to smaller areas, and large-scale landforms were often entirely overlooked.

In 1972 the United States began the Landsat project, the first satellite imagery initiative. This satellite was equipped with sensors capable of imaging the earth's surface at 80m resolution (USGS, 2013). For the first time, scientists could use remote data to view morphologic features without fieldwork. This ability to look at the Earth's surface from above offered a new tool to geomorphologists, but the 80m resolution

only showed larger features, and the images were only useful in non-vegetated areas.

The next significant advance for mapping, both in the field and remotely, was the introduction of the global positioning system (GPS) array in 1994. This allowed for 100m positioning accuracy anywhere on the planet (NOAA, 2013). GPS data, in conjunction with geo-referenced Landsat images, built the backbone of the Geographic Information System (GIS), a system of computer based mapping and data management software. GIS allowed for an accurate compilation of remote sensing data and field observations, where the locations of field observations were recorded with a GPS unit.

The greatest remaining hindrance to geomorphologists was the lack of accurate elevation models. The existing USGS topographic maps smoothed topography to an extent that made the recognition of geologic features very difficult (Figure 1.1). The

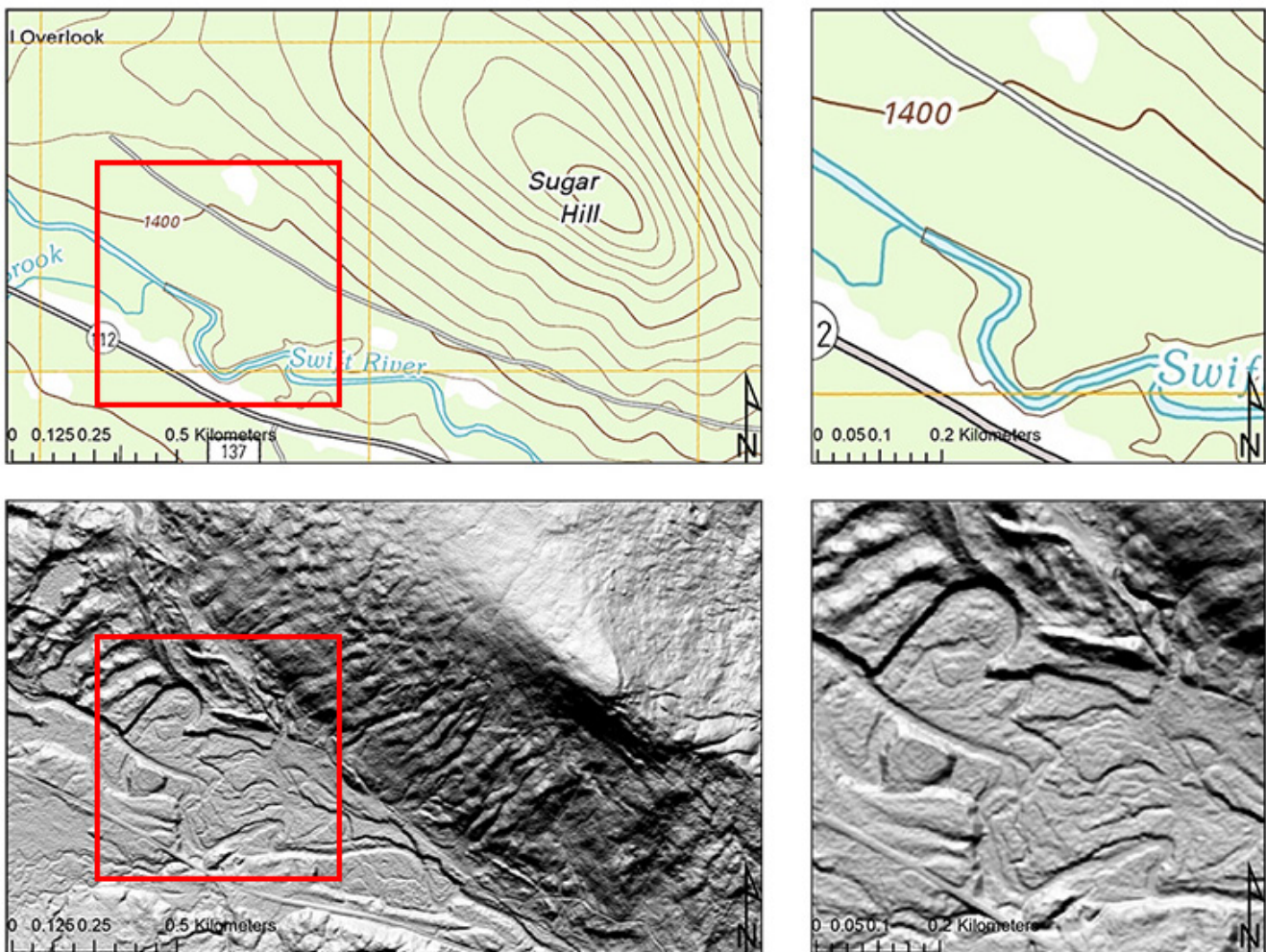


Figure 1.1 A comparison of the terrain visible in a USGS 7.5" topographic map (top) and 2m resolution LiDAR (bottom) from the Swift River study area. Old stream channels, an oxbow, and eskers can be seen in the LiDAR, but are not visible in the topo map, nor in any aerial imagery due to tree cover.

introduction of interferometric synthetic aperture radar (InSAR), in 1999, offered elevation data- achieved from satellite radar analysis- at up to 90m resolutions. This data was then converted into digital elevation models (DEM), showing the elevation in the form of a raster dataset on GIS.

By the early 2000s, geomorphologists had many useful tools at their command for remote sensing, and advances were continually being made; Landsat resolution was improved to 15m, GPS accuracy was enhanced to sub 10m, and new developments in InSAR allowed for up to 30m elevation resolutions. As a result the early 2000s saw a boom in geomorphic interest (Figure 1.2).

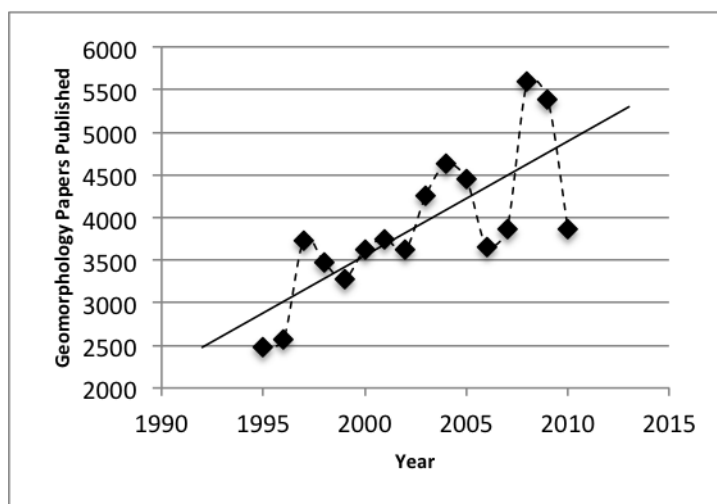


Figure 1.2 Timeline showing the increase in geomorphologic papers published between 1995 and 2010 that have been referenced on GeoRef. (GeoRef, 2013)

LiDAR, the acronym for Light Detection and Ranging, is a technology that uses lasers to calculate the distance between an object and the LiDAR generating machine (NOAA, 2013). LiDAR was developed in the 1960s, and had been implemented for use in varied fields from law enforcement to mining, but it wasn't until the late 1990s that LiDAR was used for geomorphic research.

The true usefulness of LiDAR for geomorphologists was realized when it was combined with an aircraft in the technique known as airborne laser swath mapping (ALSM) (Roering *et al.*, 2013). Here a laser is shot at the earth's surface from the plane, and the time required for the wavelength to return gives the relative distance of

the earth's surface. Early models were limited to 5,000 pts/sec, but the current ones are capable of exceeding 150,000 pts/sec (Roering *et al.*, 2013). The elevation of the aircraft and the sampling frequency together determine the resolution of the surface imagery. Sub-meter resolution is achievable; however, most data is flown at one or two meter resolution.

Once the light returns to the aircraft, the time is analyzed to determine the distance, and that ranging data is combined with readings from onboard GPS units that

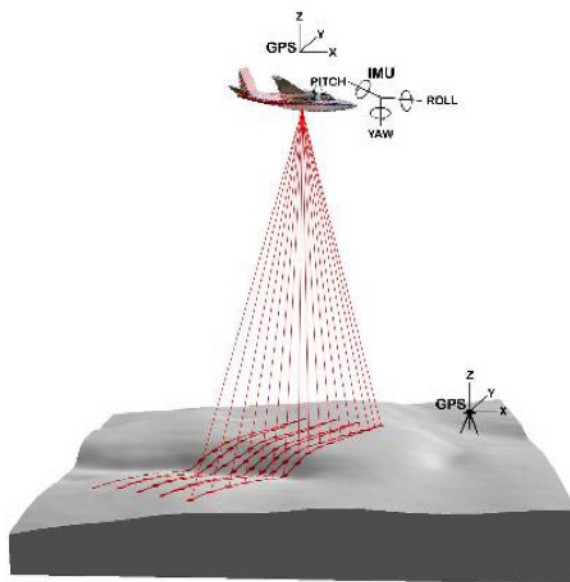


Figure 1.3. Image showing how airborne laser swath mapping (ALSM) data is achieved. (Wikipedia, 2013)

mark the location of the plane, and an internal measurement unit (IMU) which uses gyroscopes and accelerometers to determine the pitch, yaw, and roll of the plane (essentially the degree measurement off of true vertical at which the readings are taken) (Figure 1.3). Once all of these factors are combined, each relative elevation is assigned a coordinate on the earth's surface, and the relative elevations are given real world values based on a ground survey point, and are accurate to 10cm or less (Mallet & Bretar, 2009).

Besides the obvious resolution advantage achieved by airborne laser swath mapping (ALSM) over InSAR, it also has advantages in applications with thick vegetation and in bathymetric studies (Roering *et al.*, 2013). Full-waveform LiDAR data analyzes each different wavelength of the backscattered laser, allowing a three dimensional understanding of the object hit by the laser (Mallet & Bretar, 2009; Roering *et al.*, 2013). In forested areas this

is particularly important, as full-waveform LiDAR can give canopy and ground surface elevations simultaneously, something unachievable by other remote sensing techniques. Green wavelength LiDAR, a 532 nm wavelength- in comparison to the standard 1064 nm used for terrestrial mapping, is capable of penetrating shallow bodies of water, enabling some bathymetric studies (Roering *et al.*, 2013). Bare-ground LiDAR, which uses the last return of light to the sensor in order to remove tree canopy readings, can be used to map areas of thick vegetative cover that were not able to be mapped accurately with aerial imagery (Roering *et al.*, 2013). Bare ground LiDAR was the dataset used for this study. Due to these distinct advantages, LiDAR has recently become the remote sensing method of choice for geomorphologists, allowing unparalleled resolution and flexibility in terrain analysis.

The Natural Resources Conservation Service (NRCS) branch in St. Johnsbury Vermont, a subset of the Department of Agriculture, has been a part of an ongoing soil mapping effort in the White Mountain National Forest (WMNF) in New Hampshire. Using recently flown LiDAR data, from March 2013, soil specialists Roger Dekett and Jessica Philippe, and soil survey leader Bob Long have employed remote mapping techniques coupled with sporadic ground-truthing field work to quantify the soil units present in the Swift River region of WMNF (Dekett *et al.*, 2013). The power of using LiDAR and Geographic Information System (GIS) software has enabled this relatively small office of the NRCS with limited assets to thoroughly map a large wilderness area. However, as soil scientists, they often overlooked outcrops and geomorphic features. Yet, the NRCS office graciously shared their compiled LiDAR data for further geomorphic study.

1.3 Study Area

A protected forest located in north-central New Hampshire, the WMNF covers approximately 800,000 acres (USFS, 2013). The Swift River region flown with LiDAR is located in the southeastern portion of the White Mountain National Forest, in eastern New Hampshire (Figure 1.4). It is approximately 10 km by 10 km, although it is not a perfect square and is instead the uneven boundary of the White Mountain National Forest (Figure 1.4).

The study area is dominated by Mount Tremont, which is located on the northern side of the region, and has steep slopes with some exposed bedrock along the ridges and cliffs. Much of the remaining region is composed of lowlands that have been classified by the NRCS team in their initial research as glacial or fluvial (Dekett et al.,

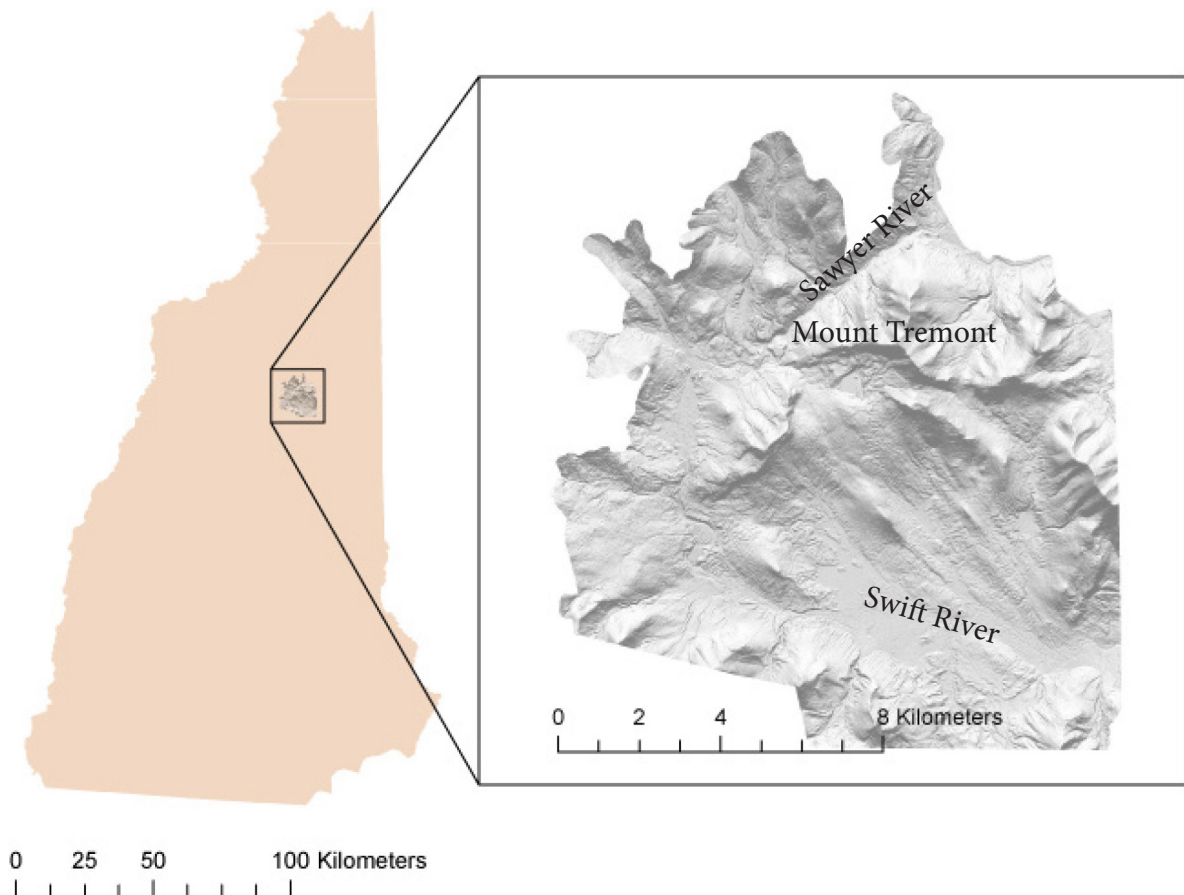


Figure 1.4 Map of New Hampshire showing the location of the Swift River study area. Major landforms are marked on the map of the study area.

2013). The Swift River runs along the southern side of the study area, and its fluvial system dominates this area.

1.4 Geologic History

1.4.1 Tectonic and Bedrock History

The Appalachian Mountain belt, of which the White Mountains are a part, were formed through a series of continental collisions, or orogenies, beginning 460 million years ago with the Taconic Orogeny (Hibbard *et al.*, 2006). The Salinic Orogeny 420 million years ago, the Acadian Orogeny 400 million years ago, the Neoacadian Orogeny 360 million years ago, and the Alleghenian Orogeny 270 million years ago followed

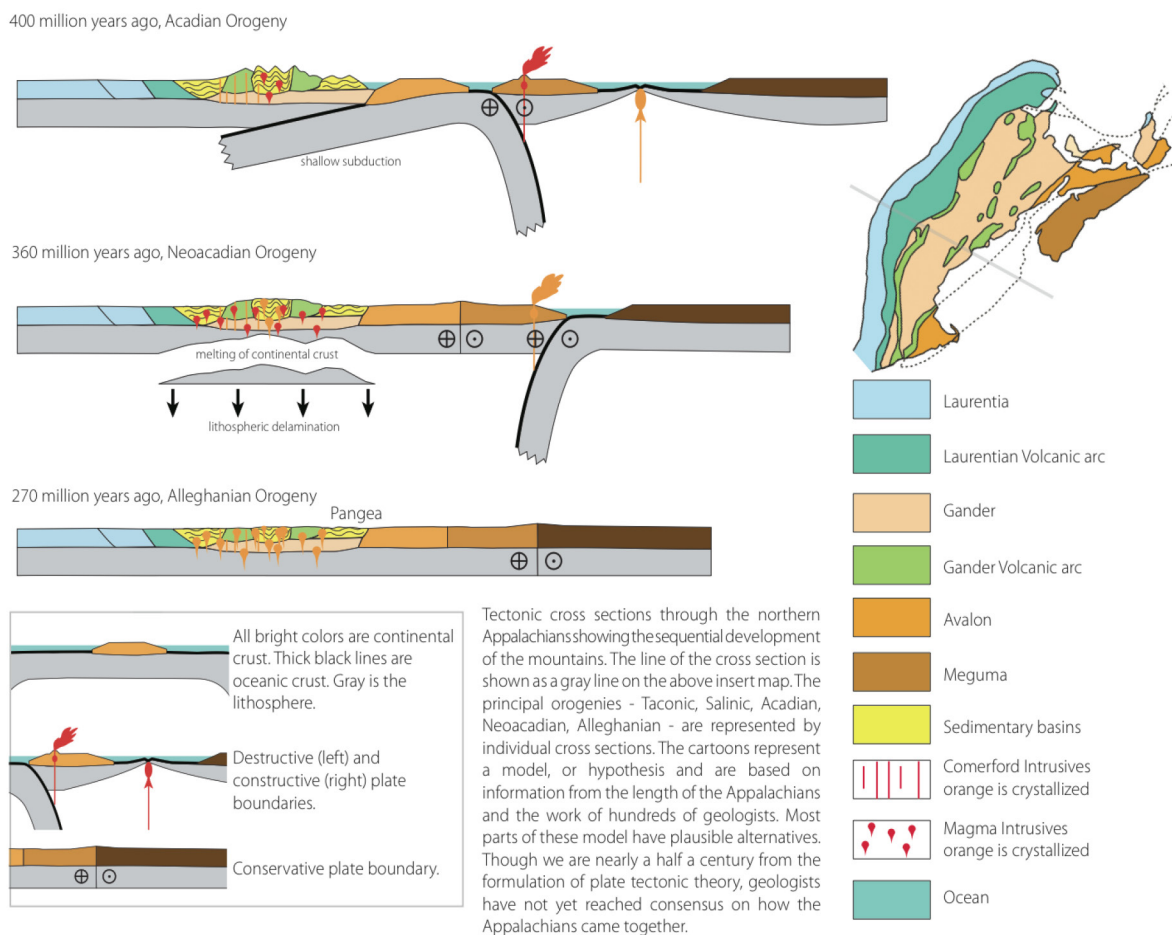


Figure 1.5 Models of the Acadian, NeoAcadian, and Alleghenian Orogenies (Hibbard *et al.*, 2006)

Swift River Study Area

Bedrock Units and Lineaments

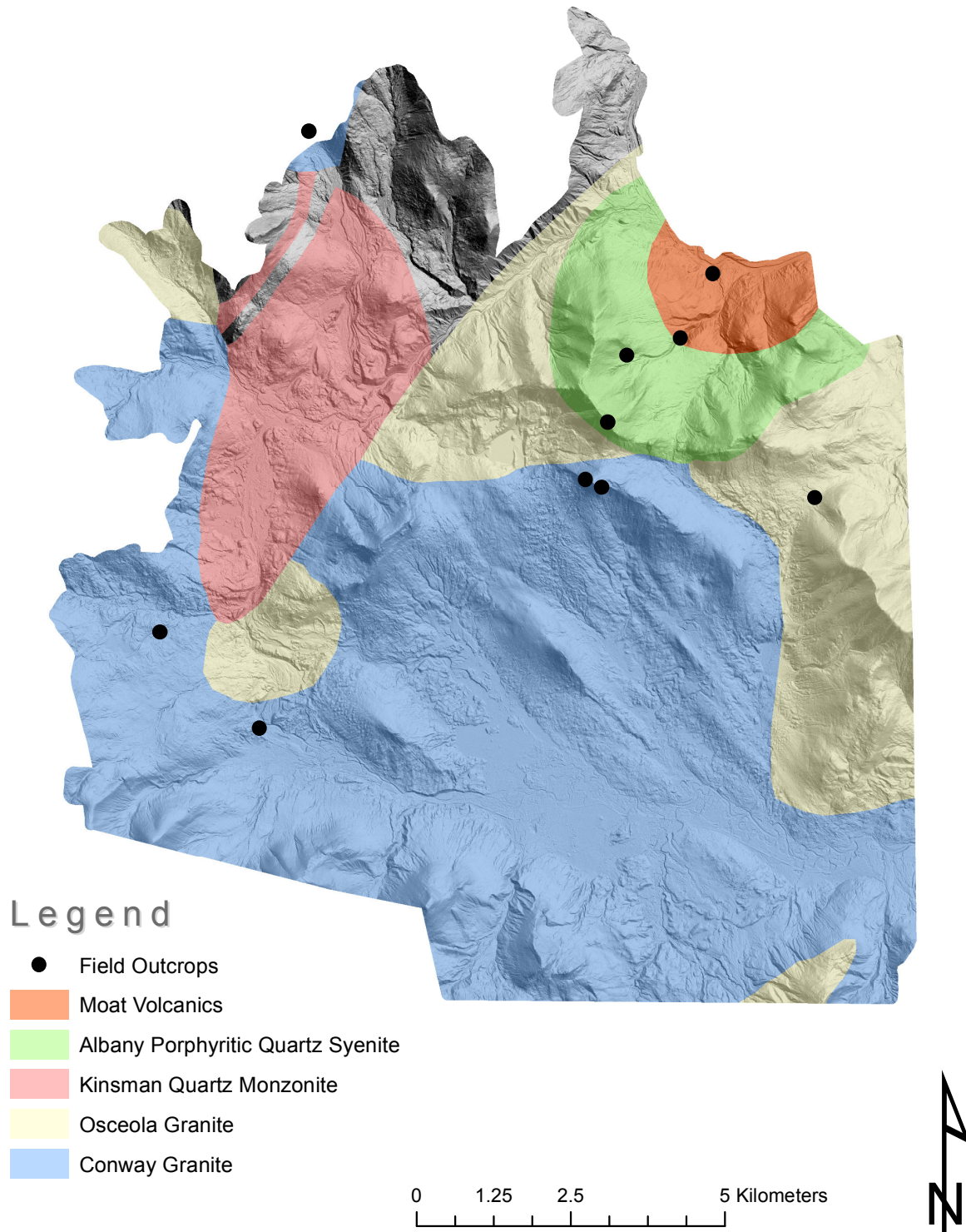


Figure 1.6 Bedrock map of the Swift River region showing the major units in this study. Outcrop locations are marked with black points.

after, with each orogeny representing a new island arc or continent accreting onto the Laurentian Continent (Figure 1.5). Together, these orogenies brought together or created almost all of the bedrock we see today between the western border of Vermont and the coast of Massachusetts- or farther north everything between Quebec City and the eastern edge of Nova Scotia.

The oldest rock unit within the Swift River region is the Kinsman Quartz Monzonite, which dates from the early Devonian, about 410-400 million years ago (Figure 1.6). This rock unit was formed during the early stages of the Acadian Orogeny, when the Avalon Plate was pushed underneath the Gander Plate, doubling the overall crustal thickness. The thicker crust settled deeper into the mantle, raising its temperature, and causing melting (Lyons *et al.*, 1997). The magma rose up into the overlying crust forming plutons where it cooled slowly.

The composition of the Devonian magmas varied regionally depending on the composition of the subducted rock. The Kinsman formation was a quartz monzonite, meaning it has somewhere between 5% and 20% quartz, and equal concentrations of Plagioclase and Orthoclase feldspars. Quartz monzonites also tend to have sodic plagioclase feldspar end members, andesine to oligoclase. In the field the Kinsman is easily recognizable due to its potassium feldspar composition (>5cm) in a fine-grained matrix. The Kinsman formation is only found in the northwestern corner of the study area, and covers only a small area.

The Alleghenian Orogeny terminated in the creation of the Pangean supercontinent. The next phase in the tectonic history of the Appalachian Mountain belt is the rifting apart of the Pangean supercontinent. The convection cells in the mantle that had brought all of the continents together switched, and began pulling them apart in the Early Triassic, 210 million years ago. As tensional forces pulled the continents apart, extensive fault systems and rift basins formed. These fractures, faults, and rift basins formed in a northeast-southwest orientation, perpendicular to

the tensional rifting forces (McHone, 1988; Faure et al., 2006; Eusden *et al.*, 2013).

The theorized explanation for the breakup of Pangaea is an upwelling of mantle material under the present day Gulf of Mexico (McHone and Butler, 1984; Schliche *et al.*, 2003). As the continents pulled apart, this magma worked its way into the faults and fractures of the rift basins, forming a period of extreme volcanism across the disassembling Pangaea. This region of volcanic activity is known as the Central Atlantic Magmatic Province (CAMP), and CAMP rocks can be found in South America, North America, Africa, and Europe (Figure 1.7) (McHone and Butler, 1984).

Within the CAMP province more regional clusters of volcanic activity are visible. The White Mountain Plutonic Suite is one such grouping of spatially and temporally correlated volcanic and plutonic rocks from the Triassic, Jurassic, and Early Cretaceous time periods. The northwest orientation of the plutons is suggestive of a mantle

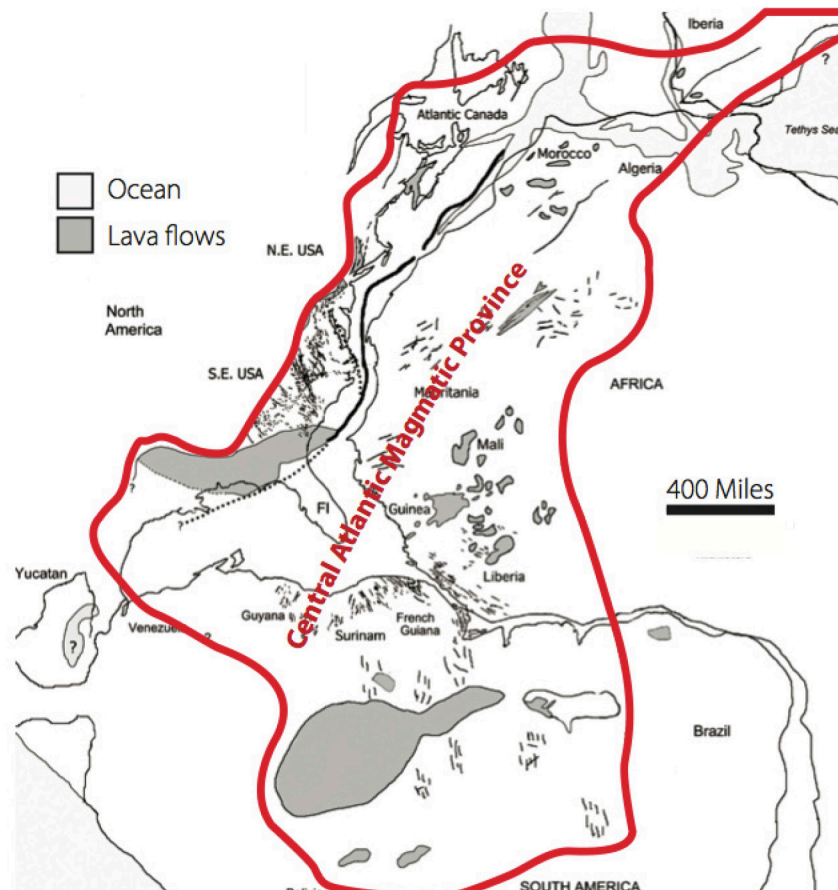


Figure 1.7 The Central Atlantic Magmatic Province is shown in red, while the dark grey areas represent magmatic intrusions (McHone and Butler, 1984).

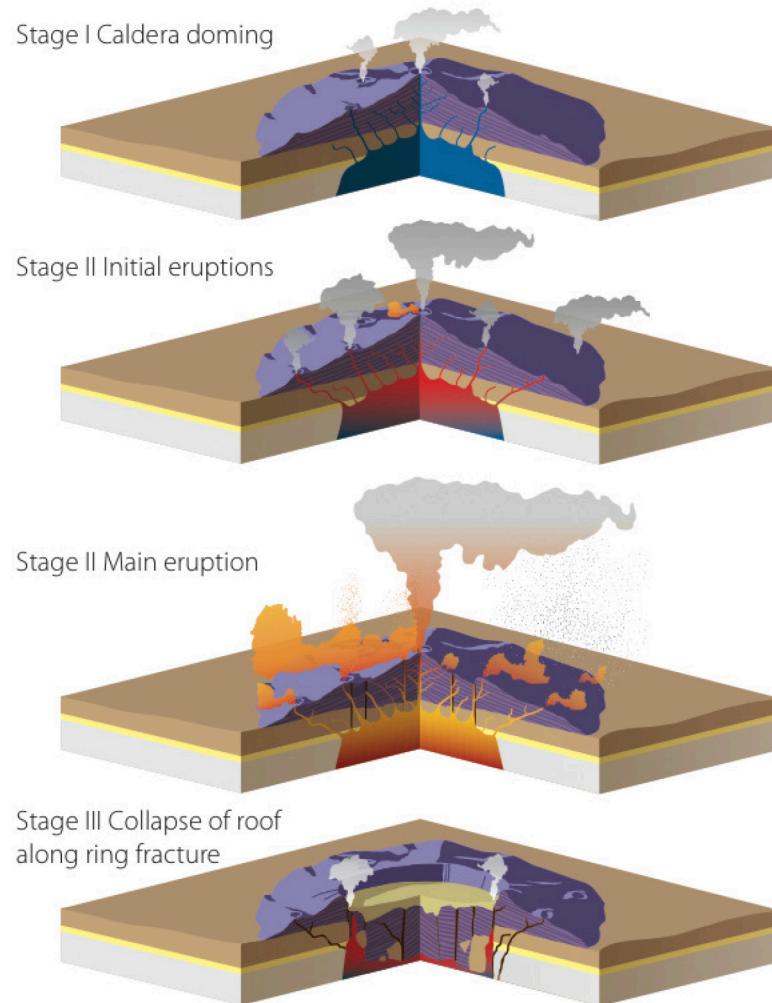


Figure 1.8 The first three stages of caldera collapse and ring dike formation as seen in the White Mountains during the Jurassic, according to Creasy (Ramberg, 2008).

hotspot as cause of this volcanic activity, but Creasy argues that it was instead caused by a five-stage process of volcanic doming, caldera collapse, and re-intrusion (Figure 1.8) (Creasy & Eby, 1993; Eusden *et al.*, 2013).

Stage one in this process involves a large intrusion of magma that forces the overlying crust to dome upwards, and some small eruptions out of ring-shaped fractures directly above the edges of this subterranean magma chamber. Stage two is marked by several large and explosive eruptions that lay down pyroclastic rocks on the slopes of the volcano. These eruptions empty the subterranean magma chamber, leading to a caldera collapse, marking stage three. These calderas are filled with large

boulders from landslides that form mega-breccias. Stage four is a second period of smaller eruptions, filling the caldera with ash flows. Magma along the ring fractures that surround the caldera cool to form ring dikes. Finally, stage five is another intrusion, this time of more granitic magma that cross cuts the earlier stages (Creasy & Eby, 1993; Eusden *et al.*, 2013).

The final three stages of this sequence are represented in the Swift River study area. The Moat Volcanics are representative of stage three mega-breccias and stage four tuffs, pyroclastic flows, and breccias (Creasy & Eby, 1993). There are also porphyritic rhyolites and some trachyte found within the Moat sequence. The Moat Volcanics are thought to be Early-Middle Jurassic.

The Moat Volcanics are surrounded by circular bands of the Albany Porphyritic Quartz Syenite, which are the ring dikes formed in stage four of the model (Figure 1.6). These ring dikes represent the original outer constraints of the magma chamber under the caldera. In this study area there are actually two units within the Albany Porphyritic Quartz Syenite, each with slightly different compositions, representing two different intrusions of magma into the ring fractures. Both units are felsic igneous rocks with a low quartz content (<5%). The outer ring has larger feldspar phenocrysts however, while the inner unit has a higher concentration of hornblende. The Albany formation is aged to be Middle Jurassic (Eusden *et al.*, 2013).

Finally, the Osceola and Conway granites represent stage five, the resurgence of granitic plutons that intrude against the overlying Moat Volcanics and Albany Porphyritic Quartz Syenite (Figure 1.6). The Conway Granite is a pink colored, biotite rich, coarse-grained, two-feldspar granite. This can be differentiated from the creamy colored, amphibole rich, one-feldspar Osceola Granite (Creasy and Fitzgerald, 1996). Together these two rocks make up about 75% of the Swift River Study Area, showing the massive size of the plutons they once were in the Middle Jurassic.

Following the intrusions of the Jurassic, the structural history of the Swift River

region is dominated by brittle deformation, predominantly in the form of fractures. The extension of Pangaea during the Jurassic, mentioned earlier as one of the causes for Jurassic intrusion, also caused extensive brittle fracturing in a northeast-southwest orientation (McHone, 1988, Faure et al, 2006). The Cretaceous tensile stress fields moved to a north-south orientation, causing east-west trending fractures (McHone, 1988; Faure, 1996; Eusden *et al.*, 2013). Both of these fracture sets may be visible on the rocks of the Swift River region.

1.4.2 Glacial History

In the Pleistocene, the Earth's climate cooled, and there were a series of glaciations that covered much of North America. The center of this continental ice sheet lay somewhere over the Hudson Bay, and extended far to the south, covering the entire state of New Hampshire, as well as the entire northeastern United States (Figure

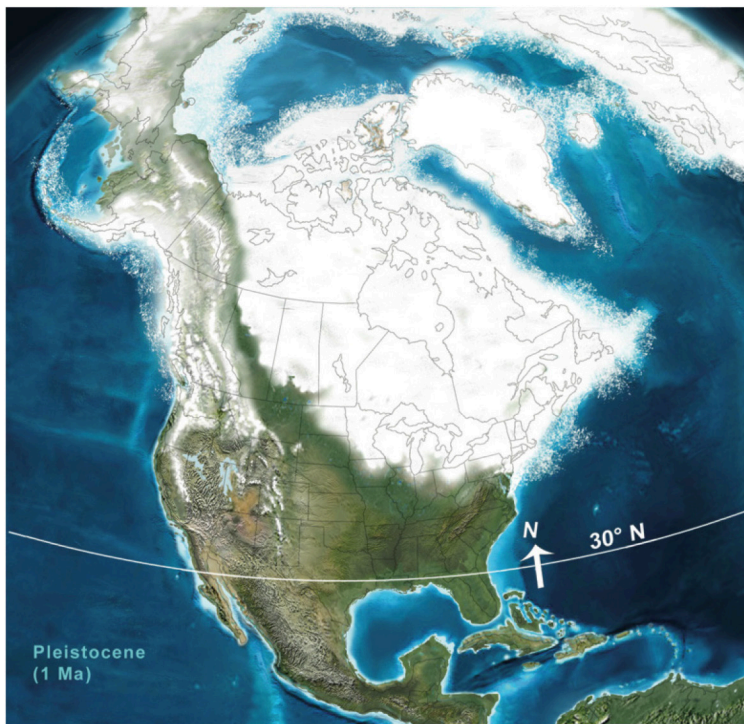


Figure 1.9 Extent of Pleistocene Ice Sheet in North America. New Hampshire and the White Mountains are entirely submerged in ice (Blakely, 2011)

1.9). The ice sheets were more than a mile thick, and covered the peaks of the White Mountains (Bradley, 1981; Anderson and Borns, 1994; Eusden *et al.*, 2013).

In the White Mountains there is only evidence of the final glaciation, the Wisconsin, as this event scoured the region, and removed all traces of previous glaciations. The Wisconsin glaciation began about 50,000 years ago, and ended 14,000 years ago. In this glaciation the ice sheet flowed predominantly

northwest-southeast, although local topography sometimes altered its course, especially near the highest peaks of the Presidential range (Bradley, 1981). Within the Swift River region, there are no large mountains that would have been able to alter the course of the ice sheet, so it likely advanced in the northwest-southeast manner.

This glaciation greatly altered the landscape, and glacial features can still be seen throughout the White Mountains. Glacially carved valleys differ from stream carved valleys in that they have a wide U-shape. This happens because in a stream valley all of the erosion is occurring at the bottom, whereas a glacier erodes all sides of the valley.

Another tell-tale glacial feature is stoss-and-lee topography on hills and mountains. These features occur when the glacier smoothens one side of a mountain,

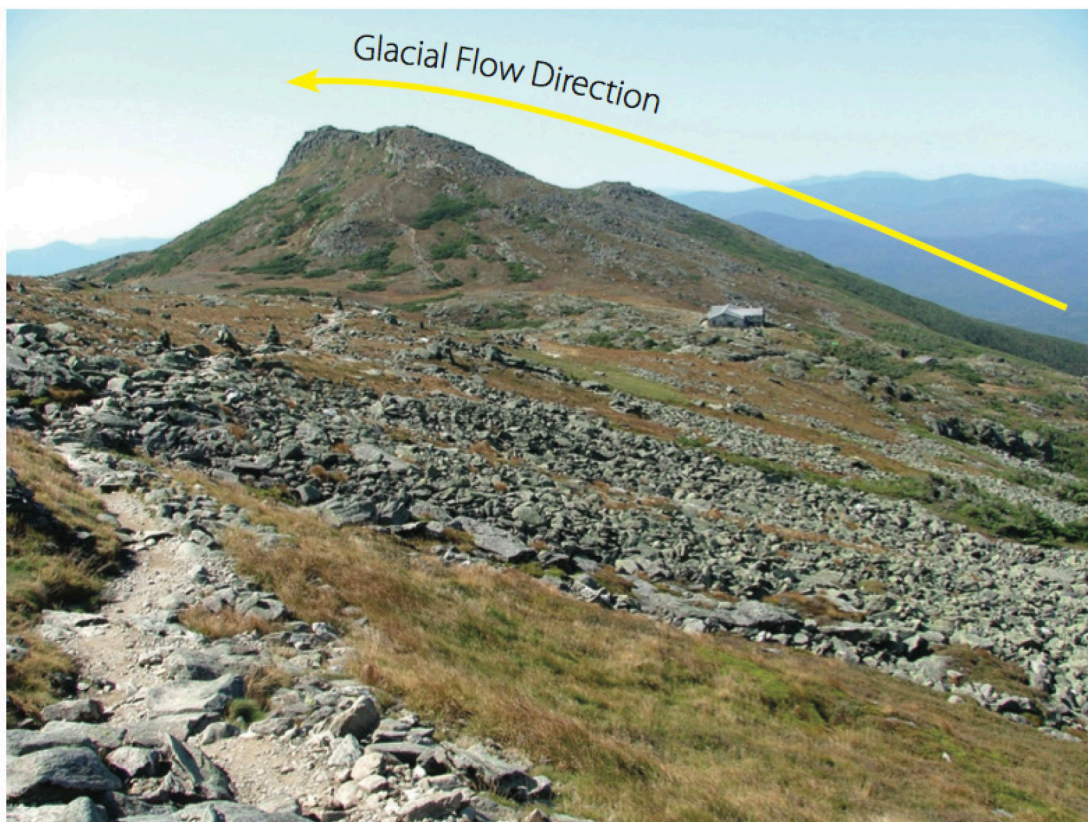


Figure 1.10 A stoss and lee feature seen on Mount Madison in the White Mountains. Similar features are seen throughout the region, and show glacial flow direction. Image from Eusden et al, 2013.

the stoss side, and breaks off blocks of rock from the lee side (Figure 1.10). The blocks break off because the ice is compacted on the stoss side, releasing water under the high pressure. This water gets squeezed over to the lee side, where the pressure is lower since the ice momentum is heading up and out, not down into the face of the mountain. Here it works its way into cracks in the rock and freezes, expanding, and breaking the rock apart. In the White Mountains the stoss side lies to the northwest, while the lee side is on the southeast (Anderson and Borns, 1994; Eusden *et al.*, 2013).

Glacial streamline features also show the glacial flow direction. The most common streamline feature is the drumlin, a rounded, elongated, and smoothed topographic ridge that varies in composition (Anderson and Borns, 1994). Drumlins are typically oval shaped, with the long axis parallel to the flow direction of the ice sheet. Unlike the stoss and lee features seen on mountains and ridgetops, the stoss face of drumlins is steeper, while the lee is long and flatly tapered (Anderson and Borns, 1994). Drumlins typically are between 250m and 1000m long and 120m and 300m wide (Anderson and Borns, 1994). Drumlin composition varies from bedrock to till to glaciofluvial sediments, and can have homogenous, conformable, or unconformable structure (Anderson and Borns, 1994).

Finally, another feature that denotes a glacial past is a striation. Striations are grooves or scratches in existing bedrock that are caused by the abrasion of the underlying bedrock by rocks included in the underside of the glacier (Anderson and Borns, 1994). The striations run parallel to the ice flow direction, and are a good indicator of regional flow directions.

1.4.3 Post-Glacial History

Two processes, fluvial and mass movement, dominate the Post-glacial history of the White Mountains (Bradley, 1981). When the Laurentide Ice Sheet retreated 12,000 years ago, it left a very smooth landscape, quite unlike the one visible today. Together, fluvial and mass movement processes have reshaped the terrain.

Mass movement processes include landslides and rockfalls. Landslides occur

when steep ground, usually more than 30° , becomes saturated with water, and loses stability. As it begins sliding down the slope it picks up speed and gains mass as other loosened areas join in. Landslides are common on the steep slopes of the White Mountains, and leave the bare scars on the mountainsides. Rockfalls are a higher energy form of mass movement, and only occur on very steep slopes.

1.5 Research Objectives

Utilizing the LiDAR data flown in March 2012, this project intended to map and classify the geomorphology of the Swift River region of the White Mountains. It was expected that the high-resolution imagery would allow new geologic features to be recognized and mapped. The geomorphology was analyzed through bedrock, glacial, and post-glacial data; each with different objectives and research questions. Finally, any interactions between these different classifications were explored further.

The bedrock was analyzed with respect to lineaments, any linear bedrock features seen in the LiDAR, representing faults, fractures, and dikes. First, it had to be determined that LiDAR could in fact be used to recognize real bedrock fractures. If this was possible, a fracture signature for each bedrock unit could potentially be determined. Each bedrock unit would either have differing joint orientations from the others, or they would all have a common regional orientation. Then, using strike and dip measurements of fractures collected in the field, it was determined if lineaments drawn from LiDAR actually matched the real world fracture sets. Subsequently, if real world fractures were represented by LiDAR lineaments, and different bedrock units were found to have unique fracture sets, then the potential uses of LiDAR bedrock mapping of remote areas would be examined. Finally, an attempt was made with the lineament data from the remote LiDAR analysis and the field data to correlate it with the tectonic history, and theorized stress fields.

The primary goal of the glacial data was to determine glacial flow direction based on glacial features in the region. Any regional variations in glacial flow direction were

analyzed. All glacial erosional features were recognized, mapped, and investigated for any relation to glacial flow direction or other glacial processes. Similarly, all glacially deposited features were identified, mapped, and examined for any information on the history of the Laurentide Ice Sheet in the Swift River region. If glacial lake features were found, they were mapped; and, the glacial lake history of the region would be unraveled.

The Swift River region was then observed for fluvial and mass movement erosional and depositional features. The fluvial features were classified by the type of deposit they represent. Mass wasting events would also be mapped, if they occurred in the Swift river region.

Using all of the data above, the temporal-spatial relationships between these three types of features were analyzed. Any interactions between types of features, overlays of features, and spatial relationships between features were determined, and any reasons for such interactions were explored.

Finally, a map was made with polygons showing bedrock controlled regions, different types of till, glacial outwash, and post-glacial fluvial depositional regions. Lineaments within the bedrock-controlled regions were also mapped. Glacial features were delineated with polygons or lines, depending on their type. Fluvial and mass movement features were also mapped with polygons. The resulting map reveals a

2.1 Introduction

This study involved two distinctly different methodologies: a set of field methods for the fracture data collected on the ground in the White Mountains, and remote sensing methodologies for GIS work. Neither methodology would result in as useful a dataset if used individually; but, the combination of the two allows for a verification and validation of the data collected.

2.2 Methods Used

2.2.1 Field Methods

The field data was collected to use as a control for the lineament data from the LiDAR mapping. As a result, it was important to collect data that represented all of the rock units from the Swift River region, and to spread the collection points out around the study area so as to be aware of regional variations. In order to have a sufficient number of data points with which to compare the LiDAR measurements, at least one hundred strike and dip measurements were taken per outcrop; although, on one large outcrop more than one hundred were collected. In order to find large enough outcrops to afford over one hundred strike and dip measurements, the study region was viewed using both LiDAR and aerial imagery, and potential outcrop locations were marked. When using the LiDAR data to find outcrops, the ideal locations were steep slopes with a rough looking texture, as soil and till tend to be smoother looking than bedrock. In the aerial images outcrops were marked, although visibility was limited to non-forested areas. The most easily accessible outcrops were given the highest priority- those along roads and trails. Other areas where outcrops were plentiful were along riverbeds, and at cliffs. The final waypoints at which data was collected were primarily near roads and along the Mount Tremont trail, although several were at the top of cliffs, or in riverbeds (Figure 2.1). At two of the cliff-top locations all one hundred strike and dips were not able to be collected safely, so forty were collected at one, and sixty more were collected at the next cliff, a few hundred meters away.

Upon arrival to a chosen outcrop, the coordinates were recorded with a handheld GPS; or, in

Swift River Study Area

Bedrock Units and Lineaments

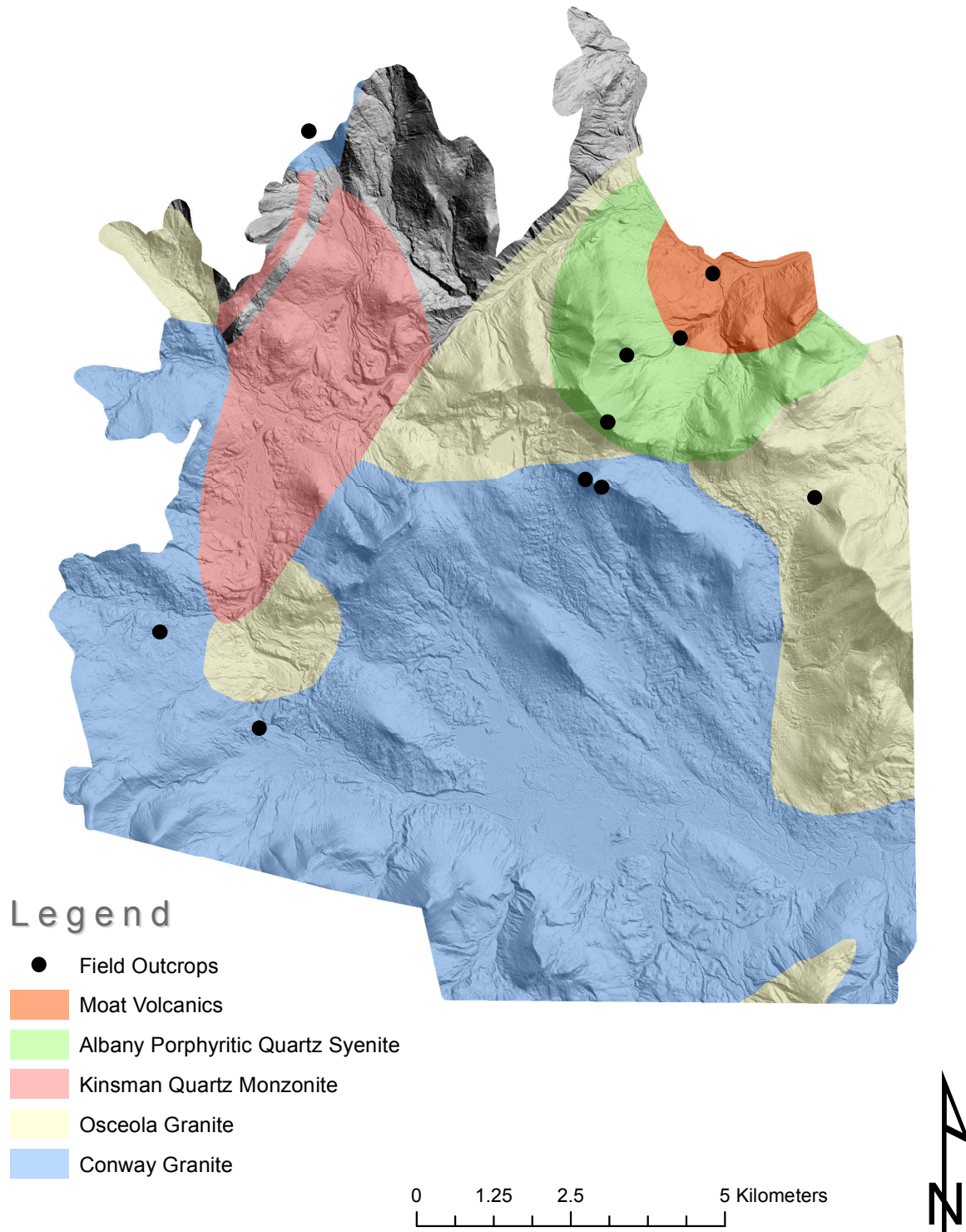


Figure 2.1 Bedrock map of the Swift River region showing the major units in this study, and outcrop locations, marked with black points.



Figure 2.2 The author taking the strike and dip of a fracture, and the rake of the slicken lines.

two instances, on a ruggedized laptop with GPS functionality. Strike and dip measurements were taken on joint and fracture planes on the rock outcrop. Only fractures with a dip greater than 45° were recorded, as sheeted fractures would not show up on aerial LiDAR imagery. Strike and dip measurements were taken with both a Brunton Pocket Transit compass, and with an iPhone 4s using the Strike and Dip app. Although hesitant at first to use an iPhone as a primary data collection device,

we calibrated the phone with the Brunton, and the two were consistently within 1° of one another when taking measurements in the field. The iPhone greatly sped up the data collection process, but the Brunton was still employed several times per outcrop to confirm the iPhone's accuracy.

The strike and dip data was recorded in a field notebook, and the data was later entered into Microsoft Excel. In the field, cross cutting relationships of joints were also recorded, if any were visible at the outcrop. Also, at several locations slicken lines were visible, and on these planes strike, dip, and rake were measured (Figure 2.2). Rake is the measurement of a line's angle off of horizontal. This shows the direction of motion of the planar joint features. Once all of this data was entered into Microsoft Excel, it was exported to OSXStereonet, where it was plotted as mirrored roseplots.

2.3 GIS Methodology

In ArcGIS, the project began with bareground LiDAR data, in the form of a raster file. The team at the St. Johnsbury NRCS office had already mosaiced the data, so it came in as a single useable raster file. From this, hillshades were created using ArcGIS' Hillshade tool, in the Spatial Analyst toolbox. When using this tool several parameters can be defined, including azimuth and altitude of the light source. Several hillshades were created for analysis, two at an azimuth of 45° and two at an azimuth of 315° . For each azimuth a low angle hillshade, with an altitude of 15° , and a standard hillshade with an angle of 45° were created. It was determined that the low altitude hillshades would not be used for this study,

because, while they offered greater contrast, they left large areas in shadow.

Next, a remote lineament analysis was carried out on the LiDAR data, based on the methods of Mabee *et al.* (1994). To do this, a researcher traces all lineaments observed on a single hillshade. Lineaments include all naturally occurring linear features, including bedrock fractures, straight sections of streams, and glacial streamline features. For this lineament analysis, the focus was on bedrock features; so, lineaments were only drawn for features that were clearly bedrock controlled, or of unknown origin, as those could possibly be attributed to the bedrock. Lineaments were drawn at two different scales, larger ones were drawn at 1:24,000, while smaller ones were drawn at 1:10,000.

The goal of the Mabee *et al.* method is to increase objectivity in the naturally subjective process of spotting and drawing lineaments (1994). In order to do so, they created the reproducibility test (Figure 2.3). This process involves the lineament drawing process being carried out on two separate occasions, each time using the same conditions (azimuth, altitude, scale...). Then the two lineament datasets are overlaid in ArcGIS, and a third set of lineaments is drawn. This set is only drawn where lineaments from the first two datasets are coincident, and any non-coincident lines are discarded.

The COGO properties of

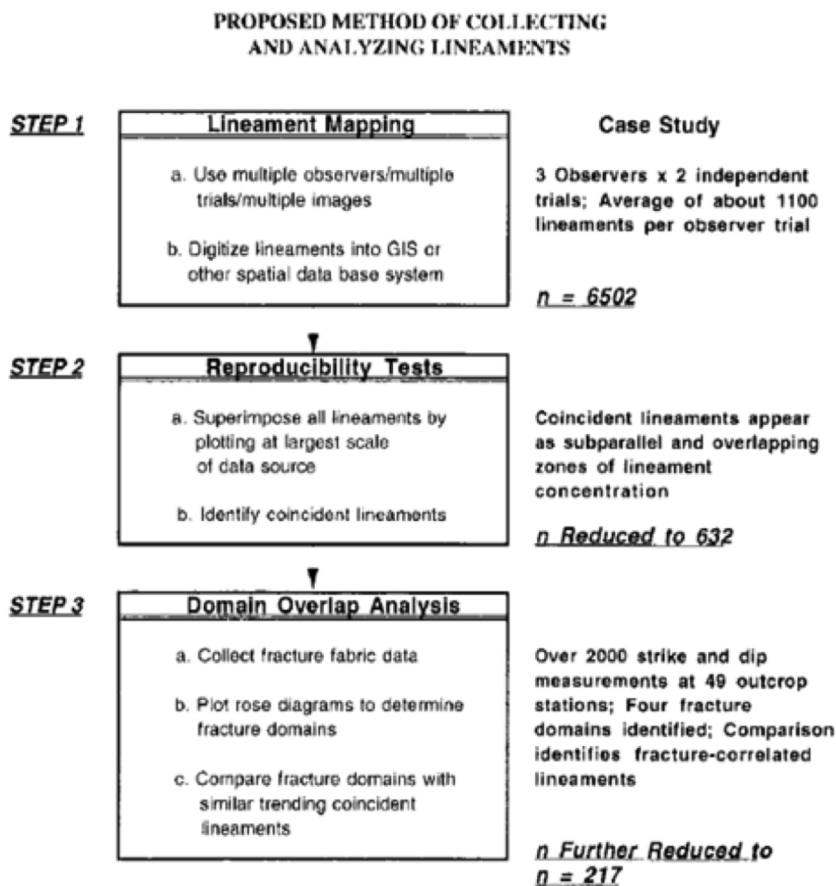


Fig. 1. Flow chart indicating the proposed method used to reduce lineament data sets collected in regional-scale studies of fractured-bedrock aquifers.

Figure 2.3 Flowchart showing the proposed lineament drawing methodology (Mabee *et al.*, 1994). Only the first two steps will be used in this analysis, as the final step requires thousands of strike and dip measurements across a wider spatial scale than this study is using.

these desired lineaments are determined by ArcGIS, and include among other values direction, an angle, essentially the strike of the given lineament. This data was exported to Microsoft Excel for each rock unit, by doing a selection of only lineaments within that rock type. In Excel it was given a dip value of 90° because no dip values can be calculated from a LiDAR image. It was then taken into OSXStereonet, and plotted as mirrored roseplots, to show the orientation of the lineaments. The data for each rock unit could now be directly compared with the real world fracture data collected on location.

Finally, all areas that appear to be bedrock outcrops or bedrock controlled were mapped in ArcGIS with polygons. These polygons were chosen based on the observed properties of the terrain- slope, altitude, and the observed smoothness in the LiDAR image. Bedrock controlled regions tend to be on steeper slopes, higher elevations, and look very rough on LiDAR, whereas lowlands and flatter topography are covered with soil and till, and are smooth appearing on the LiDAR. While this is a subjective process, it still helps give parameters to the type of morphology in each region.

Similar polygons were drawn for all the terrain that was deemed to be glacially controlled and fluvial controlled. These could overlap with the bedrock-controlled regions, and with one another, as the regions are not mutually exclusive. Any region of overlap was turned into a new polygon using the intersect tool, which allows for the creation of joint geomorphic regions (ie. fluvially dissected till).

Within the glacial polygons any linear glacial feature such as a striation or esker is marked. These lineaments are dealt with in the same way as the bedrock lineaments, and the resulting roseplots show the dominant glacial flow direction.

Potential glacial lake surfaces were modeled using ArcScene to show in 3D the receding lake levels that produced terraces. For these, a semi-transparent lake polygon was projected at the required elevations, and overlaid on a hillshade with base elevations projected from the LiDAR data.

Older, pre-digital, maps were georeferenced to fit within the study area. This was done by matching features such as lakes and rivers in the old basemap with these same features in the modern LiDAR datasets. This allowed for direct comparison between the past and present maps of the region.

Chapter 3: Results

3.1 Results Introduction

The results of this study are divided into three distinct subsections the fracture data collected in the field, the LiDAR based lineament analysis, and the LiDAR derived geomorphic maps. The strike and dip field data has been converted into stereonet and roseplots that graphically represent the data for each bedrock unit. Similarly, the lineaments are also graphed on stereonet plots and roseplots. This data is also referenced spatially with the creation of a bedrock lineament map. Finally, the geomorphic maps created in ArcGIS show the bedrock, till, glacial outwash, and post-glacial fluvial regions. These are represented in a series of maps that shed light on regions previously unmapped.

3.2 Field Data- Joints

3.1.1 Overview

Fracture data was measured at six different outcrop locations throughout the Swift River study area. These datasets represent four of the five dominant bedrock units within the region, as not enough Kinsman Quartz Monzonite outcrops were found to be measured. Shallowly dipping sheeted joints were avoided for this study, as they would not be visible in LiDAR imagery, and would disrupt any correlation between the two datasets. Three significant joint sets were found from this data by creating a Kamb contoured planes to poles stereonet plot in Stereonet 9 for Mac (Figure 3.1). For the overall dataset, a Kamb contour interval of 3, a significance level of 3, and a counting grid spacing of 20 was used. The dominant joint sets are shown by the planes on the stereonet, and strike NE-SW (avg. strike 41° dip 84°), WNW-ESE (average strike 106° dip 85°), and NNW-SSE (average strike 165° dip 85°) (Figure 3.1).

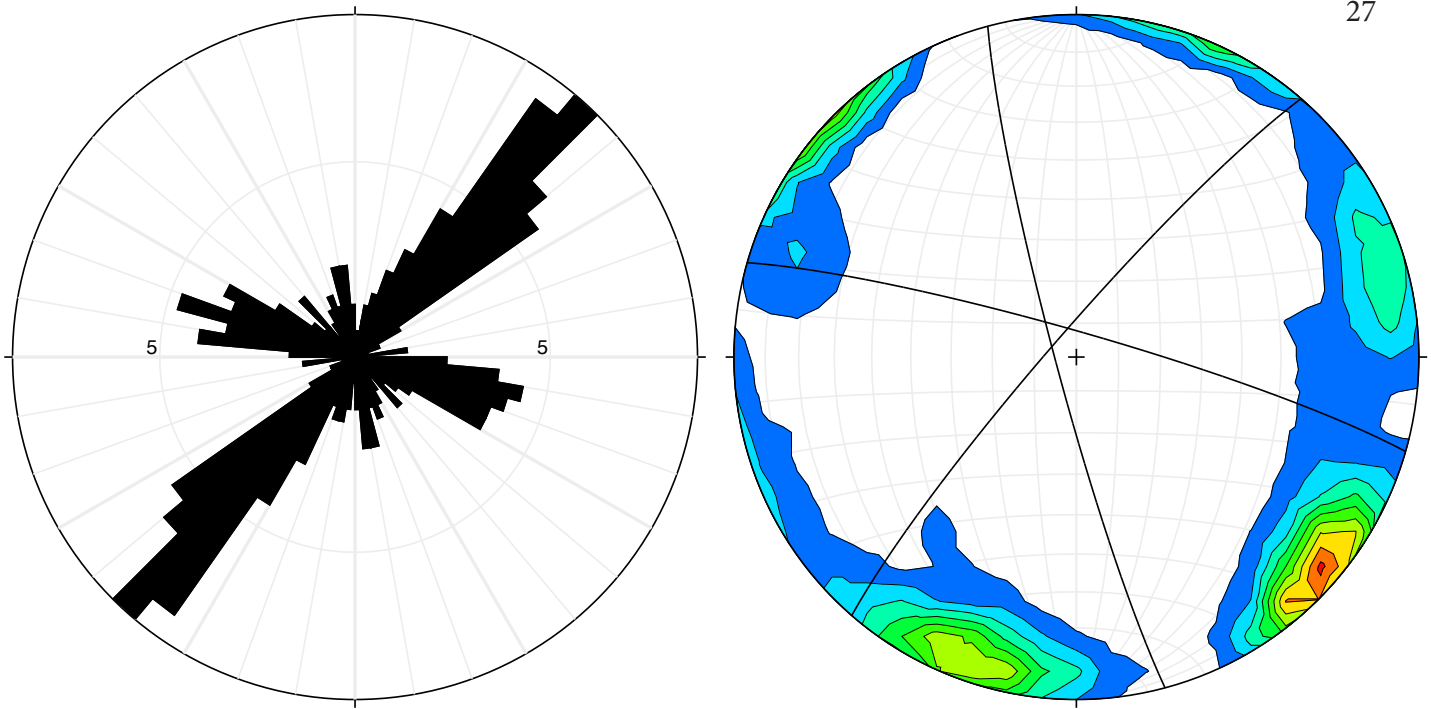


Figure 3.1 A roseplot at left, and a Kamb contoured planes to poles stereonet at right, showing the orientation of all the joint planes collected for the Swift River Study Area. $N = 400$

These three orientations are also represented on the roseplot of the dataset, also made within Stereonet 9 for Mac (Figure 3.1). The roseplot shows the dominance of certain strikes, and shows that the NE-SW joint set is the strongest, with 38% of the data falling within 15° of the average strike of this set. The WNW-ESE joint set is the second most prevalent; with 21% of the data within 15° of the average strike. Finally, 14% of the joint planes are represented by the NNW-SSE joint set. These same three joint sets are dominant throughout the different bedrock units.

3.1.2 Conway Granite

Conway Granite is characterized by the NE-SW joint set (average strike and dip 226° , 84°), as well as a secondary signal from the NNW-SSE joint set (average strike and dip 163° , 79°) (Figure 3.2). The NE-SW set contains 45% of the planes, while the NNW-SSE set has 32%.

3.1.3 Albany Porphyritic Quartz Syenite

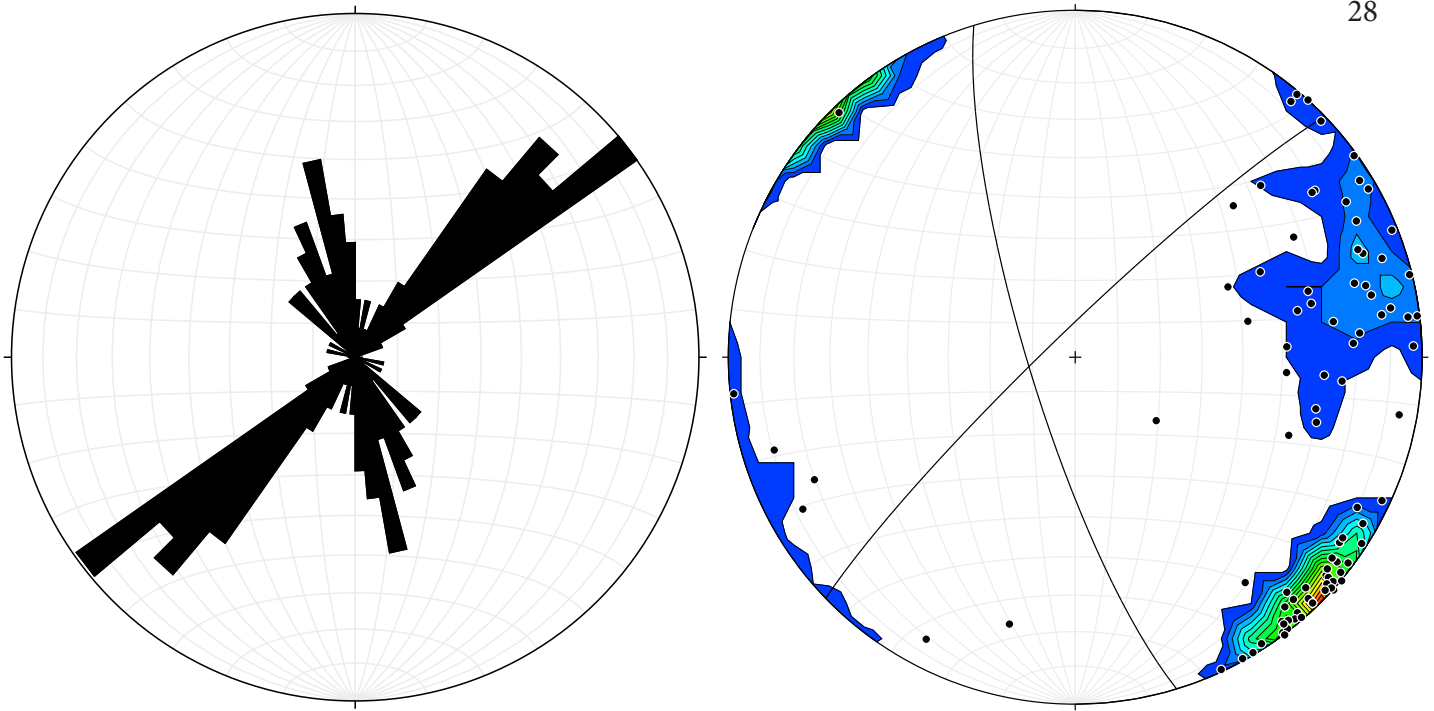


Figure 3.2 A roseplot at left, and a Kamb contoured stereonet plot to the right, showing the orientations of joints within the Conway Granite, as well as the poles of all the Conway joint planes. $N=100$

The Albany Porphyritic Quartz Syenite also has the prevailing NE-SW joint set (average strike and dip $216^\circ, 77^\circ$) with an ancillary WNW-ESE joint set (average strike and dip $283^\circ, 82^\circ$) (Figure 3.3). The NE-SW set is 48% of the planes, and 38% lies within 15° of the WNW-ESE average.

3.1.4

The Osceola Granite also has the dominant NE-SW joint set (average strike and dip $218^\circ, 82^\circ$), and a secondary joint set striking WNW-ESE (average strike and dip $284^\circ, 83^\circ$) (Figure 3.4). Here 41% of the planes are within 15° of the average NE-SW plane, and 18% are within 15° of the average WNW-ESE plane.

3.1.5

The Moat Volcanics have the WNW-ESE set as the prevailing orientation (with an average strike and dip of $294^\circ, 87^\circ$), followed by the NNW-SSE set (average strike and dip

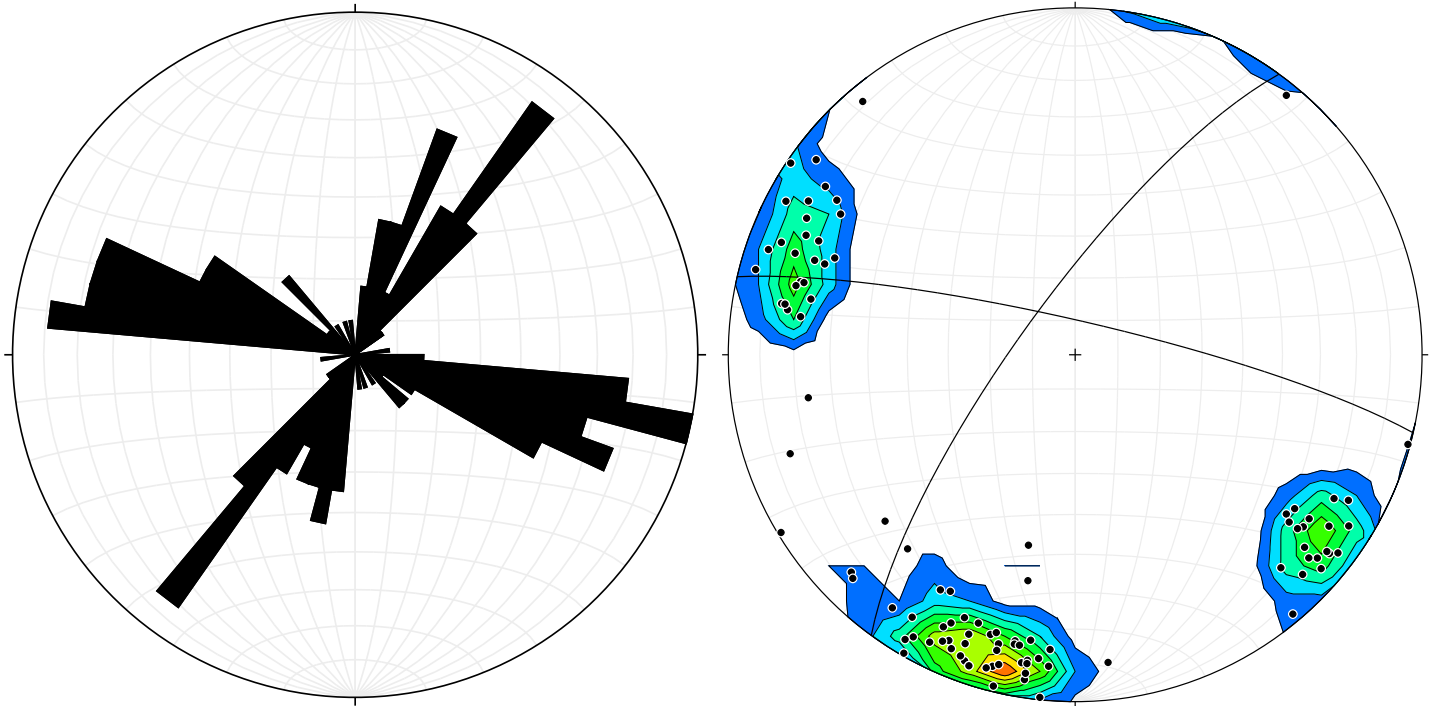


Figure 3.3 A roseplot at left, and a 1% contoured planes to poles stereonet plot to the right, showing the orientations of joints within the Albany Porphyritic Quartz Syenite, as well as the poles of all the Albany joint planes. N= 100

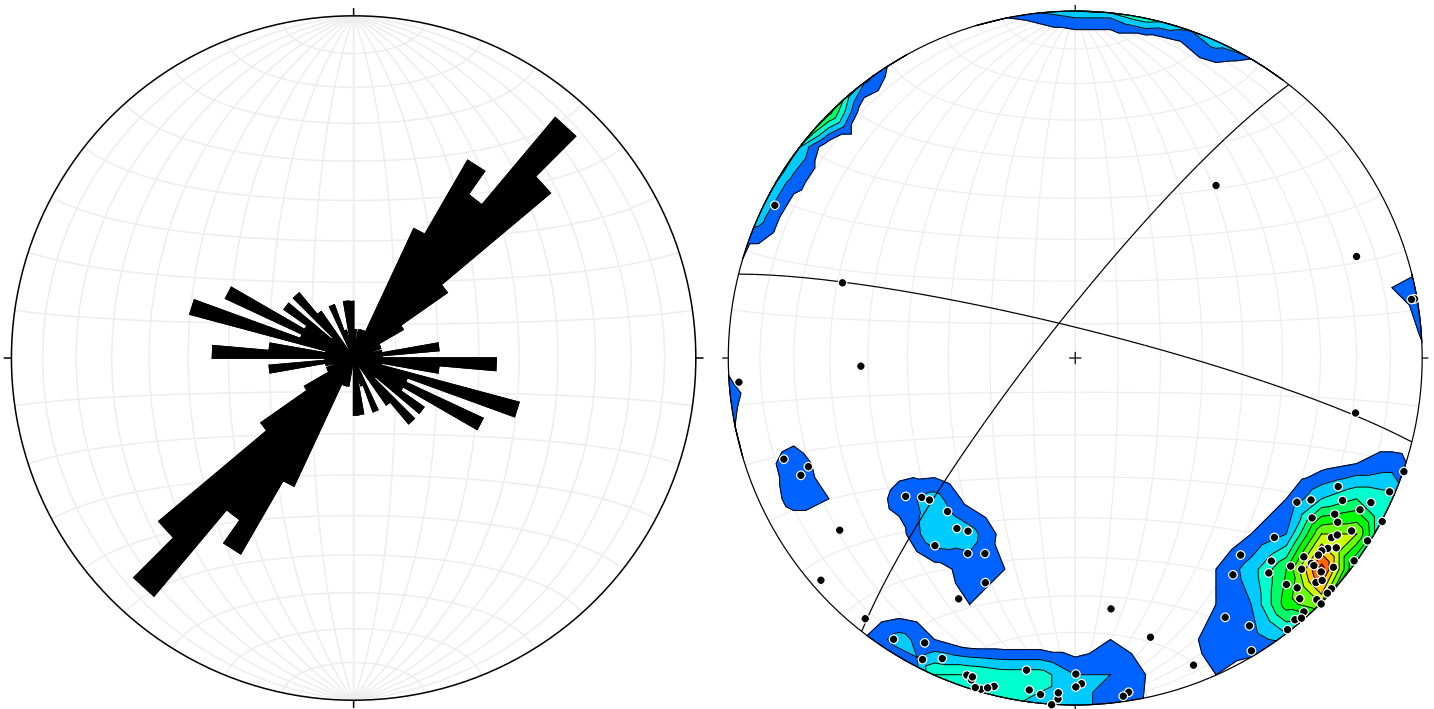


Figure 3.4 A roseplot at left, and a 1% contoured planes to poles stereonet plot to the right, showing the orientations of joints within the Osceola Granite, as well as the poles of all the Osceola joint planes. N= 100

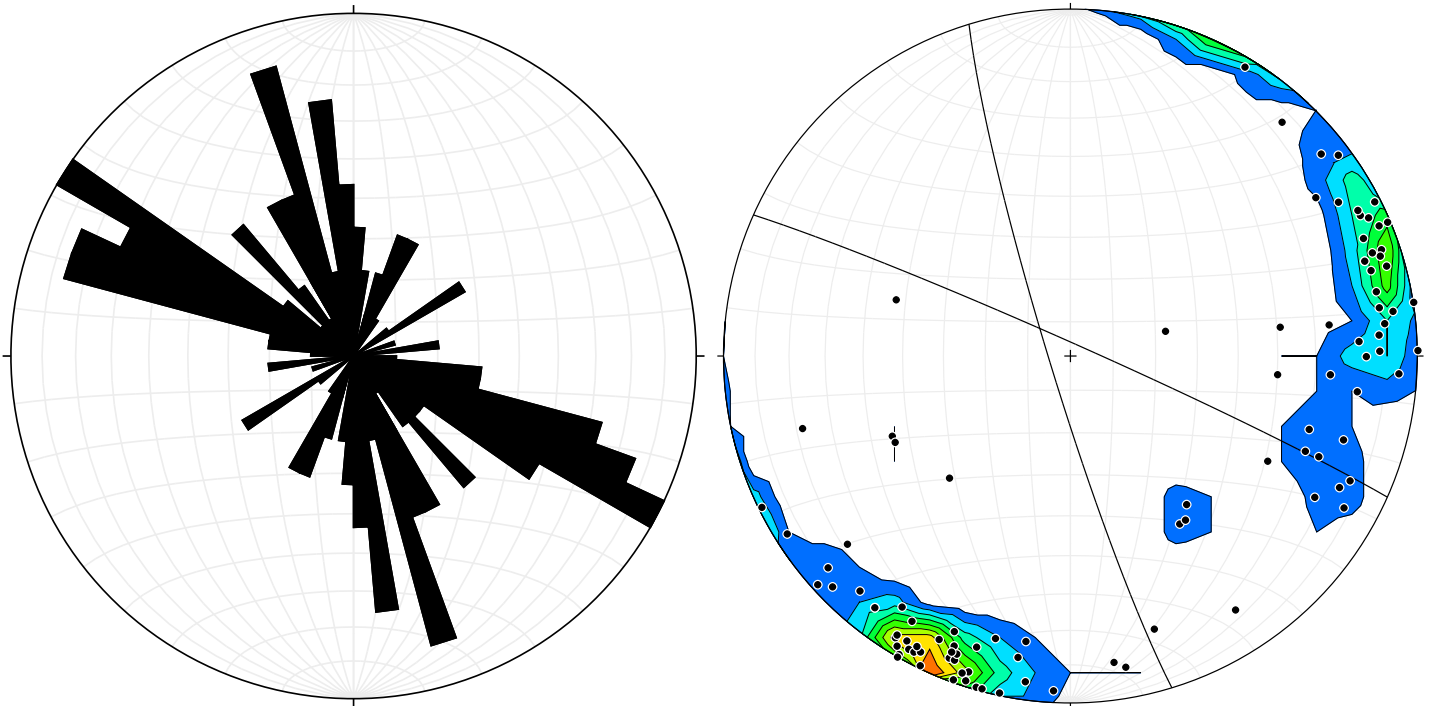


Figure 3.5 A roseplot at left, and a 1% contoured planes to poles stereonet plot to the right, showing the orientations of joints within the Moat Volcanics, as well as the poles of all the Moat joint planes. N= 100

163°, 85°) (Figure 3.5). The WNW-ESE joint set contains 47% of the data, the NNW-SSE set has 31%, and only 14% of the planes lie within 15° of the NE-SW joint set average.

3.1.6 Conclusions

All four bedrock units are consistent in that their two dominant fracture sets match two of the three sets seen on the overall stereonet. The Osceola Granite and Albany Porphyritic Quartz Syenite share similar fracture sets, with the NE-SW and WNW-ESE fractures as the dominant two for each. The Conway Granite and Moat Volcanics, while similar are distinctly different from the others, and from one another. The Conway has the NE-SW set, as well as a NNW-SSE set. The Moat Volcanics on the other hand have a WNW-ESE set and a NNW-SSE set.

3.2.1 Overview

Using the two LiDAR derived hillshades, with azimuths of 315° and 45° and altitudes of 45° each, bedrock lineaments were traced in ArcMap. Using two varying scales, 1:8000 for smaller lineaments and 1:20000 for larger lineaments, a total of 5,708 lineaments were drawn in the study area over four separate trials; two trials for each hillshade image.

Any coincident lineaments from these first four trials, those within 5° or several millimeters at the working scale, were retraced as the final lineaments. A total of 1624 lineaments were retained during this process. These lineaments were then delineated by the bedrock unit they overlaid, and mapped separately (Figure 3.6).

The dominant lineament sets are NE-SW (average strike 33°), N-S (average strike 4°), and NW-SE (average strike 141°). The NE-SW is the most prevalent, with 31% of the planes striking within 15° of the average, while the N-S and NW-SE had 26% and 19% respectively (Figure 3.7). These lineaments were drawn for comparison with the fracture data collected for each bedrock unit. Since the LiDAR offers a high resolution image of bedrock in the region, it is expected that there will be a strong correlation between fracture strikes and bedrock lineament orientations.

3.2.2 Conway Granite

A total of 378 lineaments were drawn within the Conway Granite. These are marked by dominant NE-SW, NW-SE, and N-S sets, similar to those of the overall area (Figure 3.8). This is compared to the fracture sets for the Conway Granite, which are NE-SW and NNW-SSE.

3.2.3 Albany Porphyritic Quartz Syenite

A total of 463 lineaments were drawn for the Albany Quartz Syenite, and are seen to have dominant N-S, NE-SW, and NW-SE sets, listed in decreasing order of dominance (Figure 3.9). The fracture sets for the Albany Porphyritic Quartz Syenite on the other hand were NE-SW and WNW-ESE.

3.2.4 Osceola Granite

Within the Osceola Granite unit a total of 555 lineaments were drawn. These have a dominant

Swift River Study Area

Bedrock Units and Lineaments

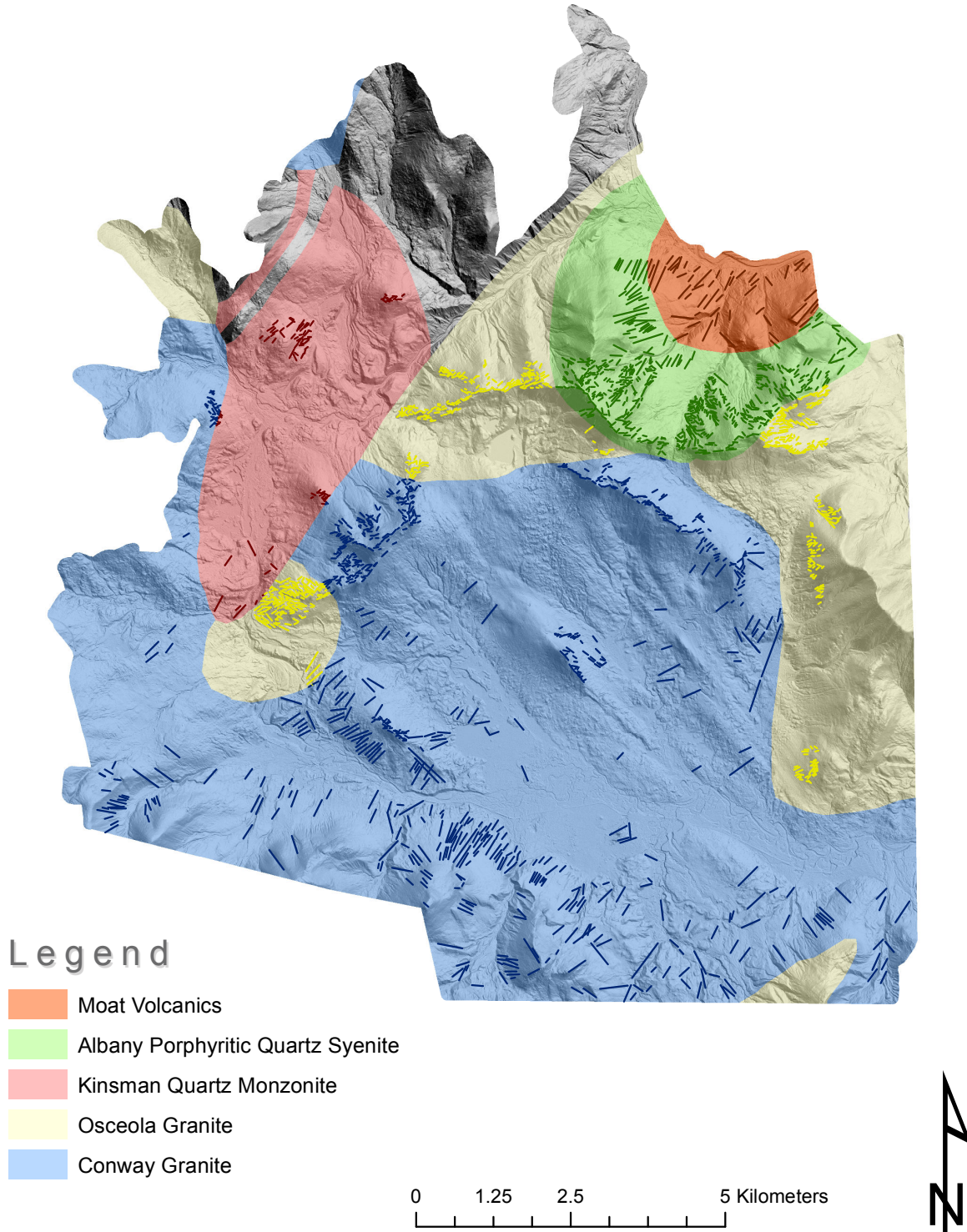


Figure 3.6 Bedrock Lineament Map of the Swift River region, showing the major bedrock units within the study area, and the lineaments drawn within each unit in the same color. The black dots are the locations of outcrops where fracture data was collected

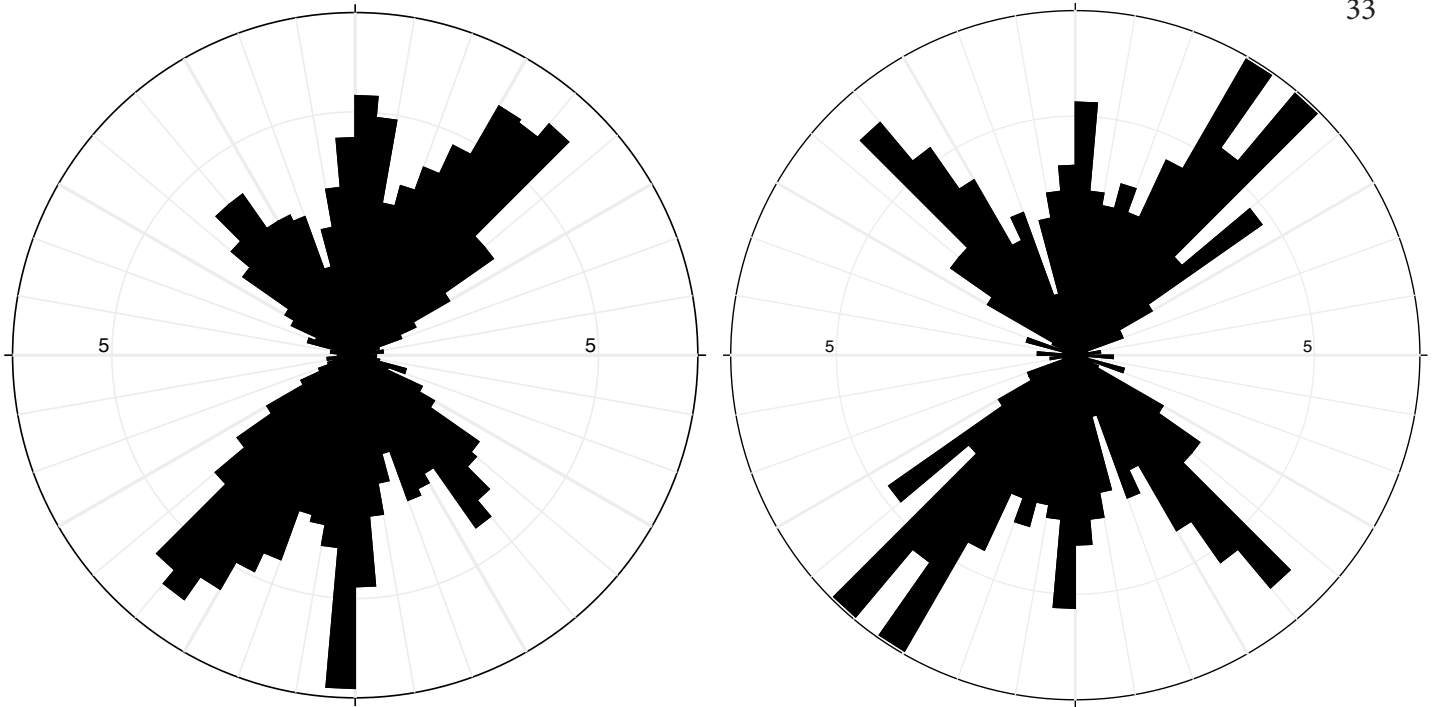


Figure 3.7 (Left) A synoptic plot of all the lineaments within the study area. N= 1624

Figure 3.8 (Right) A roseplot showing the orientations of all of the Conway Granite lineaments.
N = 378

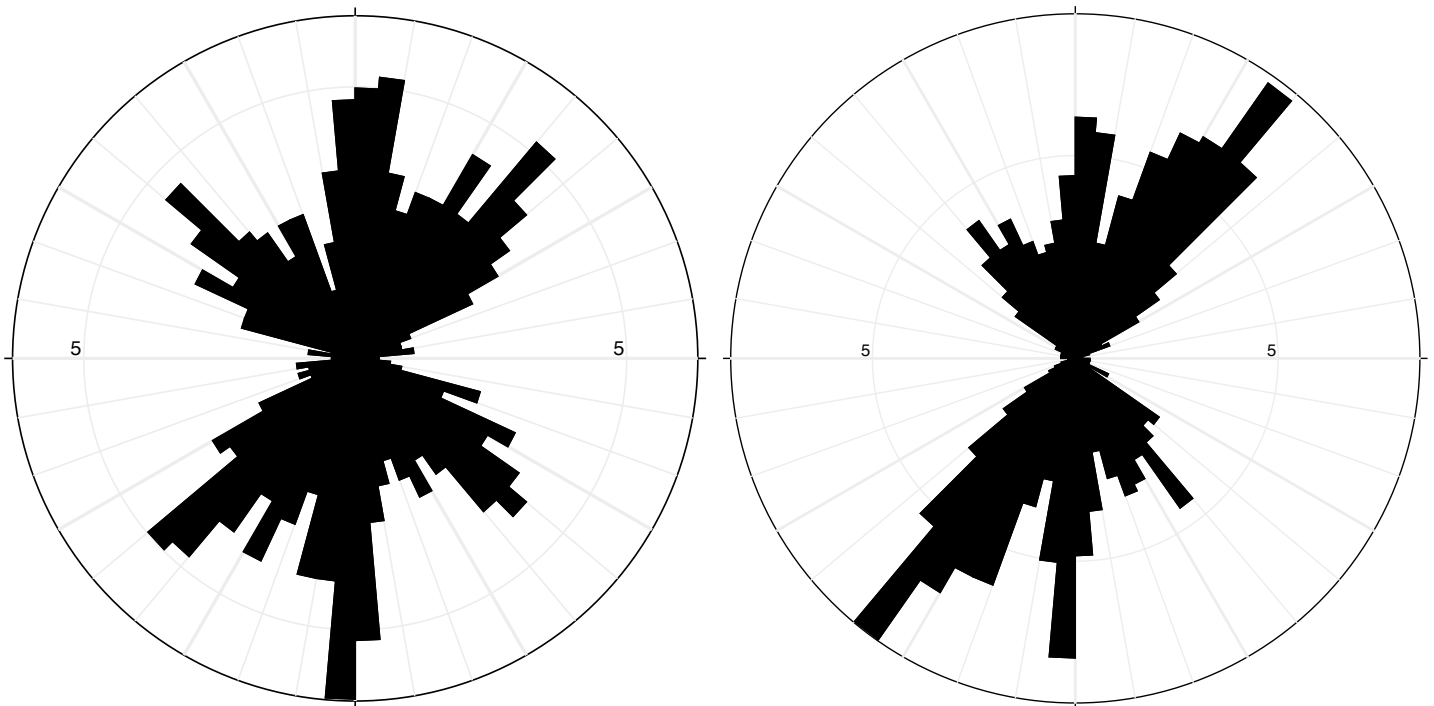


Figure 3.9 (Left) A roseplot showing the orientations of all of the Albany Porphyritic Quartz
Syenite lineaments mapped. N= 463

Figure 3.10 (Right) A roseplot showing the orientations of all of the Osceola Granite lineaments.
N = 555

orientation of NE-SW, with a secondary set at N-S, and a tertiary NW-SE set of lineaments (Figure 3.10). The bedrock fractures share the NE-SW set with an additional WNW-ESE set.

3.2.5 Moat Volcanics

There were 127 lineaments drawn in the Moat Volcanics, with a strong NE-SW dominating orientation, and a weak NW-SE set (Figure 3.11). This has one matching set with the Moat fractures, the NW-SE, although the NNW-SSE set is not found in the lineaments.

3.2.6 Kinsman Quartz Monzonite

There are 101 Kinsman Quartz Monzonite lineaments with dominant NE-SW and NW-SE sets, and a potential N-S set that is much weaker (Figure 3.12). Since no outcrops of Kinsman could be found within the study area, there are no fractures with which to compare this data.

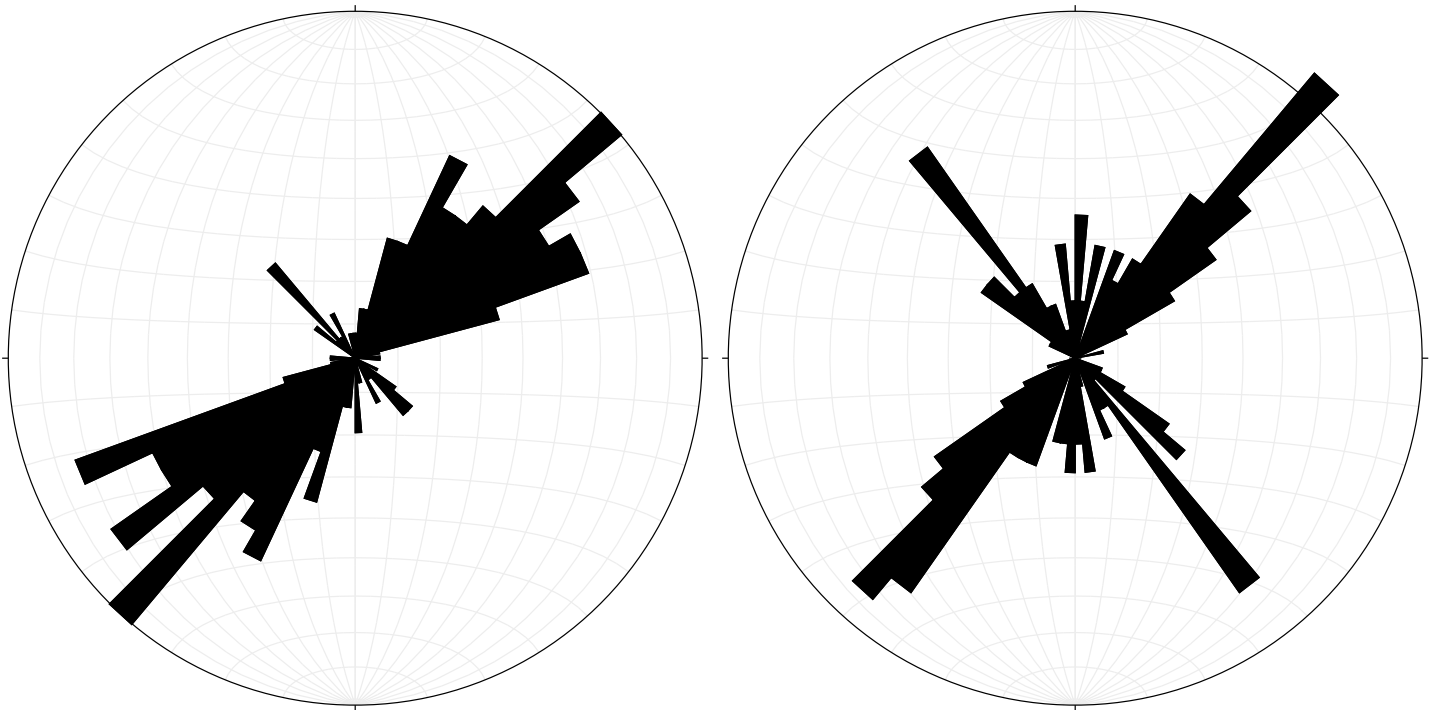


Figure 3.11 (Left) A roseplot showing the orientations of all of the Moat Volcanic lineaments mapped. N= 127

Figure 3.12 (Right) A roseplot showing the orientations of all of the Kinsman Quartz Monzonite lineaments mapped. N = 101

3.2.7 Conclusions

Although further comparisons will be made in section 4.1 of the Discussion, it is clear that some of the joint sets are well represented by the lineament data, while others are not. This may be a result of the scale of the fractures, affecting their visibility on the surface, even with high resolution LiDAR data.

3.3 Geomorphic Landscape Mapping

3.3.1 Overview

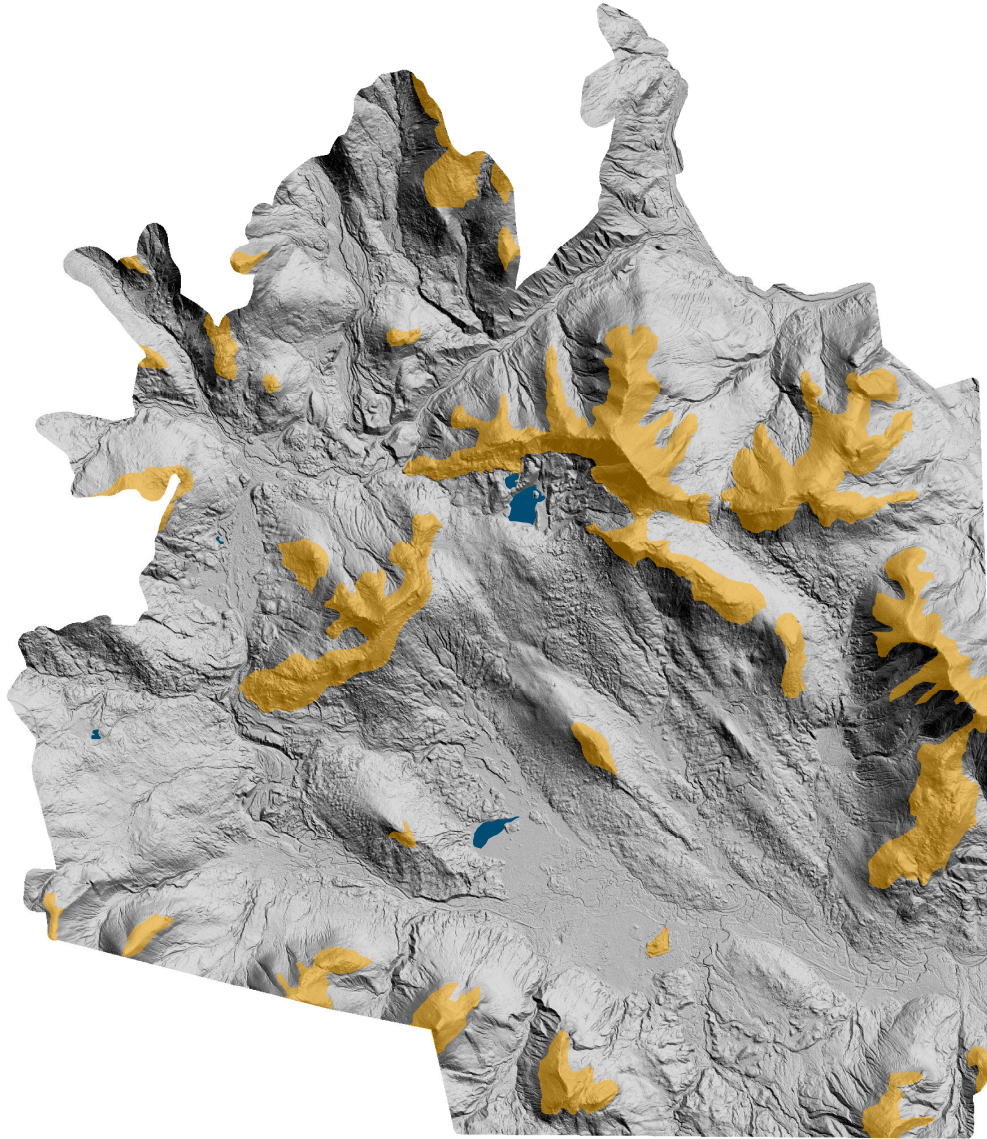
The high-resolution imagery of LiDAR allows for large scale geomorphic classifications in regions of dense forest cover. Based on the characteristics of the hillshade topography, it is possible to delineate the boundaries between major landscape surfaces, whether bedrock, bedrock controlled, glacial till, glacial outwash, or recent fluvial. Other features such as eskers, glacial flow indicators, alluvial fans, and glacial lake terraces can also be mapped using LiDAR.

3.3.2 Bedrock Controlled



Exposed bedrock has a unique signature on LiDAR; it is very sharp and angular, and linear features are often seen. Bedrock controlled regions are covered in a shallow layer of soil or till, giving them a smoother look than exposed bedrock, but linear bedrock features are still visible. Both of these features are typically seen above 600m elevation, although there are some bedrock and bedrock controlled regions well below this. For the most part, within the Swift River study area, bedrock is only exposed along steep ridges and at cliffs, and bedrock controlled areas extend a bit downslope from these. The average slope for this region is 34°. Bedrock or bedrock controlled regions make up 12.5% of the total study area, and are the only places joints are seen within these regions. (Figure 3.13).

Swift River Study Area

Bedrock Controlled



Legend

-  Water
-  Bedrock Controlled

0 1.5 3 6 Kilometers



Figure 3.13 Bedrock and bedrock controlled regions within the Swift River study area.

3.3.3 Glacial Till Deposits

Glacial till deposits are recognized by a smoother surface than the bedrock. There are three distinct till units mapped in this study; smoothed till, hummocky till, and fluvially dissected till (Figure 3.14). The smoothed till typically lies on the stoss side of uplands (the northwest), while hummocky till is found predominantly on the leeward side. Fluvially dissected till is found wherever post glacial streams have cut into this till, usually on steep slopes ($>20^\circ$). All of the till units are principally found between 360m and 600m, but can extend above and below this in places. Glacial till makes up 72.8% of the total study area; with 11.2% hummocky till, 13.8% dissected till, and 47.8% smoothed till.

3.3.4 Glacial Outwash Deposits and Glacial Lakes

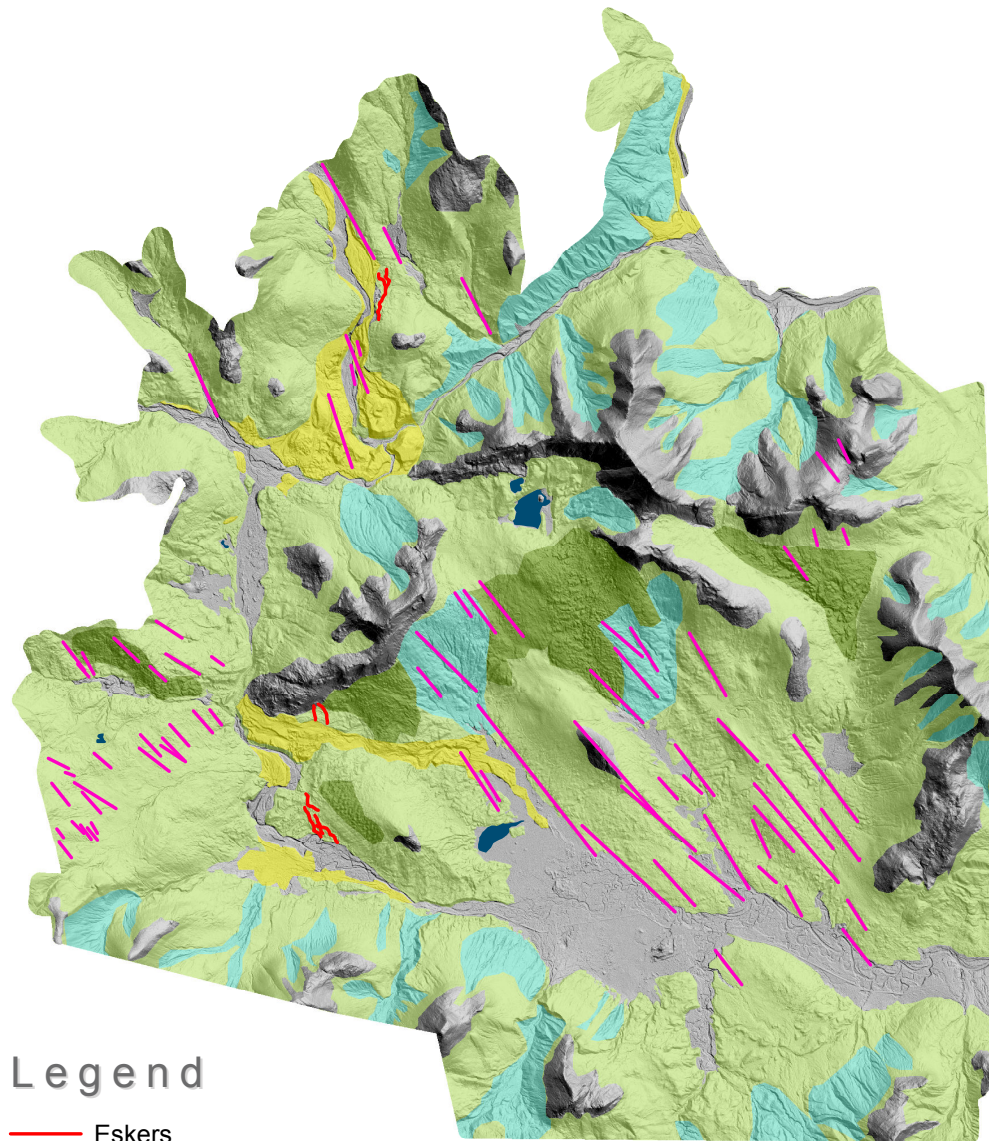
Glacial outwash deposits, whether glacio-fluvial or glacio-lacustrine, are outwash sediments which have not been reworked by more recent fluvial action (Figure 3.14). These polygons make up 5.8% of the total Swift River study area. Included in this region are a series of fifteen terrace levels ranging in elevation from 455m to 574m, although all of the largest terraces are between 483m and 563m (Figure 3.15).

These terraces all lie within the large region of glacial outwash at the northwest of the study area, and many of them are correlated across valley to terraces of the same elevation. The average slope of the terraces is only 4° , so they are quite flat. The largest riser between two adjacent terraces is 58m, between the 513m and 455m terraces, although most of the risers are under 10m. The largest of these terraces is 8.5 hectares in area. None of these terraces were visible on a USGS topographic map, or in any previous map. Only six other terraces are found outside of this region; three at the divide between the Swift and Sawyer Rivers, and three at the eastern edge of the glacial outwash in the glacial spillway.

These terraces are thought to be representative of a paleo-glacial lake that once

Swift River Study Area

Glacial Map



Legend

- Eskers
- Glacial Lineaments
- Water
- Smoothed Till
- Dissected Till
- Hummocky Till
- Glacial Outwash

0 1.5 3 6 Kilometers



Figure 3.14 A map of Glacial features within the Swift River study area including till, glacial outwash, eskers, and glacial lineaments.

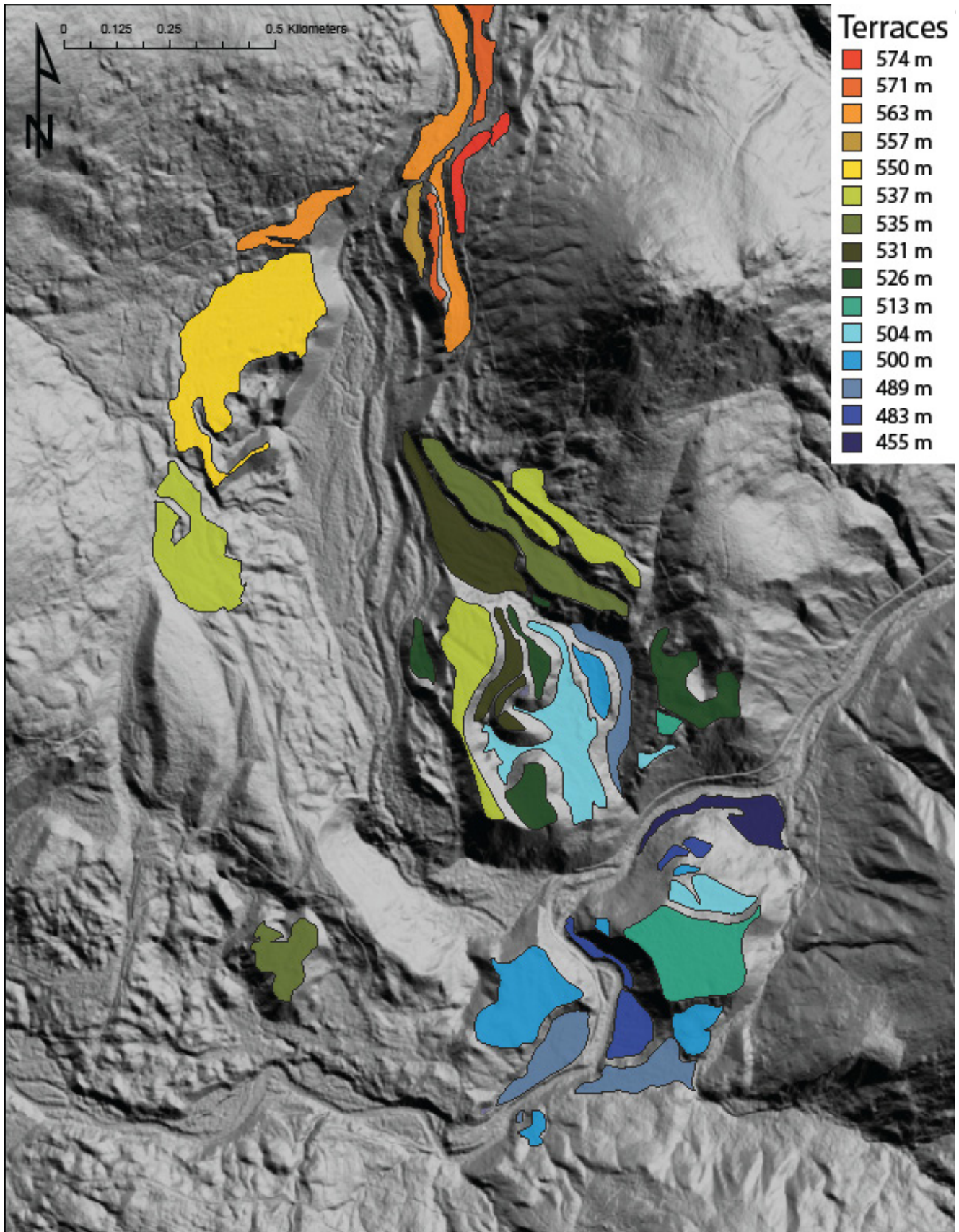


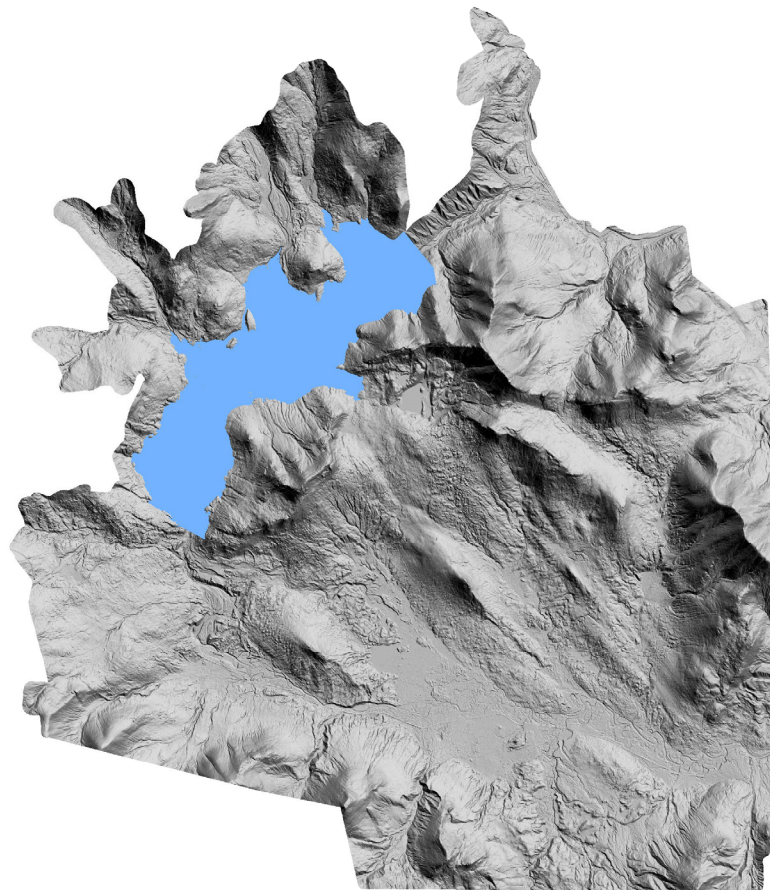
Figure 3.15 A map of glacial outwash terraces found along the Sawyer River in the Swift River study area. Each terrace is thought to represent a different lake level as a glacial lake retreated out of the region. The elevations of each terrace are given in the legend at the upper right.

filled this basin. Each terrace shows the lake surface elevation before the lake level dropped to the level of the next lower terrace. The maximum extent of this proposed glacial lake involved a lake surface elevation of approximately 554m as constrained by the outlets, and any terraces above this elevation are likely a result of a downcut glacial river delta above the lake (Figure 3.16).

A second glacial lake is also being proposed with a maximum lake surface elevation

Swift River Study Area

Glacial Lake Sawyer



0 1.25 2.5 5 Kilometers



Figure 3.16 A map of the maximum extent of the proposed Glacial Lake Sawyer, as determined by terrace elevations and outlets.

of 383m, the elevation of a paleo-shoreline (Figure 3.17). This lake does not have any glacial outwash terraces, as the entire lake floor has been reworked by more recent fluvial action, characterized by the many criss-crossing braided river segments. The only remaining clue to its existence is the well developed shoreline.

3.3.5 Glacial Eskers

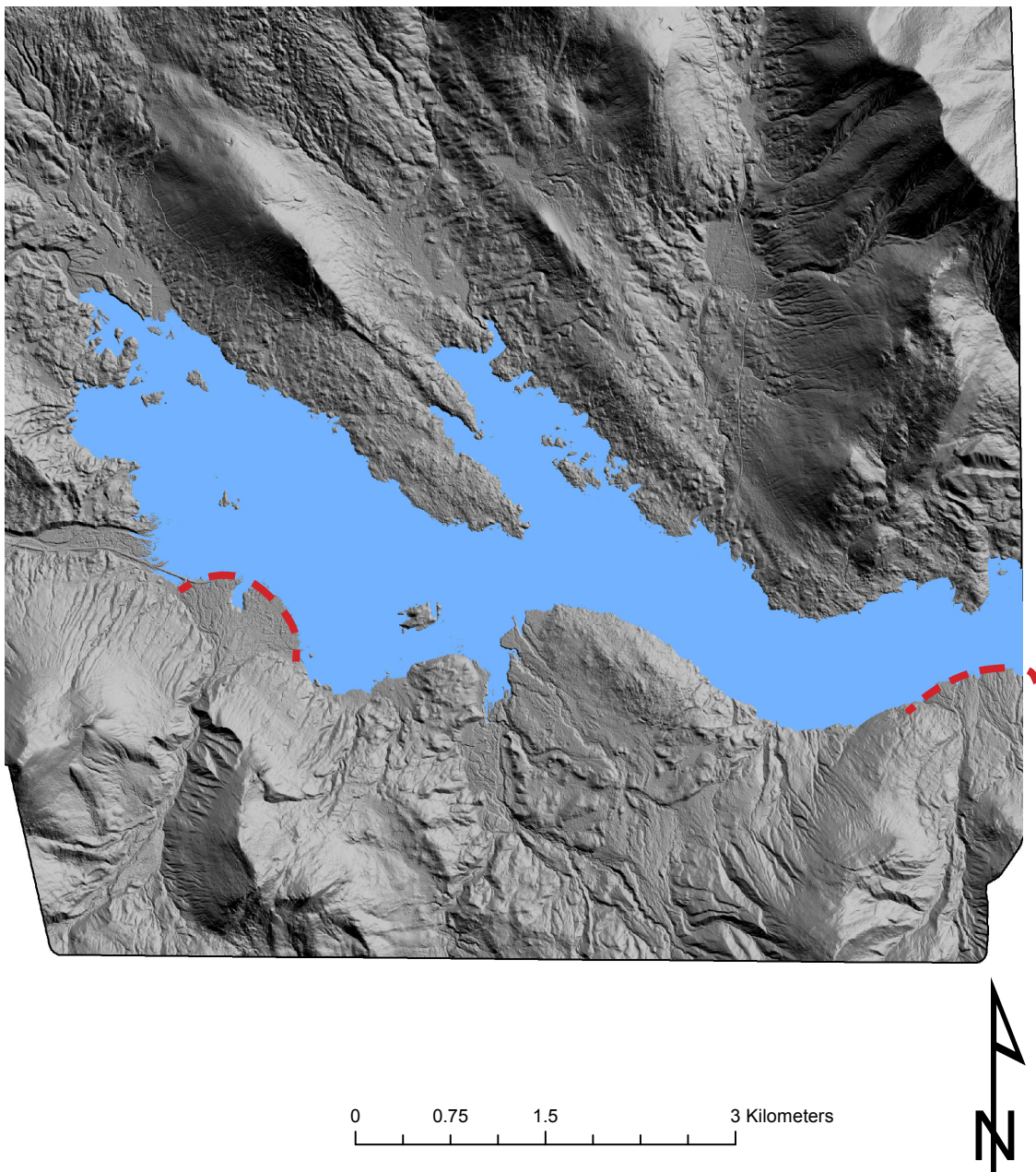


Figure 3.17 Figure showing the proposed location of Glacial Lake Swift. The blue polygon represents the glacial lake surface, as it matches up with shoreline features around the lake. Two alluvial fans are marked with red dashed lines.

Eight different eskers have been located within the study area (Figure 3.14). The longest of these is 500 m, while the rest are closer to half that length. They are all located along the edges of more recent fluvial channels, either the Sawyer or Swift Rivers, but high enough above these channels that they are not affected by erosion of these channels. They all lie on top of the smoothed till polygons, although the lowest of these eskers is at 405m and the highest is approximately 600m in elevation, so elevation does not seem to influence esker distribution.

3.3.6 Glacial Lineaments

There are several glacial features that are manifested as lines on the earth's surface. These include glacial striations, drumlins, and other glacial streamlined features. A lineament map was created in a similar fashion to the bedrock lineament map, including 57 lineaments that represent these types of features (Figure 3.14). The average orientation of these glacial lineaments is 310°. This orientation reflects glacial flow direction as the ice sheets create linear features in the direction of their flow.

3.3.7 Post-Glacial Alluvial Deposits

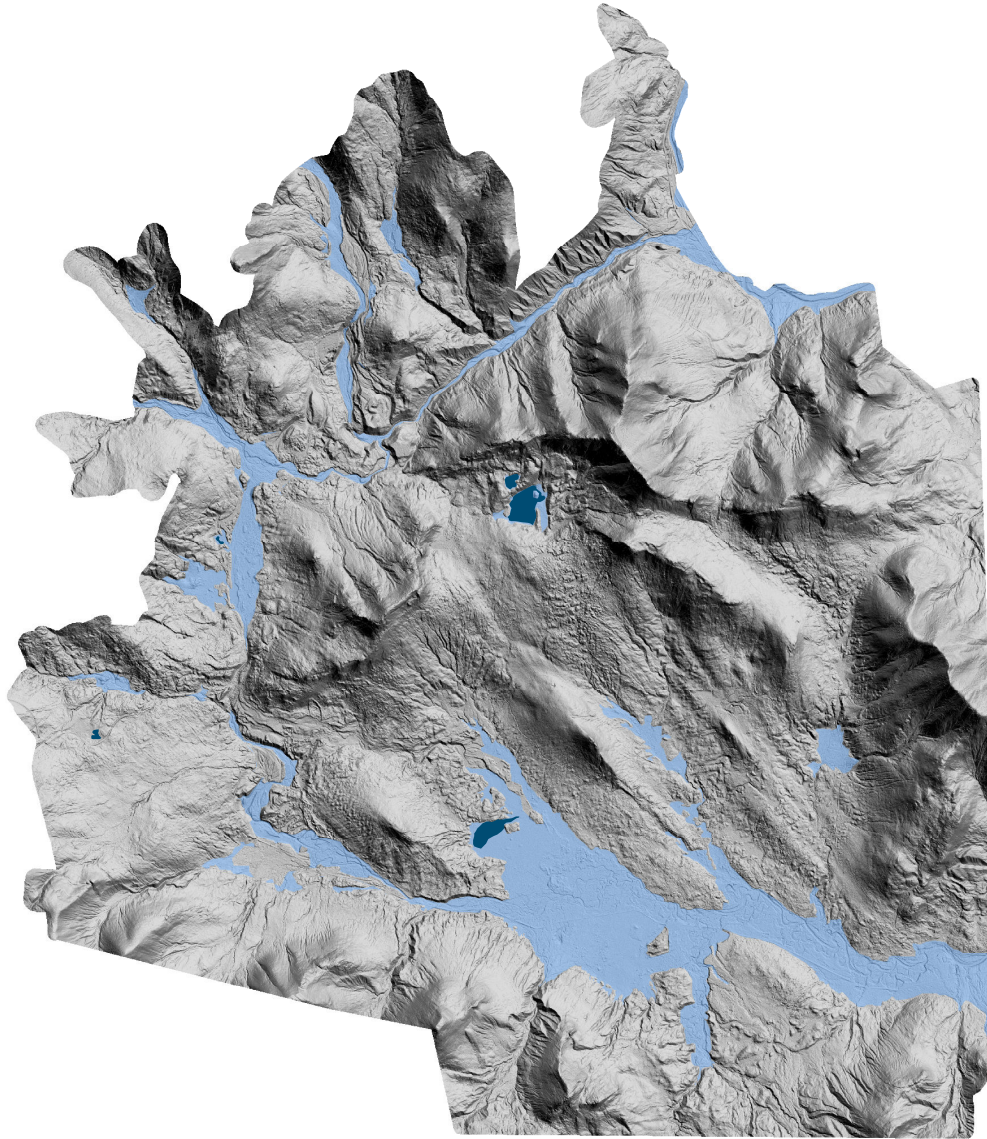
Upon the "filling" of Glacial Lake Swift to 383m, two alluvial fans become visible (Figure 3.17). These fans had not been mapped in any previous studies, but both are very good examples; coming down from the steep mountains to the south out onto the floodplain. The western of the two alluvial fans has been quarried for gravel, so although not recognized as an alluvial fan, it was recognized as a resource. Although post-glacial in origin, these features likely followed glaciation, and are not actively growing today as they are densely vegetated.

3.3.8 Holocene Fluvial Deposits



Holocene fluvial deposits include any sediment deposited by streams, rivers, or other bodies of water following the last glaciation (Figure 3.18). Much of this sediment is reworked glacial sediment, either till or outwash, but has since been eroded since by water. These eroded areas include braided rivers, large flat floodplains, and oxbows. For this classification only fluvial-depositional features are included, and fluvial erosional features that are found dissecting till on many of the steep slopes are excluded and are instead designated as dissected till. These fluvial depositional features account for 9.9% of the study area. They occur mostly below 400m; although, the upper reaches of both the Swift and Sawyer Rivers extend up to approximately 550m of elevation.

Swift River Study Area

Post-Glacial Features



Legend

-  Water
-  Post-Glacial Fluvial

0 1.5 3 6 Kilometers



Figure 3.18 Map showing the post-glacial fluvial polygons within the Swift River study area. These represent areas of sediment that are reworked and deposited following the last glaciation.

Chapter 4: Discussion

4.1 LiDAR Lineament Data as a Proxy for Bedrock Joint Sets

4.1.1 Introduction

The first lineament analyses of New England were conducted in the late 1980s, examining the relationship between topographic lineaments and the bedrock beneath (Shake & McHone, 1987). At the same time, the structural studies of New England were focused on hard rock measurements, and the study of orogenic events, while petrology studies were focused on the evolution of magma within plutons (McHone & Shake, 1992). It wasn't until more recently (the 1980s and 1990s) that the relationships between joint sets and magmatism in New England were correlated at all; and today, the strong association between extensional structures and magmatism in this region is well documented both in the Northeastern US and in Quebec (Faure et al., 2006). Since it has been shown that modern lineament studies are capable of showing structural features, a remote lineament analysis of the Swift River region could potentially be correlated with both the paleo-stress history of New England and the related igneous intrusions (Shake and McHone, 1987; Mabee et al., 1994).

4.1.2 Overall Datasets

In order to validate the effectiveness of a LiDAR based lineament study in the Swift River study area, the drawn lineaments were compared against collected bedrock joint sets. Of the 400 joints measured within the Swift River study area, three strike orientations dominated, a NE-SW set with an average strike of 41° and dip of 84° , a WNW-ESE set with an average strike of 106° and dip of 85° and a NNW-SSE set with an average strike of 165°

and dip of 85° (Figure 4.1). In comparison, the 1,396 retained bedrock lineaments (glacial lineaments were removed from this dataset) can also be paired down to three dominant orientations: a NE-SW set averaging 33° , a N-S set with an average strike of 4° , and a NW-SE set that had an average orientation of 141° . Note that in the stereonet plot the lineament data runs directly through the 90° center point since a dip value cannot be derived for a lineament based off of LiDAR data.

Plotted together, the NE-SW sets are quite similar, only 8° off from one another, and the NW-SE lineament set has moderate correlation with both the N-S joint set, offset by 18° , and the NNW-SSE joint set with 24° offset (Figure 4.1). The WNW-ESE joint set does not have any similar pattern in the lineament data. Overall, it could be said that the lineaments and the joint sets show moderate correlation. The NE-SW set was dominant in both of these datasets, although the strikes were offset by 8° .

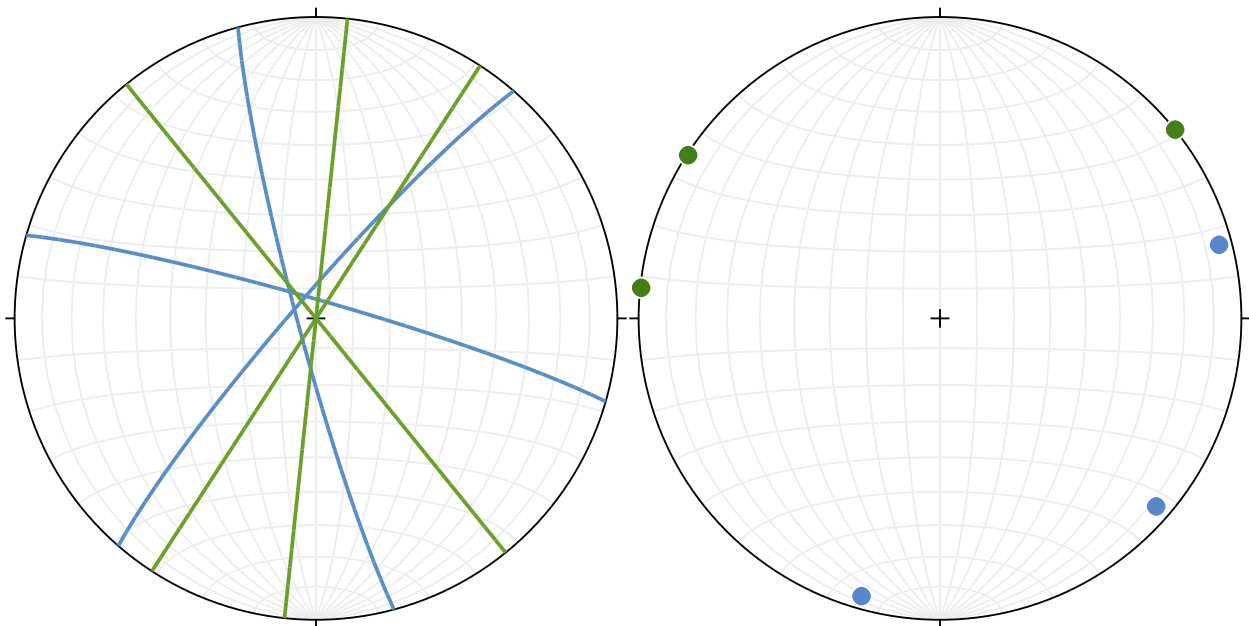


Figure 4.1 A Roseplot at left showing the three dominant joint sets overall in blue, and the three dominant lineament orientations overall in green. The NE-SW sets of each are well matched, and the NNW-SSE or the N-S joint sets and the NW-SE lineaments perhaps show some correlation. The figure to the right shows the poles of each of these planes.

4.1.3 By Bedrock Unit

Similarly, when examined individually by bedrock unit, some of the joint sets and some of the lineament sets align well, while others do not. For the Conway Granite the premier joint orientations were 48° and 163° , while the lineaments were 39° , 137° , and 3° (Figure 4.2). The NE-SW trending sets were only 7° apart revealing a strong correlation while the NNW-SSE joint set is offset from the NW-SE and N-S lineament sets by 26° and 20° respectively- meaning they may represent similar structures, but are only moderately correlated. The fact that the joints split the difference between these two lineament sets may suggest a varying orientation over the study area since lineaments were found up to 4km from the nearest measured fracture site in that unit.

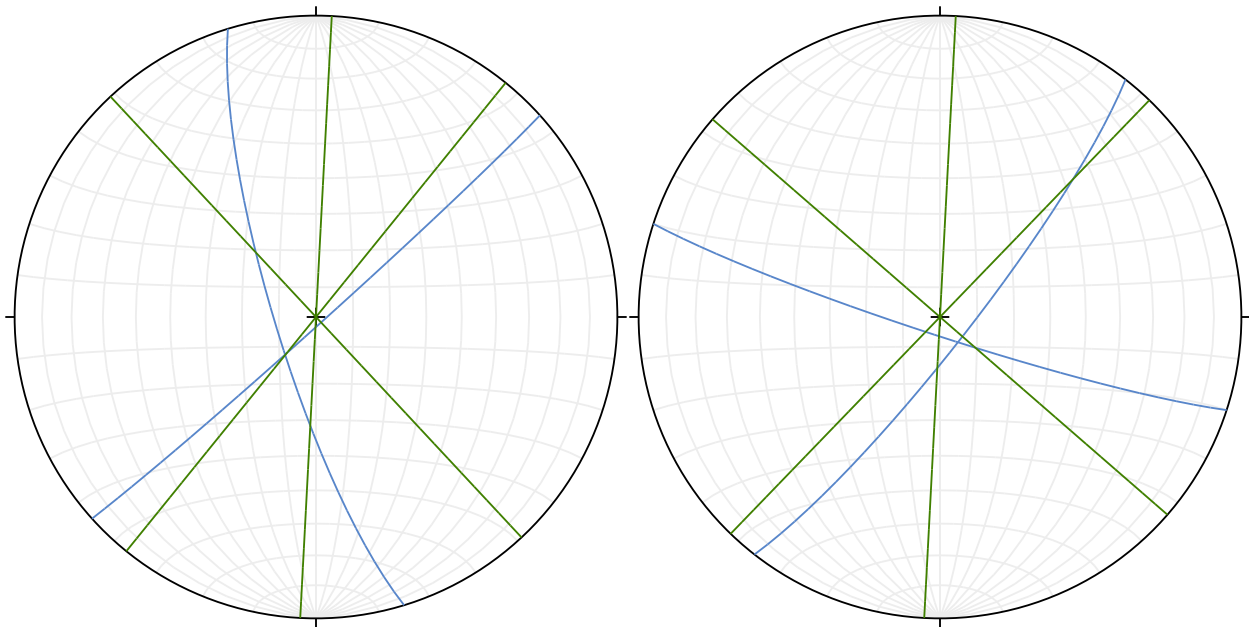


Figure 4.2 (Above Left) A Roseplot at left showing the two dominant joint sets of the Conway Granite in blue, and the three dominant lineament orientations of this bedrock unit in green. The NE-SW sets of each are well matched, and the NNW-SSE joint set and NW-SE lineament are somewhat similar, but the N-S lineaments are not correlated to a dominant joint set.

Figure 4.3 (Above Right) The Roseplot at the right shows the two dominant joint sets of the Albany Porphyritic Quartz Syenite in blue, and the three dominant lineament orientations of this bedrock unit in green. The NE-SW sets of each are once again well matched, the WNW-ESE joint set and NW-SE lineament are quite similar, and again the N-S lineaments are not correlated to a dominant joint set.

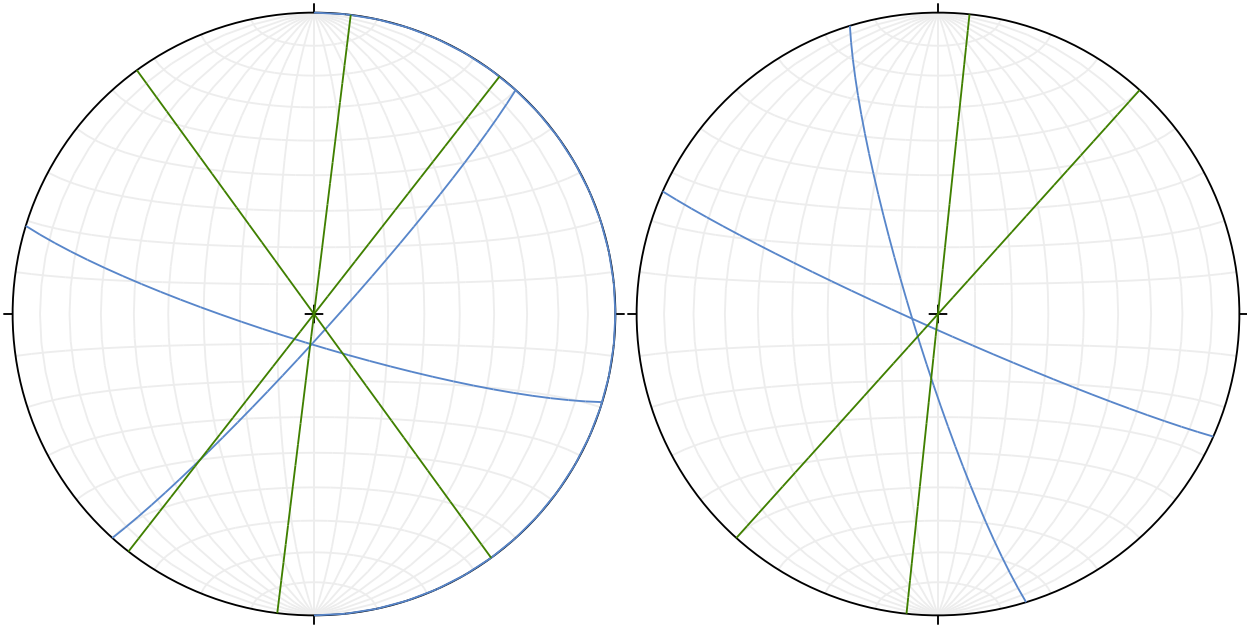


Figure 4.4 (Above Left) A Roseplot at left showing the two dominant joint sets of the Osceola Granite in blue, and the two dominant lineament orientations of this bedrock unit in green. The NE-SW sets of each are extremely well matched, the WNW-ESE joint set and NW-SE lineament are quite different, but potentially related, and the N-S lineaments are not correlated to a dominant joint set in the Osceola formation.

Figure 4.5 (Above Right) This Roseplot shows the two dominant joint planes in the Moat Volcanics in blue, as well as the two averaged dominant lineaments for this rock type in green. Unlike the other rock types, there is no reasonable correlation between any of the joint planes and lineaments. Perhaps one could be drawn between the N-S lineaments and the NNW-SSE joints, but it is not very strong.

The Albany Porphyritic Quartz Syenite also illustrates strong correlation between its NE-SW joints (average strike of 38°) and lineaments (average strike 44°), with an offset of only 6° (Figure 4.3). The WNW-ESE joint set (strike of 108°) and the NW-SE lineaments (strike of 131°) again show a moderate correlation of 21° , and the N-S lineaments (3°) are not correlated with any joint set.

The Osceola Granite, like the other bedrock units, has a strong association between the NE-SW joints (42°) and lineaments (38°), with just 4° separating the two (Figure 4.4). There is potentially weak correlation between the WNW-ESE joints (107°) and NW-SE lineaments (144°) as they are a full 37° off from one another, and the N-S lineaments (7°) have no equivalent among the joint sets.

The Moat Volcanics are unlike the other rocks in that there is no NW-SE joint set, although this lineament orientation (42°) still exists, but without good correlative joints (Figure 4.5). The strongest correlation in the Moat Volcanics is only moderate, with 23° separating the N-S lineaments (6°) and the NNW-SSE joint set (163°). The WNW-ESE joint set (114°) also lacks any correlated lineaments.

4.1.4 Analysis

The lineament data only represents some of the joint planes accurately, while some joint planes lack a corresponding lineament set, and some lineaments lack a corresponding joint plane. The orientation that showed the strongest correlation between datasets was the NE-SW striking planes, with an 8° offset overall, and even less offset for each of the bedrock units. This is also the dominant orientation for each, making up 43% of the joint planes, and 31% of the lineaments. For the secondary and tertiary joint orientations there is moderate to poor correlation to the secondary and tertiary lineament orientations. As a result, for the Swift River study area, lineaments are a good proxy for the dominant extensional features, but they do not display subordinate features well.

This could be a result of limited sampling points that do not cover the entire breadth of the sampling area, and since the LiDAR lineaments cover the entire region, they might be offset due to a gradual shift in orientation across the study area. In order to check for this, much more strike and dip data would need to be collected at a much higher spatial resolution, necessitating the use of more outcrops than were found in this study. Also, perhaps the N-S lineament is at a more regional scale than the others, and therefore wouldn't show up as well at an outcrop. This could explain the relative lack of N-S fracture planes.

Interestingly, this study appears to be one of the first attempts to directly correlate joint orientations with lineament orientations from LiDAR in New England. There are many studies that tie the presence of lineaments to the presence of fractured bedrock,

particularly in relation to hydrologic well drilling (Mabee et al., 1994; Kim et al., 2004; Corgne et al., 2010). Mabee et al. (1994) found that wells positioned within 30m of a major lineament were more likely to have a high water yield than wells placed without this methodology. This paper attributes this correlation with the proximity of fractured bedrock to the lineament. It does not address however the ability of a lineament to predict the orientations of these bedrock fractures (Mabee et al., 1994).

Other studies, such as Shake and McHone (1987) and McHone and Shake (1992) only examine macro-scale lineaments, exceeding 20km. It was found that generally these lineaments lined up well with mapped faults and bedrock fracture sets, although they mentioned that the NE-SW trending lines they found in New Hampshire did not directly tie to the geology (McHone and Shake, 1992). The reasoning for this very large scale was twofold: first their study area included a range extending from the Adirondack mountains in New York to the White Mountains in New Hampshire, so it too massive to analyze the hundreds of thousands of smaller lineaments that likely existed. Also, they were limited by the resolution of the datasets at that time; they created hillshades by literally illuminating four plastic 1:250,000 raised relief maps of the region with directional lights (Shake and McHone, 1987).

Another lineament study, conducted by the USGS over the entire State of New Hampshire, used higher resolution topographic information and imagery than was available to Shake and McHone (1987; 1992) (Ferguson et al, 1998; Ferguson et al., 1999). This study found lineaments ranging in size from just under 500m to ones well over 10km using a 1:48,000 working resolution. Three dominant sets of lineaments from this study can be found within the Swift River study area; a NE-SW set, a NW-SE set, and a N-S set (Figure 4.6).

These are the same three orientations found in the LiDAR lineament analysis, which suggests that these orientations may represent real features. Although many of the individual lineaments are different, likely due to the differing resolutions and working

scales, the two studies are clearly identifying the same sets of lineaments. Due to the scale difference, it is possible that the LiDAR derived lineaments represent the surficial expression of fractures while the Ferguson et al. (1998) lineaments show subsurface linear features.

One feature that differs between the two studies is the relative abundance of NW-SE lineaments. In the Ferguson et al. (1998; 1999) studies there are many large lineaments running NW-SE (Figure 4.6). These lineaments were removed from the bedrock portion of the LiDAR lineament data, as they were seen to represent glacial streamline features, not bedrock features. Without the ability to penetrate tree canopy it would have been difficult for the Ferguson et al (1998;1999) studies to differentiate the two without field work.

With a workable resolution in excess of 1:15,000 and an approximately 13km by 13km study area, the LiDAR hillshades used in the Swift River region were used to produce lineaments ranging from just under 10m to 1.5 km. It is logical that larger lineaments from the previous studies would only represent major bedrock features, while smaller lineaments could vary much more. That being said, the Ferguson et al. (1998;1999) maps show strong correlation with the LiDAR lineament data.

4.1.5 Conclusions

For future studies, at least in this region of the White Mountains, LiDAR based lineaments are a good proxy for the dominant fracture orientation, but do not accurately represent all of the joint patterns found when measuring the bedrock at outcrops. It would be impossible to accurately differentiate bedrock units within the study area based on lineament data without significant field work.

4.2 Reconstructing the Tectonic History

4.2.1 Introduction

Swift River Study Area

NH Lineament Analysis 1998 and 1999

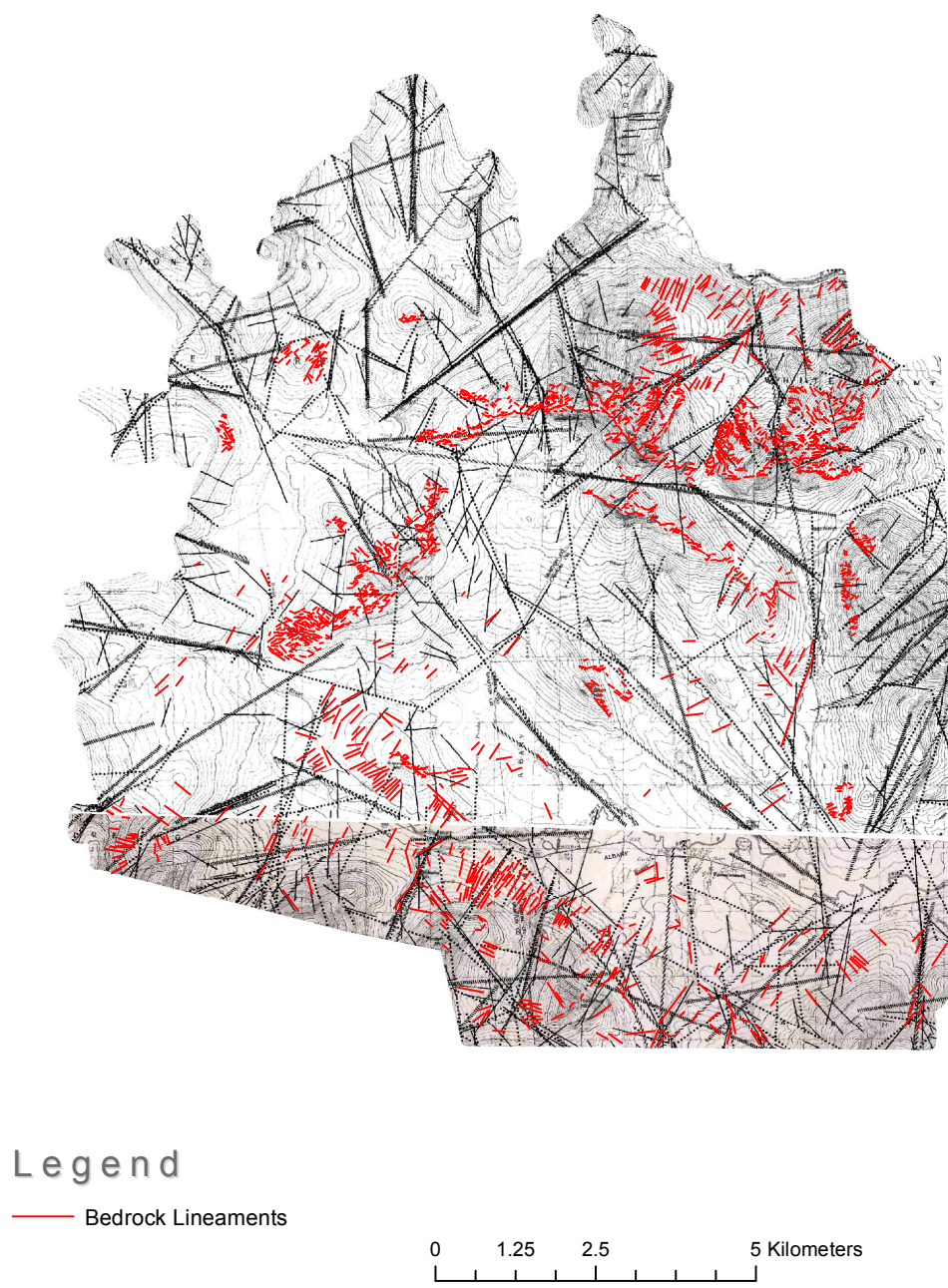


Figure 4.6 The two lineament maps created for the USGS cropped to the Swift River study area (Ferguson et al, 1998; Ferguson et al, 1999). The 1998 map lies to the south while the 1999 map is to the north. Overlain in red are the LiDAR derived bedrock lineaments from this study.

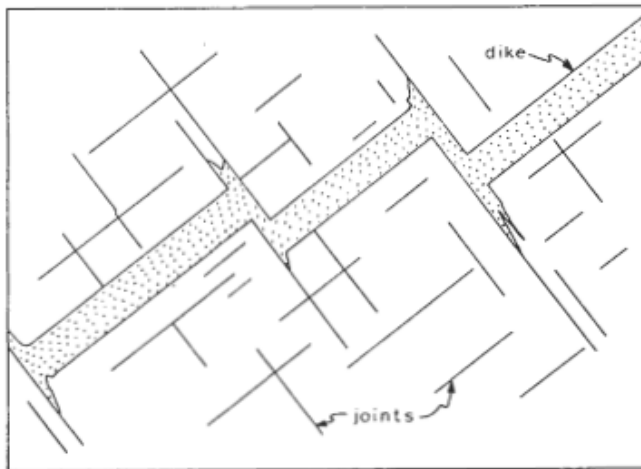


Figure 4.7 Image from McHone's (1988) paper, illustrating what extensional features would form from a given stress orientation, and in which direction these features would propagate (McHone, 1988).

Joint Sets, dike swarms, and faults in the Appalachian Mountains have been used to reconstruct the paleo-stress history of the region (McHone & Butler, 1984; McHone, 1988; Faure et al., 2006). Magma takes the path of least resistance to the surface, and this is often in fractures opened up due to extensional stress. Once this magma cools in the fracture, it forms a dike, and remains an indicator of the paleo-stress at a given time. Although joint planes also open up due to extension, dikes are more useful as they offer a rock product that allows for radiometric dating (McHone, 1988). Once a dike swarm has been dated, it can be inferred that undated joints and dikes of the same orientation were created in the same paleo-stress environment, and at the same time.

Joints and dikes propagate perpendicular to an extensional stress as represented by σ_3 in Figure 4.7. Some fractures will also form parallel to the σ_3 direction, but these are typically smaller and less common. This type of extensional regime, where joints form perpendicular to the direction of least compression (σ_3) is predominantly found in regions of tectonic plate movement (McHone, 1988).

As a result, dike swarms in certain regions of the Appalachian Mountains have undergone similar stresses, and therefore have similar orientations (Figure 4.8). The central New England portion of the Appalachians, including the White Mountains and the

Joint Sets, dike swarms, and faults in the Appalachian Mountains have been used to reconstruct the paleo-stress history of the region (McHone & Butler, 1984; McHone, 1988; Faure et al., 2006). Magma takes the path of least resistance to the surface, and this is often in fractures opened up due to extensional stress. Once this magma cools in the fracture, it forms a dike, and remains an indicator of the paleo-stress at a given time. Although joint planes also open up due to extension, dikes are more useful as they offer a rock



Figure 4.8 A map from McHone's (1988) paper, illustrating the dike orientations along the Appalachians. Rose diagram C represents Central New England, including the White Mountains and the White Mountain Magma Series (WMMS) (McHone, 1988). The red circle represents the location of the Swift River study area.

Swift River study area have a very strong NE-SW orientation, as collected from 239 dikes (McHone, 1988).

4.2.2 Swift River Paleo-stress Reconstruction

Using the same methodology as McHone (1988), it is possible to recreate the dominant stress fields that created the measured joint sets within the Swift River study area. Since the joint system is dominated by the NE-SW striking joints, this is the joint set that will be used to recreate the paleo-stress. The sigma 3 direction will be perpendicular to the 41° striking average joint orientation, or at 131° (Figure 4.9).

There are several possible methods of creating these secondary and tertiary joint sets, namely that they each represent a mode 1 joint for different stress fields, or that two sets are conjugate pairs for a single stress event (Fossen, 2010). Since the secondary WNW-

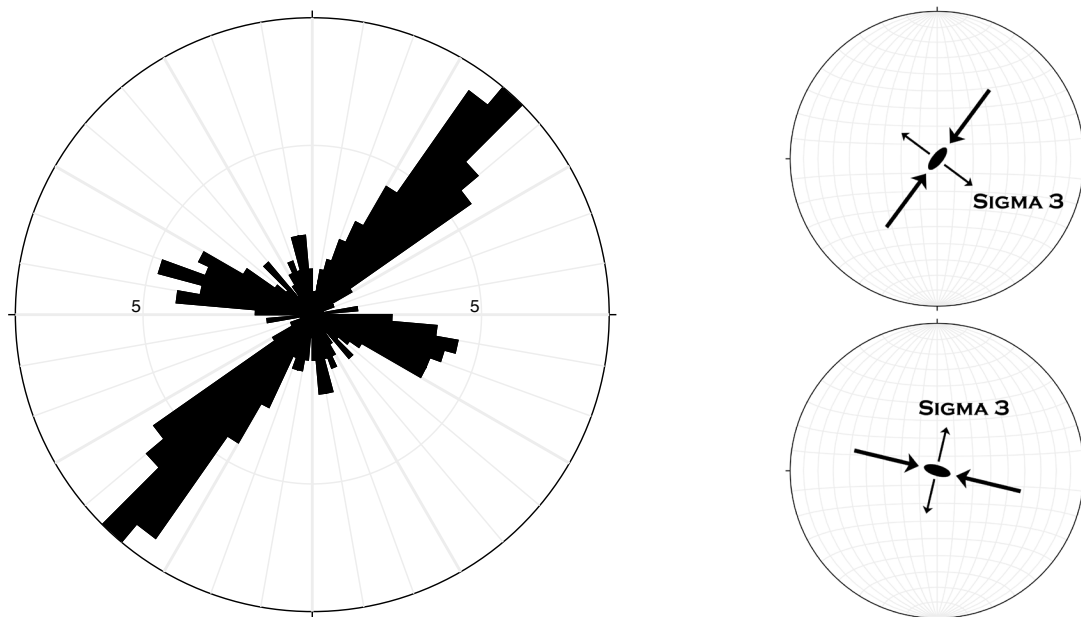


Figure 4.9 A roseplot showing the joint data collected from 400 planes within the Swift River study area is on the left, while to the right are two stress diagrams, showing the stress directions associated with each of the two dominant joint sets. The stress field to the upper right represents the NE-SW striking joints, while the lower right stress diagram represents the WNW-ESE joint set. Sigma 1 and 2 are interchangeable here, with one of them pointing directly into the page, and the other lying as shown. Sigma 3, the direction of lowest stress (i.e. extension) lies perpendicular to the strike of the joints, or at 131° for the NE-SW joints, and 16° for the WNW-ESE joints.

ESE joint set made up a significant portion of the measured joint sets it too was analyzed for paleo-stresses. It yielded a sigma 3 direction of 16° (Figure 4.9).

4.2.3 Paleo-Stress Analysis

The two dominant joint orientations of the Swift River study area are almost identical to the orientations of joints found in McHone's study of Appalachian tectonics (1988) (Figure 4.10). Although the secondary WNW-ESE joint set resembles dikes measured in Southern Quebec and Northern Vermont, not in New Hampshire, the distance between the Swift River study area and these regions is not so great as to make it impossible for these stresses to come into play.

This can be seen in figure 4.11, where the two sigma 3 directions found in the Swift River study area (Figure 4.9) are shown on a map of New England. The Swift River study area, although lying south of the Salem-Rangeley lineament which is used as the stress field divider by McHone, is quite close to the boundary between the two. Therefore it is quite plausible that although the Cretaceous aged extension here was dominated by a sigma 3 orientation of somewhere around 131° , it was still feeling the effects of the 16° sigma 3 stress field to the north.

This in turn can be compared to the more recent Northern Appalachian paleo-stress analysis conducted by Faure et al. (1996; 2006). The Faure et al. (1996; 2006) analysis is also based primarily upon dike trends for the New England area, and these two papers determined the same general sigma 3 directions as McHone (1988), although instead of a NNE-SSW set, Faure et al. (1996) found a more N-S stress field (Figure 4.12, 4.13). Although there is some variation in the N-S stress fields proposed by Faure et al. (1996; 2006) and McHone's (1988) NNE-SSW fields, they are similar enough to be considered equivalent. They are also quite similar to the secondary sigma 3 orientation in the study area. The dominant NW-SE sigma 3 orientation is very similar between the two papers, and matches the dominant sigma 3 orientation determined for the study area.

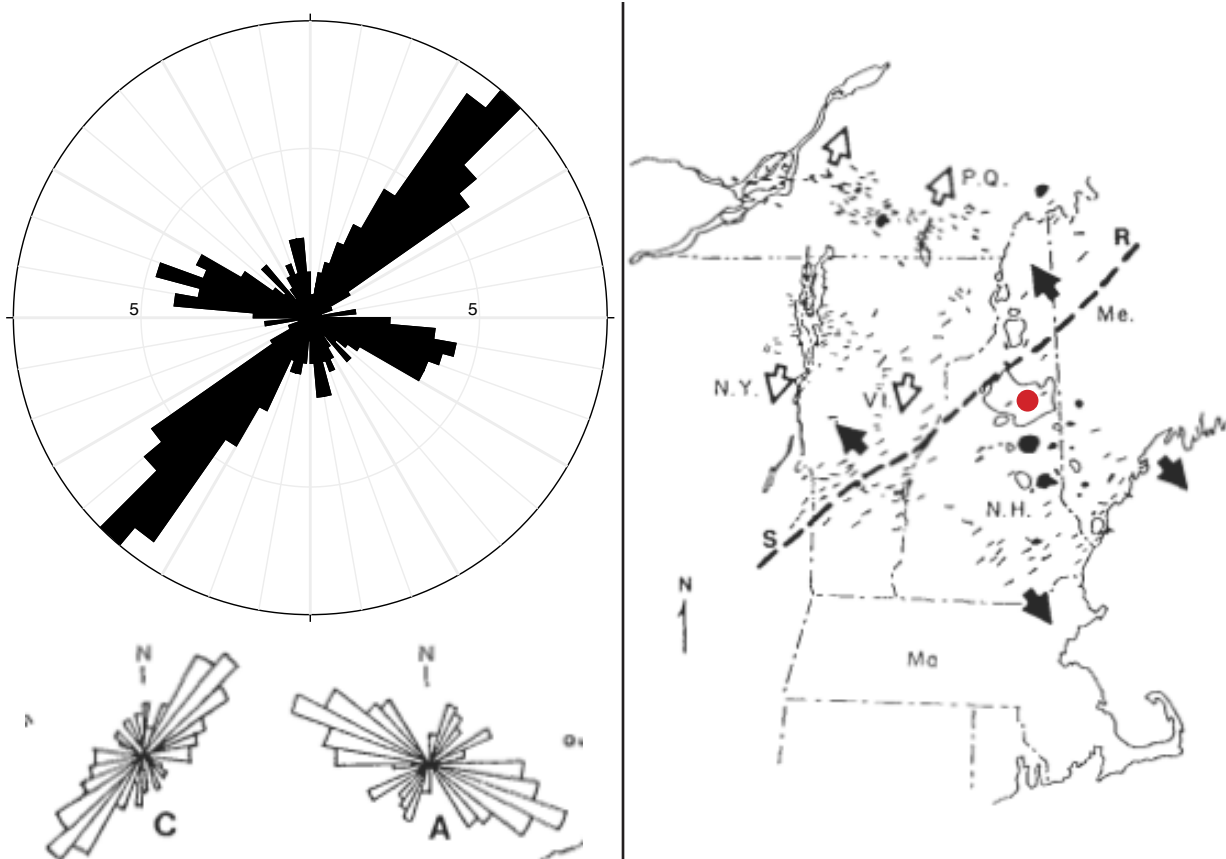


Figure 4.10 (Left) Roseplot showing the joints measured in the Swift River study area (top) compared with two roseplots from McHone's study (1988). Roseplot C represents dikes in central and eastern New England. Roseplot A represents dikes in southern Quebec and Northern Vermont.

Figure 4.11 (Right) Map showing the dominant paleo-stress σ_3 directions, as inferred by McHone (1988). The solid arrows represents stress fields found south of the Salem-Rangeley lineament (dashed line), while the hollow arrows represent the stress fields found north of the S-R lineament. The red circle represents the location of the Swift River study area.

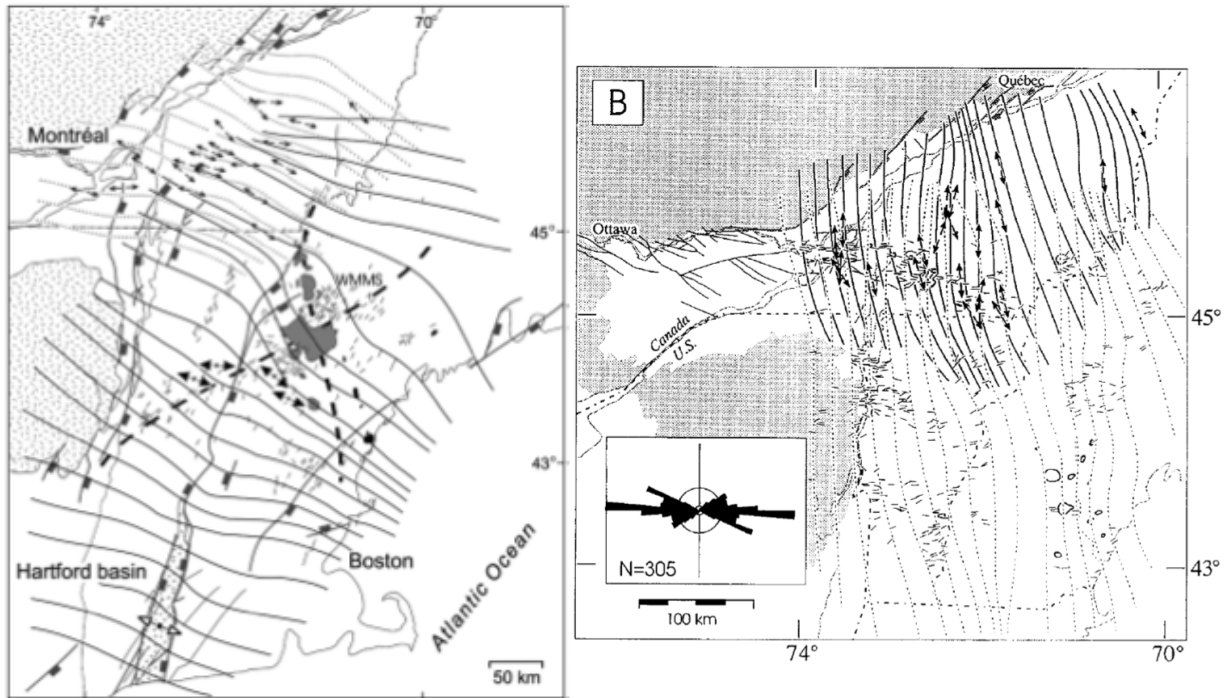


Figure 4.12 (Left) A map from Faure et al. (2006) showing the Jurassic paleo-stress sigma 3 directions in New England. The sigma 3 directions vary somewhat, but predominantly run NW-SE.

Figure 4.13 (Right) A Map from Faure et al. (1996) showing the Cretaceous paleo-stress sigma 3 directions in New England, New York, and southern Canada. These stress directions run N-S.

4.2.4 Tectonic Significance of Paleo-stress

As mentioned in section 4.2.1, dike forming extensional regimes are often related to large scale tectonic activity (McHone, 1988). In this instance, these Late Triassic- Early Jurassic extensional features are a result of the breakup of Pangea, and rifting of the Atlantic Ocean (McHone, 1988; Faure et al, 2006). The orientation of the extensional features is approximately parallel to the rifting Atlantic Ocean at that time (Figure 4.14). As can be seen in this map, the extensional dikes run almost parallel to the rift, but since the rift itself isn't straight, this variation is translated into the dike orientations causing the local variations in stress fields seen in New England.

Eusden et al. (2011) matched fracture orientations found in the Great Gulf with their

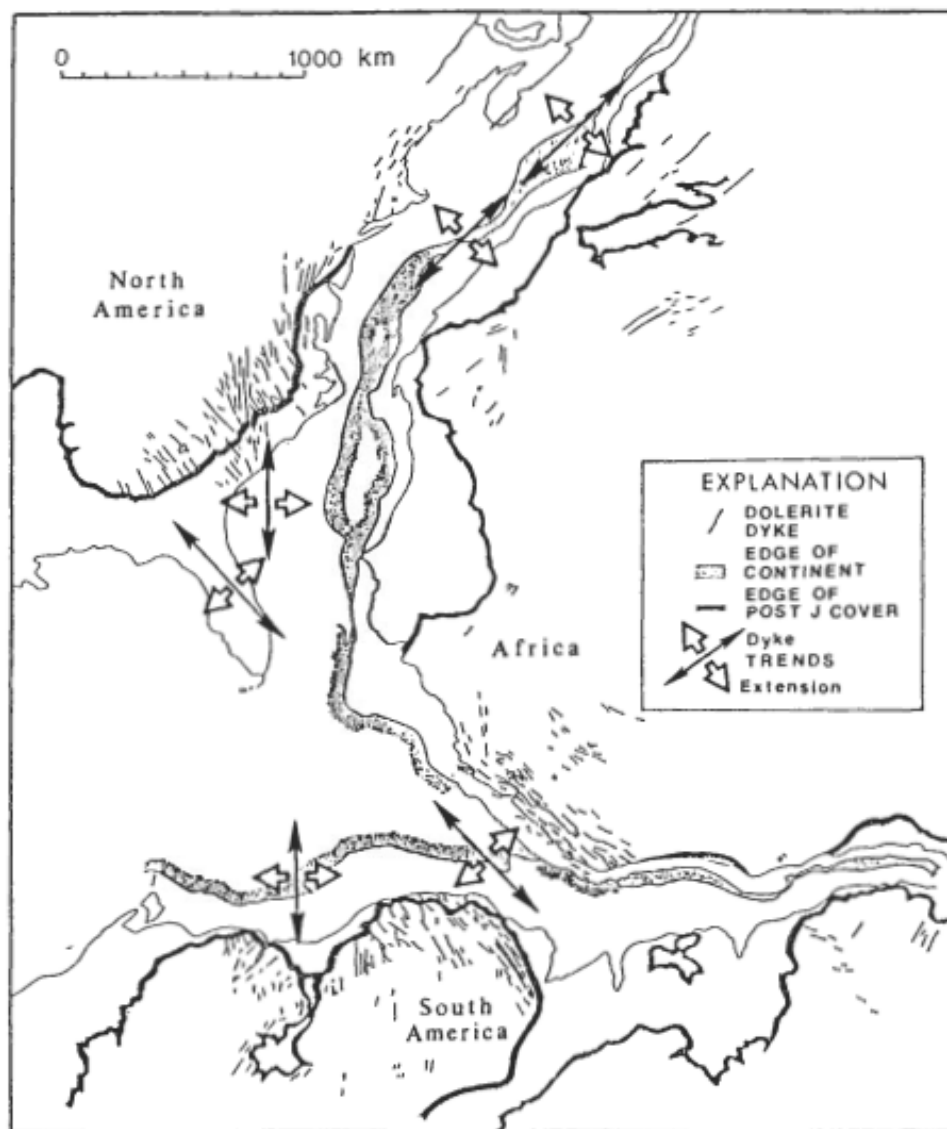
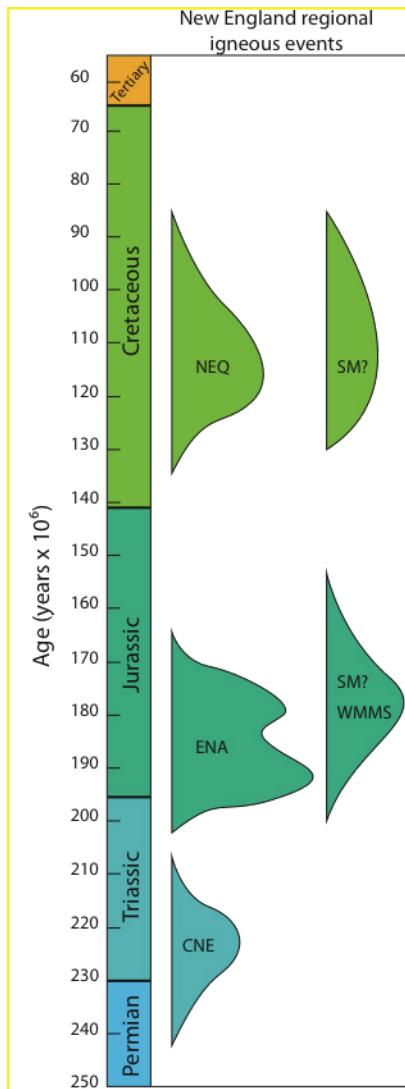


Figure 4.14 A map from McHone (1988) modified from Dooley and Wampler (1983) showing the Atlantic Ocean rift opening, extensional directions, and dike trends.



Great Gulf n = 1558

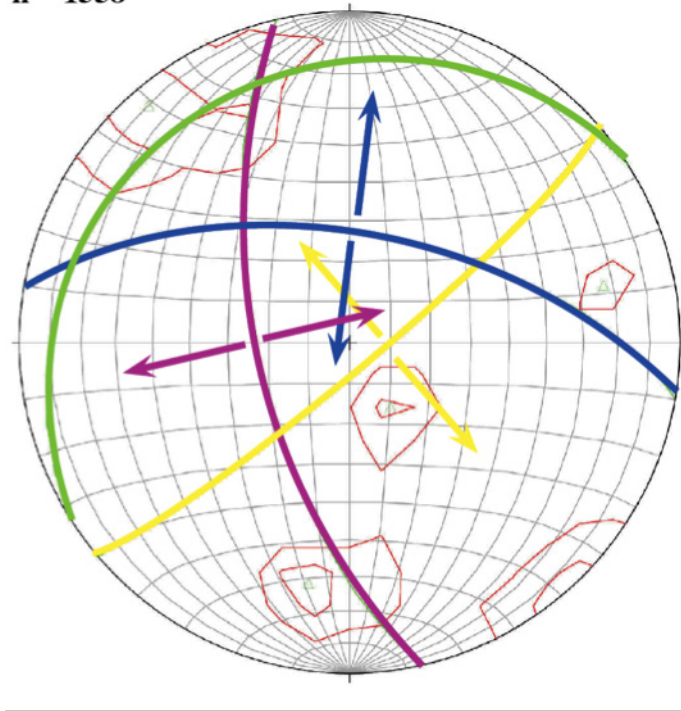


Figure 4.15 A stereonet (above) showing the three major joint sets and sigma 3 orientations found in the Great Gulf, on the side of Mount Washington, New Hampshire (Eusden et al, 2011). Each joint set is matched to a color coded line on the time scale of igneous intrusions in New England (Eusden et al, 2011).

location on a geologic timescale of New England igneous intrusions. Although they vary slightly in orientation, likely due to the 25 km distance between the two study areas, the Swift River NE-SW, WNW-ESE, and NNW-SSE joint sets are represented by the yellow, blue, and purple joint sets respectively (Figure 4.15). This study supports the theory that the NE-SW joints are related to Pangean rifting in the Jurassic, and intrusion of the White Mountain Magma Series. The WNW-ESE set on the other hand was created during the early-mid Cretaceous, and the NNW-SSE set was late Cretaceous in age.

4.3 Glacial Lineaments and Regional Laurentide Ice Flow Analysis

4.3.1 Introduction

The Pleistocene glaciation events covered the White Mountain region in over one kilometer of ice, and as a result, this ice played a major role in shaping the surface of the land underneath. In the Swift River study area much of the geomorphology is glacially altered, with 76.6% of the surface being covered in till. As the ice sheet flowed southeast through the study area, it left behind linear features that represent the flow direction of the ice at that time.

Given the rather subdued topography in the Swift River area during peak ice cover, topography likely had no effect on flow direction. However, in late stage glaciation, as the ice thinned, some of the higher ridges in this region, including Mount Tremont and Mount Carrigan, may have directed ice flow around them (Bradley, 1981; Anderson and Borns, 1994; Eusden *et al.*, 2013).

4.3.2 Glacial Lineament Analysis

In the process of drawing bedrock lineaments off of a LiDAR hillshade, it is inevitable that some glacially derived lineaments were drawn accidentally as well. These glacial lineaments were separated based on the substrate they were found in, and their nature as glacial lineaments are more smooth than bedrock lineaments. After removal from the bedrock lineaments, it was found that the average lineament orientation was 310°.

While no previous glacial lineament studies have been undertaken in this region, the Ferguson *et al.* (1998; 1999) bedrock lineament maps appear to also show glacial lineaments (4.16). There are an abundance of long, 2km or greater, lineaments running in a NW-SE direction. Furthermore, many of these lineaments are mapped in regions that have been mapped as stratified drift and till by LiDAR classification of hillshades in this study.

Swift River Study Area

NH Lineament Analysis 1998 and 1999

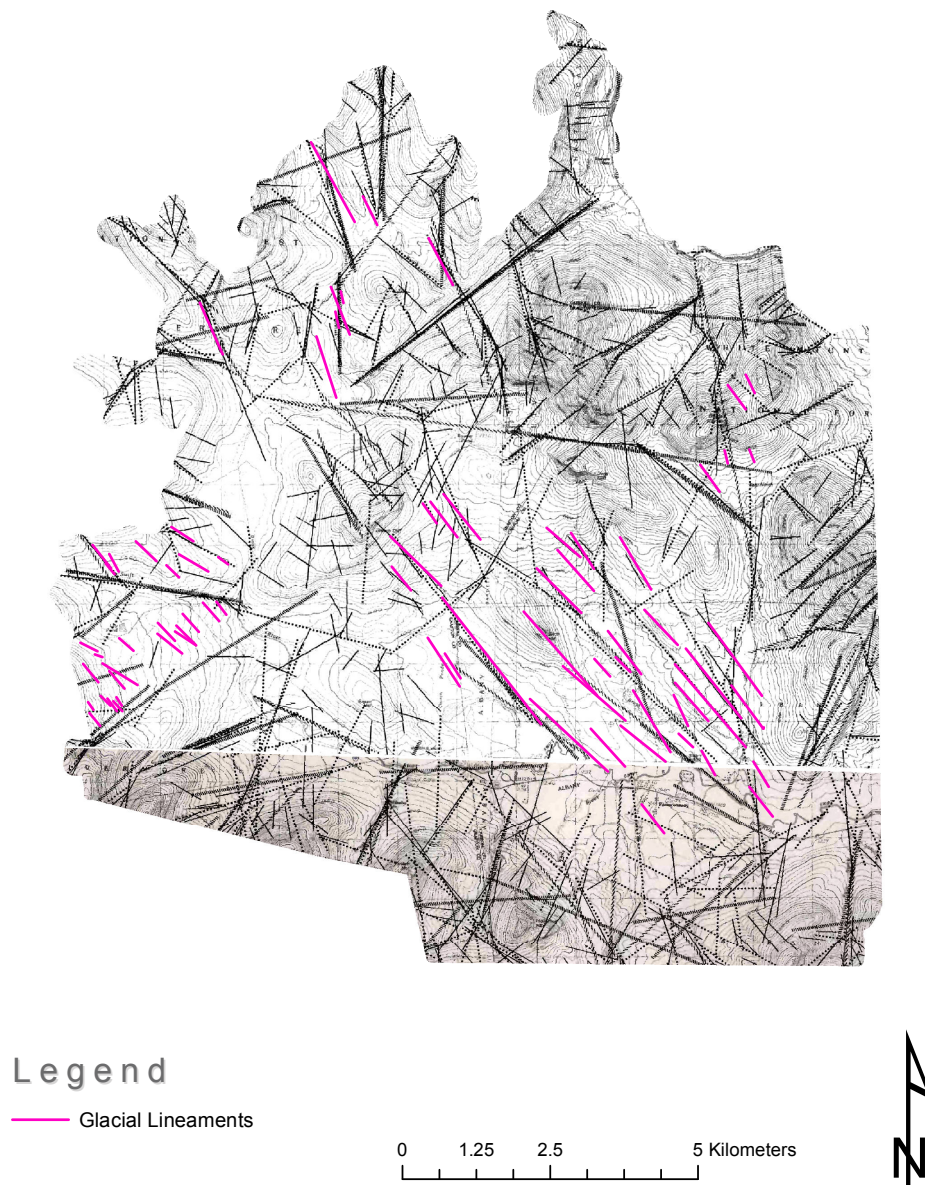


Figure 4.16 The two lineament maps created for the USGS cropped to the Swift River study area (Ferguson et al, 1998; Ferguson et al, 1999). The 1998 map lies to the south while the 1999 map is to the north. LiDAR derived glacial lineaments from this study are overlain in pink.

Many of these lineaments line up with the glacial lineaments drawn from the LiDAR, and are likely just glacial lineaments that were indiffereniable without LiDAR.

4.3.3 Glacial Flow Analysis

Glacial lineaments can be used as glacial flow indicators, as features are lengthened in the direction of flow. Common features with a linear component that could potentially be translated to lineaments are drumlins and large bedrock striations (Anderson and Borns, 1994). As the ice flows, it stretches “tails” onto drumlins and other raised features in the direction of flow.

The average orientation of these flow indicators, 310° , may be the best representation of overall ice flow. This is very similar to other estimates of flow direction in the area; 320° based off of Anderson and Born’s (1994) map of North American Laurentide

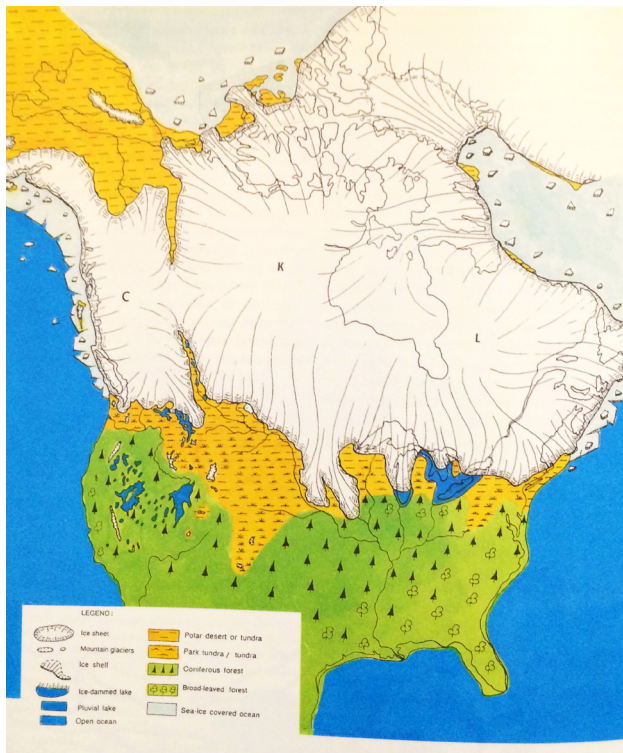


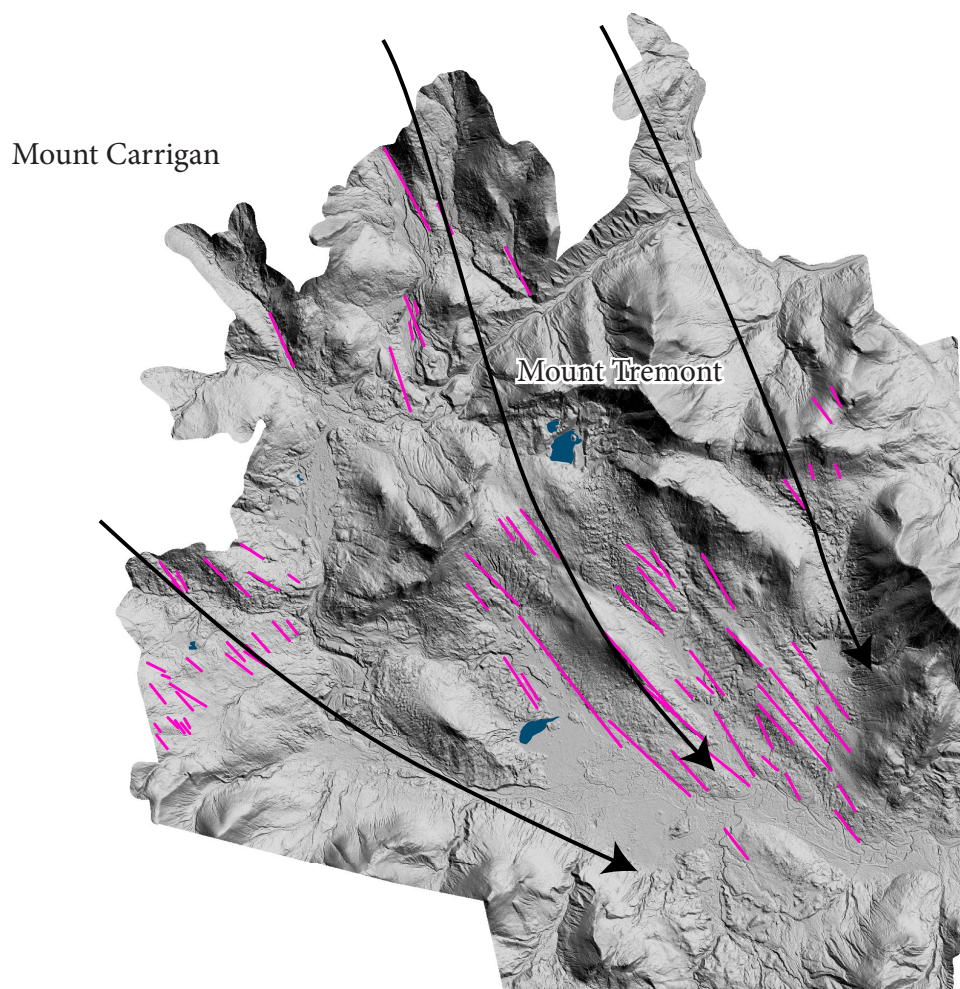
Figure 4.17 Map showing the extent of the Laurentide Ice Sheet, with flow lines representing flow direction as of 15,000 years ago (Anderson and Borns, 1994).

flow, and 300° based off of Dyke and Prest’s (1987) map of Laurentide extent and flow (Figure 4.17).

In the late stages of the Wisconsin Glaciation, approximately 14,500 years ago topography may have started to influence flow. The ice sheet had thinned by this point so that major peaks, such as Mount Carrigan (1,427m) and Mount Tremont (1,027m) would have been a major barrier to ice flow. Instead the ice would have found preferred routes through the lower topography. A map of these preferred routes is inferred from late stage flow indicators that differ from

Swift River Study Area

Glacial Flow Direction Map



Legend

- Glacial Lineaments
- Water

0 1.5 3 6 Kilometers



Figure 4.18 Glacial flow direction map as inferred from the glacial lineaments (in pink). Some variation in flow direction can be seen around Mount Tremont (north of center) and Mount Carrigan (off map to the NE). Black arrows represent the proposed late stage ice flow direction. The locations of Mounts Carrigan and Tremont are labeled.

the peak stage flow direction (Figure 4.18). By 14,000 years ago, this region was likely seeing the end of its ice, and was ice free by 13,000 years ago (Dyke and Prest, 1987).

4.4 Paleo-Glacial Lakes in the Swift River region



Figure 4.19 A Nunatak sticking through the Antarctic Ice Sheet (British Antarctic Survey).

4.4.1 Introduction

As the Laurentide Ice Sheet retreated, higher elevations may have been the first to deglaciate. Although perhaps counterintuitive, in the ablation zone of an ice sheet or glacier, the melting of ice outpaces the falling of new snow, and as a result topography inhibits flow rather than adding to glacial mass (Anderson

and Born, 1994). Since all of New Hampshire was within the ablation zone- the domes of accretion lay close to the Hudson Bay- the highest peaks of the White Mountains were the first to deglaciate and became Nunataks, or rock peaks sticking above an ice sheet (Figure 4.19).

As the Laurentide Ice Sheet continued to melt, it filled in all of the major valleys on the North, East, and West sides of the White Mountains. On the West side of the White Mountains there is ample evidence that the retreating ice sheet in the valleys blocked rivers flowing out of the White Mountains, and formed glacial lakes (Thompson and Svendsen, 2013; Eusden et al., 2013). Then, when the ice retreated further, the water passed through a spillway, a channel carved through till.

One similar glacial lake has been identified on the Eastern side of the White Mountains, lake Pigwacket (Thompson in Eusden et al., 2013). This lake was caused by the

damming of the Saco River Valley, and lasted into post-glacial times. Two newly identified glacial lakes are being proposed in this study, each located in the Swift River study area.

4.4.2 Proposed “Glacial Lake Sawyer”

The first of the two proposed glacial lakes to form temporally will be referred to as “Glacial Lake Sawyer” in this paper, as it existed primarily in what is now the Sawyer River drainage. This lake likely formed early on in the deglaciation of the area, when only the highest regions were deglaciated, as it requires two distinct glacial dams to have formed, one to the northeast, in the current Sawyer River channel, and one to the south, at the current headwaters of the Swift River. It formed in the saddle that lies between these two drainages.

The glacial lake is inferred from a series of large dissected terraces that fill this basin, and glacial outwash deposits (Figure 3.14 and Figure 3.11 respectively). In the White Mountains, glacial lake locations are recognized by “flat deltas whose upper surfaces mark the approximate elevations of the former lake surfaces” (Thompson in Eusden et al., 2013). This is exactly what is exhibited in this example, with each terrace representing a different lake level as the lake was drained. Between each draining event, a horizon of outwash was formed, and was dissected during the next drainage event. The water sources for the lake were streams running in from the deglaciated Mount Carrigan and Mount Tremont. Several of the lake levels are modeled in a 3D scene created using ArcScene, showing the northern outlet on the left, and the southern outlet on the right (Figure 4.20 and Figure 4.21). It is proposed that the maximum lake level was at 554m above current sea level, as this is the elevation of the highest, and likely oldest, large terrace, with only a braided stream channel uphill. As the lake level subsequently fell, it left several progressively lower terraces. When the lake level dropped to below 534m the lake was split in two, a north and south lake cut by a spit of land (Figure 4.20). It is likely that the southern lake drained entirely shortly after this point, as no more major terraces are found on this side of the divide. Between

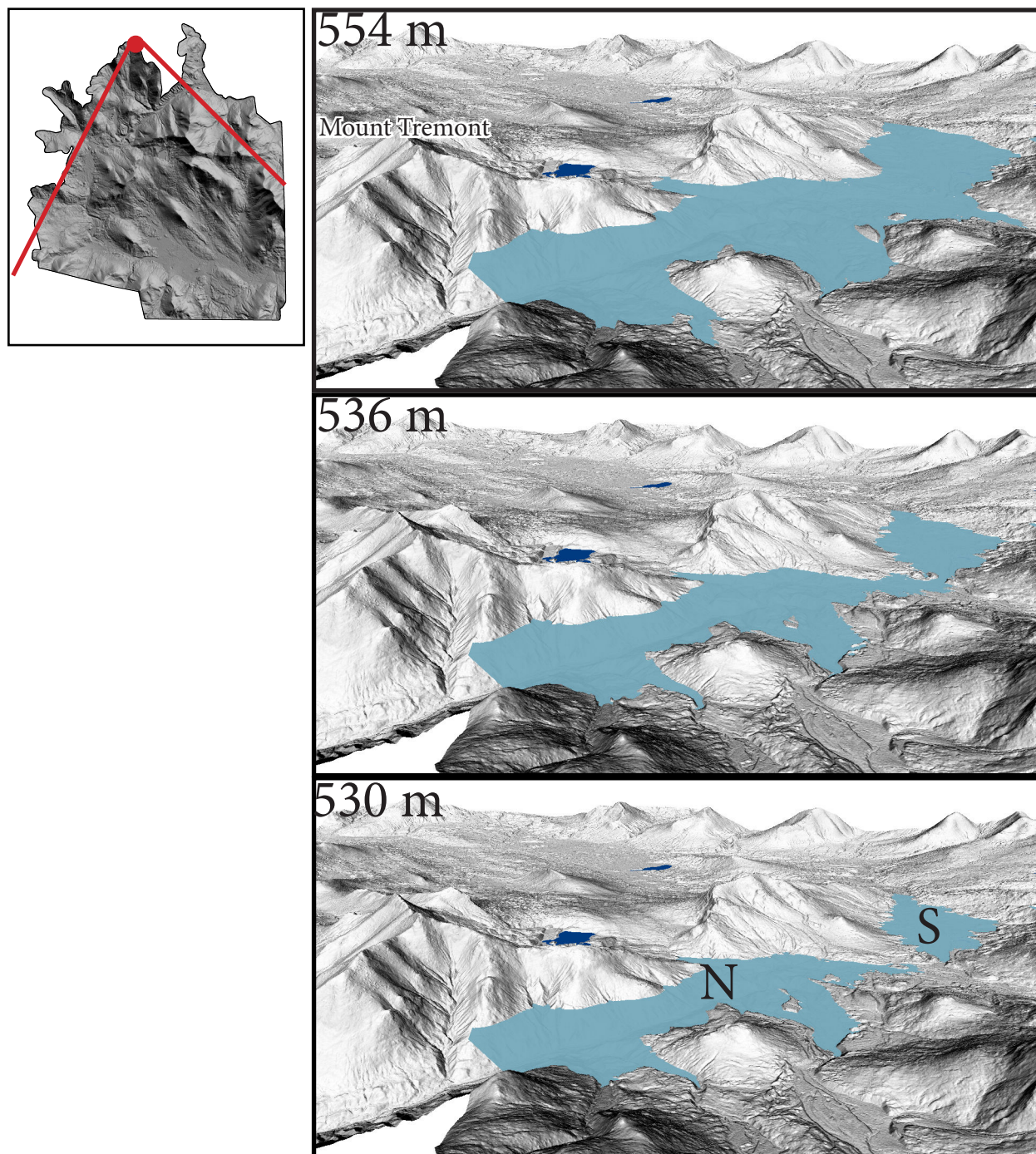


Figure 4.20 Three 3D models of Glacial Lake Sawyer representing different lake surface elevations. The lake surface elevation of each is marked in meters at the upper left of the image. The glacial lake is in light blue, while dark blue ponds represent current bodies of water. The extent of the view can be seen in the map inset at the top left, with the red dot marking the viewpoint location, and the two lines marking the boundaries of the line of sight. After the splitting of Glacial Lake Sawyer, the two parts, North and South are marked with an N and an S respectively.

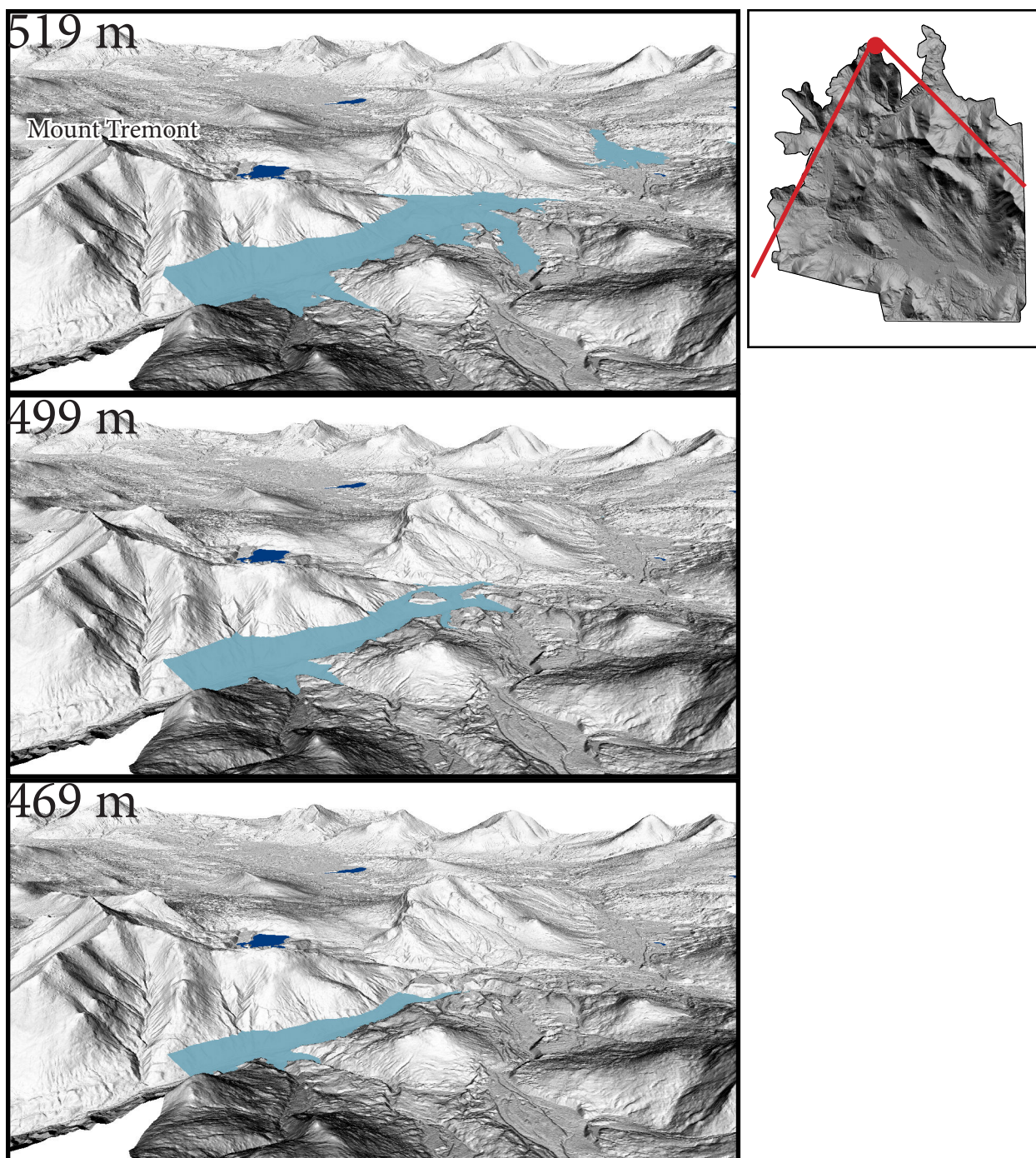


Figure 4.21 Three 3D models of Glacial Lake Sawyer representing different lake surface elevations. The lake surface elevation of each is marked in meters at the upper left of the image. The glacial lake is in light blue, while dark blue ponds represent current bodies of water. The extent of the view can be seen in the map inset at the top right, with the red dot marking the viewpoint location, and the two lines marking the boundaries of the line of sight.

519m and 500m some of the largest terraces were formed, marking a period of slow drainage, and much deposition (Figure 4.21).

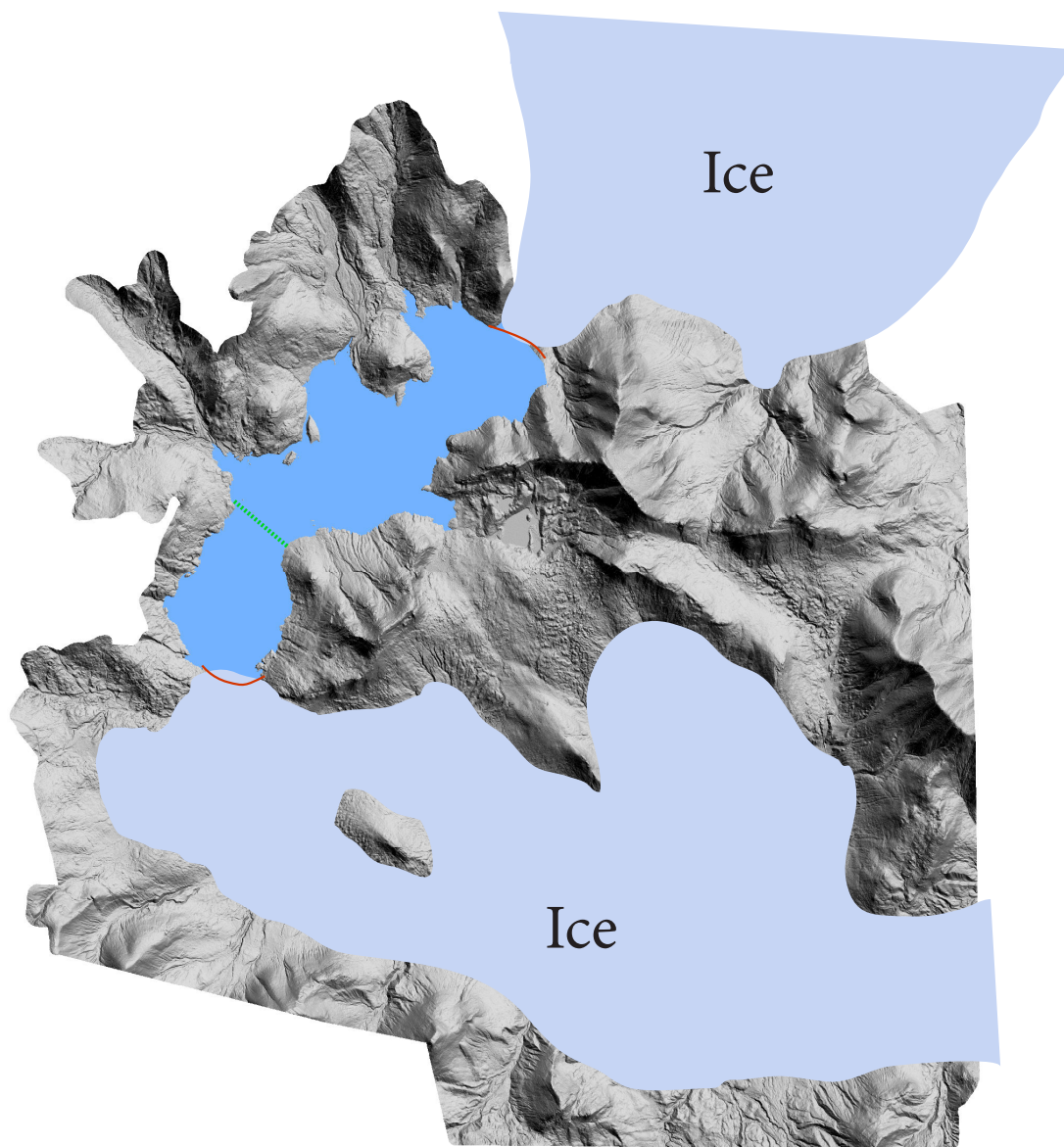
Below the 495m mark, there are very few terraces and each is quite small. This represents a period of increased drainage, with less time to deposit sediment horizons (Figure 4.21). By the time the lake surface had reached 460m it is likely that the ice dam released entirely, leaving one final terrace and a spillway that has since become the channel of the Swift River.

Unlike Lake Pigwacket or the other glacial lakes of the White Mountains, Glacial Lake Sawyer is not the result of a single outlet being blocked by glacial ice, but two outlets each being blocked. This would be highly unusual, but is the best explanation for the terraces found here. If the ice did retreat off the highest elevations first, it would have left two remaining glaciers in the Swift and Sawyer river valleys as is seen in Figure 4.22. These glaciers would have stopped flowing, there no longer being an ice input pushing them, and would slowly ablate in place. This would explain why no glacial flow indicators show this stage of glaciation. As they melted, they slowly allowed more and more water to escape Glacial Lake Sawyer, until they retreated enough for a large outwash event, which formed the spillways seen (Figure 4.23).

4.4.3 Proposed "Glacial Lake Swift"

Upon ice dam release of the Southern Lake Sawyer, it can be seen that the water would flow through the spillway only to be blocked again by more ice filling the Swift River valley (Figure 4.23). This is thought to be the beginning of the second glacial lake, called "Glacial Lake Swift" due to its location. A similar blockage may have occurred in the Saco River valley to the water released from the northern lake, but it is outside of the study area, so remains unknown.

As the ice continued to melt, the ice extent receded down the Swift River Valley (Figure 4.24). This glacial lake had a maximum surface elevation of 383m, which is the



0 1.25 2.5 5 Kilometers

Figure 4.22 A map showing the proposed ice extent at the time of maximum filling of Glacial Lake Sawyer. The ice is shown in blue/grey, the ice dams are marked with red lines, and the future land bridge between the North and South Sawyer Lakes is marked with a green line.

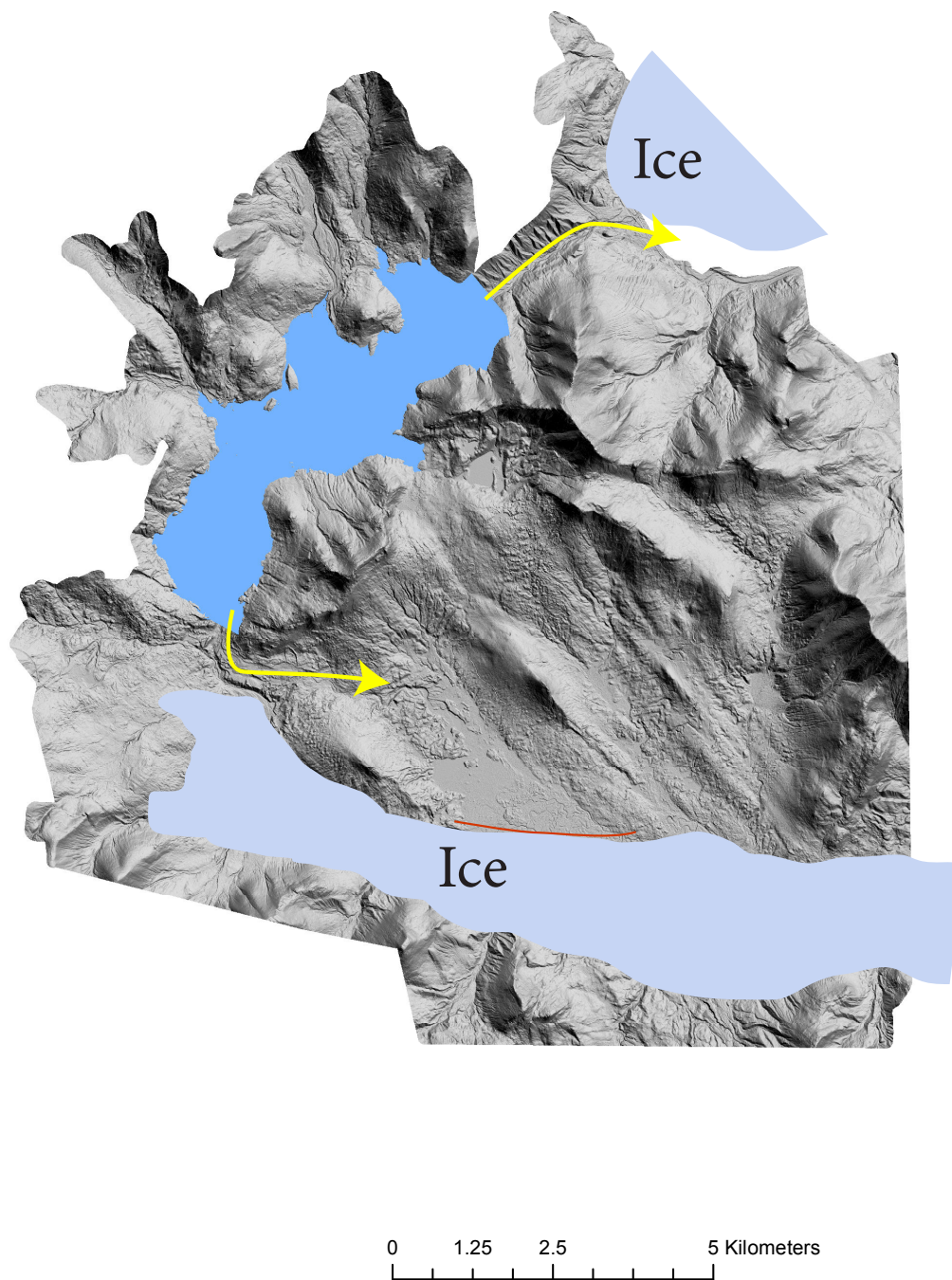


Figure 4.23 A map showing the proposed ice extent at the time of lake drainage. The ice is shown in blue/grey, the ice dams are marked with red lines, and the spillways as seen in the LiDAR imagery are drawn with yellow arrows.

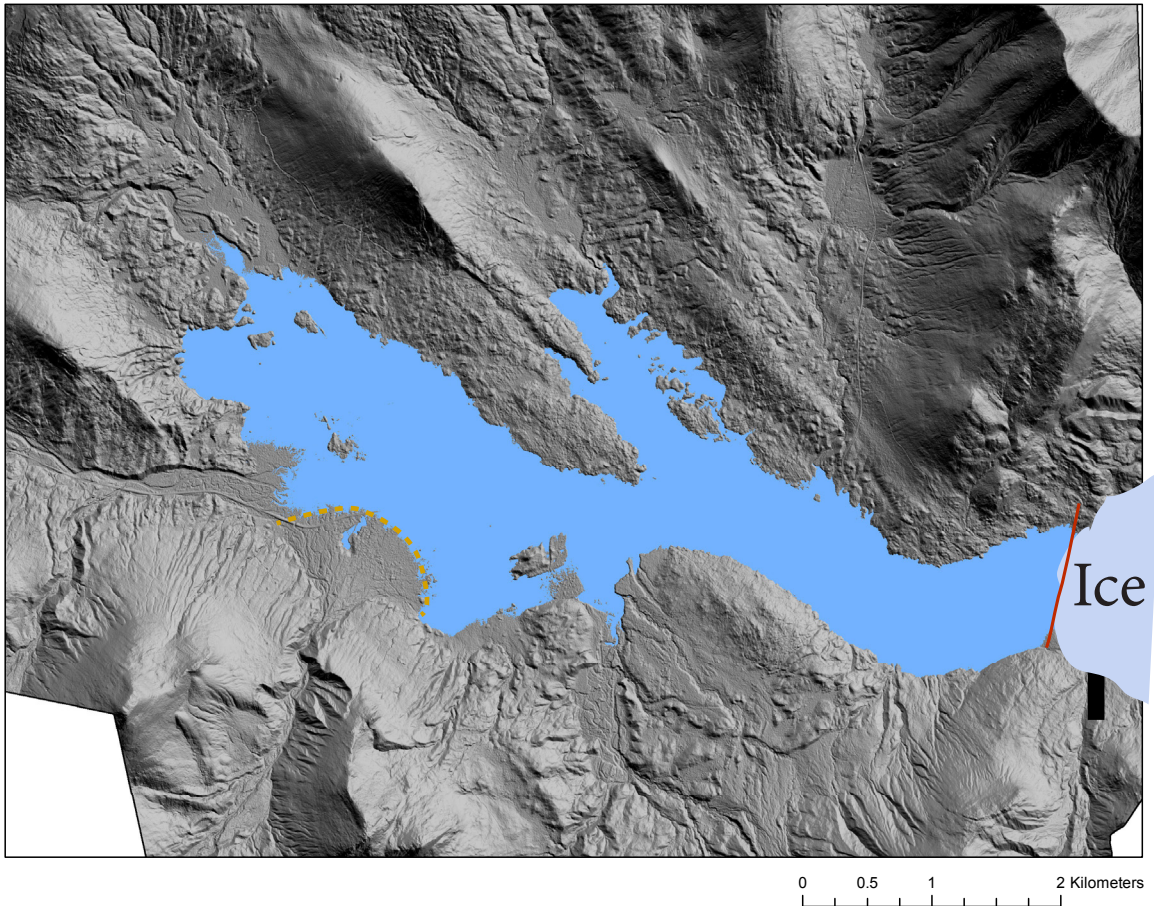


Figure 4.24 A map showing the maximum extent of Glacial Lake Swift, although the lake may have continued further east as the ice retreated. The maximum lake level of 383m is shown in bright blue, the ice is shown in blue/grey, and the ice dam is marked with a red line. The extent of the alluvial fan is marked with an orange dashed line.

elevation of a long paleo-shoreline feature. The existence of this shoreline represents a relatively long period of stagnating lake level, perhaps representing the filling of the lake at the same time as the ice retreated, increasing lake volume (Figure 4.24).

At some point, the ice dam either gave way, or retreated far enough down the Swift River valley that this region was no longer Glacial Lake Swift. It instead became a peri-glacial braided river valley that likely flowed to a glacial lake farther down the Swift River Valley. A modern analog of this is the Hooker River Valley above Lake Pukaki in New Zealand (Figure 4.25). The Hooker River is glacially fed, but this paleo-Swift River was likely groundwater and runoff fed, as the glaciers were at a lower elevation, not in the



Figure 4.25 The Hooker River Valley, with Mt Cook in the background (www.portwallpaper.com). The braided Hooker River runs through the valley; although not very braided in this image the previous channels can be seen, they are only hidden due to the lush environment that allows for immediate re-vegetation. The steep walls of this valley are lined with alluvial fans.

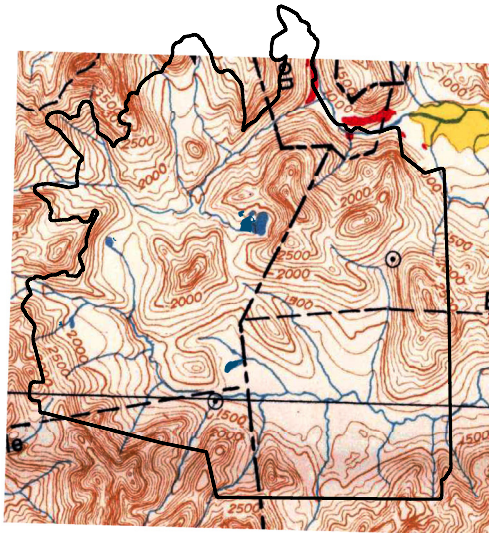
mountains. Otherwise the two are quite similar, a braided river with alluvial fans flowing from the steep slopes into the valley floor (Figure 4.25). Only one well defined alluvial fan is present in the Swift River valley, but another potentially lies right at the edge of the LiDAR coverage (Figure 4.24).

4.5 Geomorphic Mapping

4.5.1 Comparison to Goldthwait

This region of the White Mountains has seen almost no prior geomorphic mapping.

Swift River Study Area
Goldthwait 1950 Surficial Map

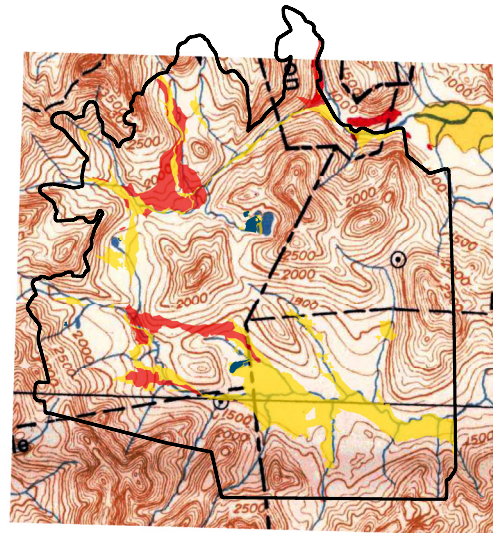


Legend
Water

0 1.5 3 6 Kilometers



Swift River Study Area
Goldthwait 1950 Surficial Map
Comparison



Legend

Water

Goldthwait Style Fluvial

Goldthwait Style Outwash

0 1.5 3 6 Kilometers



Figure 4.26 (Left) The original 1950 Goldthwait surficial map, with the red regions representing fine grained and potential varved sediments, and the gold representing gravel deposits.

Figure 4.27 (Right) The original 1950 Goldthwait surficial map with polygons derived from this LiDAR based study overlain. The red regions represent fine grained and potential varved sediments or regions classified as outwash in this study, and the gold represents gravel deposits represented as post glacial fluvial in this study.

The only study that attempted to do so was done by Goldthwait in 1950. This study only delineated two surficial features, a fine grained sediment sometimes including varves, and coarser grained gravel without varves. The study was focused along major roads, and the only polygons drawn within the Swift River study area were along the Saco River and Rte. 302, just along the northern boundary of the study area (Figure 4.26).

These surficial groups defined by Goldthwait (1950) are very similar in expected sediment type to the units delineated in the LiDAR based geomorphic mapping. The unit labeled outwash would likely have a fine grained matrix with varved layers in some regions. The post-glacial fluvial regions would likely be gravel dominated with potential cobbles and boulders intermixed as well. Therefore, these two units were compared to the two Goldthwait units, and in the limited regions of Goldthwait's study that lie within the LiDAR

coverage, the two overlapped almost perfectly (Figure 4.27). Although this is simply an estimate, and fieldwork would be needed to accurately determine the sediment types, the overlap of units suggests the LiDAR classification is at the very least a good starting point for field work., and with these LiDAR derived classifications, a much higher percentage of the region can be tentatively mapped than was possible in Goldthwait's time.

Chapter 5: Conclusion

5.1 Conclusion

LiDAR mapping within the Swift River region of the White Mountain National Forest has allowed the opportunity to test mapping techniques previously unused in New England. These include creating a LiDAR based lineament map, and an entirely remote geomorphic map. The merits of such a study include the ability to view features below tree canopy, ability to map large regions with a limited budget and personnel, and create a base-map quickly for use in the field. At the same time, like any remote study, LiDAR analyses have drawbacks as well.

The fracture data collected from outcrops within the study area shows that the remote LiDAR based lineament analysis is extremely successful in recognizing the dominant fracture set for a region. The secondary fracture set could be somewhat correlated to the lineament data, although not strongly, and the tertiary set could not be recognized at all. This makes LiDAR lineament mapping, at least in this part of the White Mountains that has limited exposed bedrock, a moderate proxy for fractures measured on the ground. Although some of the fracture sets can be identified, ground-truthing is required as well.

Similarly, while LiDAR allows for delineations to be made between surficial deposits with good certainty, the composition of these surficial units remains an estimate without further fieldwork. For example, while fluvial regions could easily be differentiated from till, till units were differentiated from one another based off of appearance (smoothed, hummocky, and fluvially dissected), and not by composition. In order to do so would still require extensive fieldwork.

The remote LiDAR mapping techniques excelled in other ways however: namely determining glacial flow direction from glacial flow indicators, and the demarcation of new macro-scale features that were invisible with lower resolution imagery that couldn't

penetrate tree canopy. Glacial flow direction indicators stood out starkly as lineaments when illuminated in a hillshade from the northeast. This allowed variations in late stage glacial flow to be recognized. Some of the other macro-scale features uncovered by LiDAR that were previously unmapped include a set of glacial lake terraces, a glacial lake shoreline, eskers, alluvial fans, and glacial spillways.

As a result, LiDAR based mapping, either structural or geomorphic, cannot be accurately done in the White Mountains without a component of fieldwork. LiDAR derived maps would, however, greatly streamline the field mapping process. By having an estimate of surficial unit boundaries or dominant fracture sets, researchers could determine their fieldwork approach before stepping foot in the study area. At the same time, LiDAR may allow these researchers to find and map macro-scale features that could be easily overlooked in the field. LiDAR will likely become an important tool for any future geologic study in the White Mountains.

5.2 Future Work

As the New Hampshire Geological Survey continues to do bedrock quadrangle mapping, these basemaps could be instrumental in helping quad mappers find bedrock outcrops. All of the mapped non-bedrock regions of the study area, 87.5% of the total, could be overlooked, with the possible exception of stream channels that are downcut to bedrock. This would greatly streamline the bedrock mapping study, allowing the mappers to focus on the bedrock regions only.

Furthermore, since the geomorphology Swift River region of the White Mountain National Forest has now been mapped using LiDAR, future field work needs to be done to prove or disprove some of the claims made from this remote analysis. This includes better differentiation of surficial units based off of composition, rather than by their appearance in a hillshade. While these maps may help future surficial mappers approach this region

in a more organized fashion, they cannot stand alone without field testing. At the same time, some of the features found in this study are brand new, and could benefit from more fieldwork as well. For example, the outwash terraces, while assumed to be lacustrine sediments, could in fact represent downcut glacio-fluvial terraces. This differentiation could only be made by a sediment analysis from these terraces, and is just an estimate without that.

Finally, as more of the White Mountain National Forest continues to be flown with LiDAR, the amalgamation of these datasets could allow much greater knowledge of the region. For example, Glacial Lake Swift extends beyond the boundaries of this study area, and would require further mapping in another region yet to be flown with LiDAR. Similarly, a map of regional glacial flow direction could be created for the entire White Mountains if the entire region were flown with LiDAR and glacial lineaments drawn throughout. This could offer more insight on the late stage glacial movement in the region than previous datasets have been able to offer. As LiDAR availability in this region increases over the next several years, LiDAR will likely become an integral part of mapping efforts in the White Mountains, and New England as a whole.

5.3 Acknowledgements

The continued mentoring and guidance of J. Dykstra Eusden has been instrumental throughout the project, from the field work that was conducted out of his summer home, to the weekly thesis meetings. Matt Duvall is a GIS guru, whose help I have had to enlist several times. Mike Retelle took the time to meet with me several times in the later stages of the project, and offered insight on the glacial features in the region. The team from the NRCS of Roger Dekett, Jessica Phillipe, and Bob Long took the time to meet with me at the outset of the study, and shared the LiDAR dataset with me. Rick Chormann, the New Hampshire State Geologist, met with me to discuss the potential usefulness of these maps

for his team. Most importantly, I would like to thank Josh Sturtevant, my field partner and fellow GIS mapper for his help throughout the project. Having another person to bounce ideas off of was instrumental throughout the thesis process.

References

- ANDERSON, B. G. & BORN, H. W. 1994. The Ice Age World: *Scandinavian University Press*. p. 70-103.
- BLAKEY, R. 2011. Library of Paleogeography on the World Wide Web, accessed [December 13, 2013], at URL [<http://cpgeosystems.com/paleomaps.html>]
- BRADLEY, D. C. 1981. Late Wisconsinan mountain glaciation in the Northern Presidential Range, New Hampshire: *Arctic and Alpine Research*. **13**: 3, p. 319-327.
- BRITISH ANTARCTIC SURVEY. 2014. Image from British Antarctic Survey website on the World Wide Web, accessed [January 20, 2014], at URL [<http://www.antarctica.ac.uk>]
- CORGNE, S., MAGAGI, R., YERGEAU, M. & SYLLA, D. 2010. An integrated approach to hydro-geological lineament mapping of a semi-arid region of West Africa using Radarsat-1 and GIS, *Remote Sensing of Environment*, **114**: 9, p. 1863-1875.
- CREASY, J. W., & EBY, G. N. 1993. Ring Dikes and Plutons: a deeper view of calderas as illustrated by the White Mountain Igneous Province, in Cheney, J. T. Hepburn, J. C., eds. Field Trip Guidebook for the Northeastern United States, Geological Society of America Annual Meeting, Boston: Contribution No. 67. Department of Geology and Geography, University of Massachusetts, Amherst, MA. P. N1-N25.
- CREASY, J. W., & FITZGERALD, J. P. 1996. Bedrock Geology of the Eastern White Mountain Batholith, North Conway Area, N. H. *New England Intercollegiate Geologic Conference Guidebook to Field Trips in Northern New Hampshire and Adjacent Regions of Maine*. P. 255-272.
- DEKETT, R., LONG, R., & PHILIPPE, J. 2013. Natural Resources Conservation Service of Vermont: United States Department of Agriculture. St. Johnsbury, Vermont.
- DYKE, A. S., & PREST, V. K. 1987. Late Wisconsinan and Holocene History of the Laurentide Ice Sheet. *Géographie physique et Quaternaire*. **41**: 2, p.237-263.
- EUSDEN, J. D., GARDNER, P., KINDLEY, C., CASTRO, C. 2011. Paleostress Fields of Mesozoic Dikes and Joints. NEGSA bulletin. p. 1-16.
- EUSDEN, J. D., THOMPSON, W. B., FOWLER, B. K., DAVIS, P. T., BOTHNER, W. A., BOISVERT, R. A., CREASY, J. W. 2013. The Geology of New Hampshire's White Mountains. Durand Press, Lyme NH. p. 47-87.
- FAURE, S., TREMBLAY, A. & ANGELIER, J. 1996. Alleghanian paleostress reconstruction in the

- Northern Appalachians: Intraplate deformation between Laurentia and Gondwana. *Geological Society of America Bulletin*, **108**: p. 1467-1480.
- FAURE, S., TREMBLAY, A., MALO, M. & ANGELIER, J. 2006. Paleostress analysis of Atlantic Crustal Extension in the Québec Appalachians. *Journal of Geology*; **114**: p. 435-448.
- FERGUSON, E. W., CLARK, S. F., JR., MARCOUX, G. J., SHORT, H. A., & MOORE, R. B. 1998. Lineament map of Area 8 of the New Hampshire bedrock aquifer assessment, north-east-central New Hampshire. *USGS Open-File Report*: p. 98-191.
- FERGUSON, E. W., CLARK, S. F., JR., MARCOUX, G. J., SHORT, H. A., & MOORE, R. B. 1999. Lineament map of Area 11 of the New Hampshire bedrock aquifer assessment, north-east-central New Hampshire. *USGS Open-File Report*: p. 99-165.
- Fossen, H. 2010. Structural Geology. *University Press, Cambridge*. p. 1-150.
- GEOREF, 2013, Search for “geomorphology” on GeoRef database on the World Wide Web, accessed [November 7, 2013], at URL [<http://www.ebscohost.com/academic/georef>]
- GOLDTHWAIT, J. W. 1950. Surficial Geology of New Hampshire. *New Hampshire State Planning and Development Commission*.
- HAUGERUD, R. A., HARDING, D. J., JOHNSON, S. Y., HARLESS, J. L., WEAVER, C. S., & SHERROD, B. L. 2003. High-Resolution Lidar Topography of the Puget Lowland, Washington- A Bonanza for Earth Science: *GSA Today*; June 2003, p. 4-10.
- HIBBARD, J.P., VAN STAAL, C.R., RANKIN, D.W., & Williams, H. 2006, Lithotectonic Map of the Appalachian Orogen, Canada: Geological Survey of Canada “A” Series, 2 sheets.
- HIBBARD, J.P., VAN STAAL, C.R., AND RANKIN, D.W., 2010, Comparative analysis of the geological evolution of the northern and southern Appalachian orogen: Late Ordovician-Permian: From Rodinia to Pangea: The Lithotectonic Record of the Appalachian Region: *Geological Society of America Memoir*, v. 206, p. 51-69.
- KIM, G., LEE, J. & LEE, K. 2004. Construction of lineament maps related to groundwater occurrence with ArcView and Avenue™ scripts, *Computers & Geosciences*, **30**: 9–10, p. 1117-1126.
- LYONS, J. B., BOTHNER, W. A., MOENCH, R. H., & THOMPSON, J. B. 1997. Bedrock Geologic Map of New Hampshire: U.S. Geological Survey, Denver, CO, 2 plates- 1:250,000 scale bedrock and 1:500,000 scale derivative maps.
- MABEE, S. B., HARDCASTLE, K. C., WISE, D. U. 1994. A method of collecting and analyzing lineaments for regional-scale fractured-bedrock aquifer studies: *Ground Water*; **32**: 6, p. 884-894.

- MALLET, C. & BRETAR, F. 2009. Full-Waveform Topographic Lidar: State-of-the-Art. *ISPRS Journal of Photogrammetry and Remote Sensing* **64**: 1, p. 1-16.
- MCHONE, J. G., & BUTLER, J. 1984. Mesozoic Igneous Provinces of New England and the opening of the North Atlantic Ocean: *Geological Society of America Bulletin*: **95**: 7, p. 757-765.
- MCHONE, J. G. 1988. Tectonic and paleostress patterns of Mesozoic intrusions in eastern North America: *Triassic–Jurassic rifting, continental breakup and the origin of the Atlantic Ocean passive margins, part A*: Elsevier. P. 608-620.
- MCHONE, J.G. AND SHAKE, S.N. 1992. Structural control of Mesozoic magmatism in New England, in *Mason, R., ed., Basement Tectonics 7*: Boston, Kluwer Academic. p. 399-407.
- NATIONAL OCEANIC AND ATMOSPHERIC ASSOCIATION, 2013, GPS information available on the World Wide Web, accessed [November 13, 2013], at URL [<http://www.noaa.gov/index.html>]
- PAVLIS, T. L., & BRUHN, R. L. 2010, Application of LIDAR to resolving bedrock structure in areas of poor exposure: An example from the STEEP study area, southern Alaska: *Geological Society of American Bulletin*.
- PAVLIS, T. L., LANGFORD, R., HURTADO, J., & SERPA, L. 2010. Computer-based data acquisition and visualization systems in field geology: Results from 12 years of experimentation and future potential: *Geosphere*; **6**: 3, p. 275-294.
- PORT WALLPAPER. 2014. Image from Port Wallpaper website on the World Wide Web, accessed [February 20, 2014], at URL [<http://www.portwallpaper.com/gallery/world/new-zealand-list/>]
- RAMBERG, I. B. 2008, The Making of a Land: Geology of Norway: *Geological Society of London*.
- ROERING, J.J., MACKEY, B.H., MARSHALL, J.A., SWEENEY, K.E., DELIGNE, N.I., BOOTH, A.M., HANDWERGER, A.L., AND CEROVSKI-DARRIAU, C., 2013, 'You are HERE': Connecting the dots with airborne lidar for geomorphic fieldwork: *Geomorphology*, v. 200, p. 172-183.
- SCHLISCHE, R.W., WITHJACK, M.O., AND OLSEN, P.E., 2002, Relative timing of CAMP, rifting, continental breakup, and inversion: tectonic significance, in Hames, W.E., McHone, G.C., Renne, P.R., and Ruppel, C.R., eds., *The Central Atlantic Magmatic Province: Insights from Fragments of Pangea*: American Geophysical Union Monograph 136, p. 33-59.

- SHAKE, S.N., AND MCHONE, J.G., 1987. Topographic lineaments and their geological significance in central New England: *Northeastern Geology*, **9**: 3, p. 120-128.
- THOMPSON, W. B., & SVENDSEN, K. M. 2013 Glacial Lakes and related deglaciation features in the northern White Mountains, New Hampshire (abstract): *Geological Society of America Abstracts with Programs*. **45**.
- U.S. DEPARTMENT OF AGRICULTURE FOREST SERVICE, 2001, White Mountain National Forest on the World Wide Web, accessed [November 7, 2013], at URL [<http://www.fs.usda.gov/whitemountain>]
- U.S. GEOLOGICAL SURVEY, 2001, National Water Information System data available on the World Wide Web, accessed [November 10, 2013], at URL [<http://waterdata.usgs.gov/nwis/>].
- WIKIPEDIA, 2013, image from LiDAR page available on the World Wide Web, accessed [November 10, 2013], at URL [<http://en.wikipedia.org/wiki/Lidar>].